


8-2021

Synthesis of the Diazonium Zwitterionic Polymer/Monomer for Use as the Electrolyte in Polymer Electrolyte Membrane (PEM) Fuel Cells

Josiah Marshall
East Tennessee State University

Follow this and additional works at: <https://dc.etsu.edu/etd>

 Part of the [Materials Chemistry Commons](#), [Organic Chemistry Commons](#), and the [Polymer Chemistry Commons](#)

Recommended Citation

Marshall, Josiah, "Synthesis of the Diazonium Zwitterionic Polymer/Monomer for Use as the Electrolyte in Polymer Electrolyte Membrane (PEM) Fuel Cells" (2021). *Electronic Theses and Dissertations*. Paper 3968. <https://dc.etsu.edu/etd/3968>

This Thesis - unrestricted is brought to you for free and open access by the Student Works at Digital Commons @ East Tennessee State University. It has been accepted for inclusion in Electronic Theses and Dissertations by an authorized administrator of Digital Commons @ East Tennessee State University. For more information, please contact digilib@etsu.edu.

Synthesis of the Diazonium Zwitterionic Polymer/Monomer for Use as the Electrolyte in
Polymer Electrolyte Membrane (PEM) Fuel Cells

A thesis

presented to

the faculty of the Department of Chemistry

East Tennessee State University

In partial fulfillment

of the requirements for the degree

Master of Science in Chemistry

by

Josiah Marshall

August 2021

Dr. Hua Mei, Chair

Dr. Cassandra Eagle

Dr. Robert Standaert

keywords: proton exchange membrane, diazonium, perfluoro 3(oxapent-4-ene) sulfonyl
fluoride, perfluoroalkylsulfonylimide

ABSTRACT

Synthesis of the Diazonium Zwitterionic Polymer/Monomer for Use as the Electrolyte in Polymer Electrolyte Membrane (PEM) Fuel Cells

by

Josiah Marshall

My research goals are to synthesize new zwitterionic perfluorosulfonimide (PFSI) monomer/polymers. They are expected to replace traditionally used perfluorosulfonic acid (PFSA) polymers as the electrolyte in PEM fuel cells. For the PFSI monomer preparation, we designed a nine-step synthesis route. Thus far, I have successfully completed the synthesis of 4-(2-bromotetrafluoroethoxy)-benzenesulfonyl amide, 4-acetoxybenzenesulfonic acid sodium salt, and 4-chlorosulfonyl phenyl acetate. The coupling reaction of 4-(2-bromotetrafluoroethoxy)-benzenesulfonyl amide with 4-chlorosulfonyl phenyl acetate, was troublesome due to slow reaction kinetics and byproducts. Additionally, I did a methodology study for the homopolymerization of the perfluoro 3(oxapent-4-ene) sulfonyl fluoride monomer. We compared the weight average molecular weight (M_w) of different reaction conditions. The best M_w was achieved when the polymerization was carried out for five days at 100 °C and 150 psi with 2 wt % initiator and 5 g of monomer. All the compounds were characterized by melting point, GC-MS, GPC, FT-IR, and $^{13}\text{C}/^1\text{H}/^{19}\text{F}$ NMR.

Copyright 2021 by Josiah Marshall

All Rights Reserved

DEDICATION

I would like to dedicate this work to my late grandparents, Roy and Shirley Hardin, as well as all my friends and family whose support has been instrumental in my achievements.

ACKNOWLEDGEMENTS

I would like to express my sincerest gratitude to Dr. Mei for her mentorship and patience throughout the entirety of my research experience at ETSU.

A thank you to the undergraduate research assistant, Adam Badawi, for all the help setting up and executing experiments.

Another thanks to Dr. Robert Standaert and Dr. Cassandra Eagle for serving on my thesis committee.

A big thank you to Dr. Ray Mohseni for his help with the operation of the analytical instruments and assistance with data interpretation.

Lastly, I would like to recognize the entire ETSU faculty/staff and graduate students in the department of chemistry during my time in the program. Thank you for the support, motivation, and continued investment in my success as a student.

TABLE OF CONTENTS

ABSTRACT	2
DEDICATION	4
ACKNOWLEDGEMENTS	5
LIST OF TABLES	11
LIST OF FIGURES	12
LIST OF SCHEMES	14
LIST OF ABBREVIATIONS	15
CHAPTER 1. INTRODUCTION	17
Preface.....	17
Research Aims.....	17
Fuel Cells.....	18
Polymer Electrolyte Membrane (PEM) Fuel Cells	20
Membrane Electrode Assembly (MEA).....	22
Proposed MEA System	26
Polymer Electrolyte Membrane	26
Aim 1: Diazonium N-bis[(perfluoroalkyl) benzenesulfonyl] imide (PFSI) Monomer	30
Aim 2: Methodology study for the homo-polymerization of perfluoro 3-(oxapent-4-ene) sulfonyl fluoride.....	33
CHAPTER 2. RESULTS AND DISCUSSION	35

Synthesis of 4-(2-bromotetrafluoroethoxy)-benzenesulfonyl amide	35
Synthesis of 4-acetoxybenzenesulfonic acid sodium salt	38
Synthesis of 4-chlorosulfonyl phenyl acetate	40
Coupling reaction of 4-(2-bromotetrafluoroethoxy)-benzenesulfonyl amide with 4- (chlorosulfonyl) phenyl acetate	44
Synthesis of perfluorobenzoyl peroxide [(2,3,4,5,6-pentafluorobenzoyl) 2,3,4,5,6- pentafluorobenzenecarboperoxoate]	47
Homo-polymerization of Perfluoro 3(oxapent-4-ene) sulfonyl fluoride.....	50
CHAPTER 3. EXPERIMENTAL.....	53
General Considerations	53
NMR Spectroscopy	53
Gas Chromatography-Mass Spectroscopy	53
Infrared Spectroscopy	53
Gel Permeation Chromatography	54
Souza-Design Dual Manifold High Vacuum Line System	54
Experimental Practice	55
Synthesis of 4-(2-bromotetrafluoroethoxy)-benzenesulfonyl amide	56
Liquid-liquid extraction & concentration of purified product	57
Synthesis of 4-acetoxybenzenesulfonic acid sodium salt	58
Synthesis of 4-(chlorosulfonyl) phenyl acetate	59

Coupling Reaction of 4-(chlorosulfonyl) phenyl acetate with 4-(2-bromotetrafluoroethoxy)-benzenesulfonyl amide	60
Synthesis of perfluorobenzoyl peroxide [(2,3,4,5,6-pentafluorobenzoyl) 2,3,4,5,6-pentafluorobenzenecarboperoxoate]	63
Homo-Polymerization of perfluoro-3(oxapent-4-ene) sulfonyl fluoride Monomer	64
CHAPTER 4. CONCLUSIONS	68
REFERENCES	69
APPENDICES	75
Appendix A1: ¹ H NMR spectrum of 4-(2-bromotetrafluoroethoxy)-benzenesulfonyl amide, 400 MHz, CD ₃ COCD ₃	75
Appendix A2: ¹⁹ F NMR spectrum of 4-(2-bromotetrafluoroethoxy)-benzenesulfonyl amide, 400 MHz, CD ₃ COCD ₃	76
Appendix A3: FT-IR spectrum of 4-(2-bromotetrafluoroethoxy)-benzenesulfonyl amide	77
Appendix B1: ¹ H NMR spectrum of 4-acetoxybenzenesulfonic acid sodium salt, 400 MHz, D ₂ O.....	78
Appendix B2: ¹³ C NMR spectrum of 4-acetoxybenzenesulfonic acid sodium salt, 400 MHz, D ₂ O.....	79
Appendix B3: FT-IR Spectrum of 4-acetoxybenzenesulfonic acid sodium salt.....	80
Appendix C1: ¹ H NMR spectrum of 4-(chlorosulfonyl) phenyl acetate, 400 MHz, CD ₃ COCD ₃	81

Appendix C2: FT-IR spectrum of (4-chlorosulfonyl) phenyl acetate	82
Appendix C3: GC-MS Chromatogram of (4-chlorosulfonyl) phenyl acetate.....	83
Appendix D1: ¹⁹ F NMR spectrum of Coupling Reaction of 4-chlorosulfonyl phenyl acetate with 4-(2-bromotetrafluoroethoxy)-benzenesulfonyl amide, 400 MHz, CD ₃ COCD ₃	84
Appendix E1: ¹⁹ F NMR spectrum of (2,3,4,5,6-pentafluorobenzoyl) 2,3,4,5,6- pentafluorobenzenecarboperoxoate, 400 MHz, CD ₃ COCD ₃	85
Appendix E2: FT-IR spectrum of (2,3,4,5,6-pentafluorobenzoyl) 2,3,4,5,6- pentafluorobenzenecarboperoxoate.....	86
Appendix F1: ¹⁹ F NMR spectrum of perfluoro 3(oxapent-4-ene) sulfonyl fluoride monomer, 400 MHz, CD ₃ COCD ₃	87
Appendix F2: (Expanded region -110 to -137 ppm) ¹⁹ F NMR spectrum of perfluoro 3(oxapent-4-ene) sulfonyl fluoride monomer, 400 MHz, CD ₃ COCD ₃	88
Appendix G1: ¹⁹ F NMR spectrum of homo-polymerization run #1 of CF ₂ =FCOCF ₂ CF ₂ SO ₂ F, 400 MHz, CD ₃ CN	89
Appendix G2: Gel Permeation Chromatography (GPC) for homo-polymerization run #1 of CF ₂ =FCOCF ₂ CF ₂ SO ₂ F in 1, 1, 1, 3, 3, 3-hexafluoroisopropanol (HFIP)	90
Appendix H1: ¹⁹ F NMR spectrum of homo-polymerization run #2 of CF ₂ =FCOCF ₂ CF ₂ SO ₂ F, 400 MHz, CD ₃ CN	91
Appendix H2: Gel Permeation Chromatography (GPC) for homo-polymerization run #2 of CF ₂ =FCOCF ₂ CF ₂ SO ₂ F in 1, 1, 1, 3, 3, 3-hexafluoroisopropanol (HFIP)	92

Appendix I1: ^{19}F NMR spectrum of homo-polymerization run #3 of $\text{CF}_2=\text{FCOCF}_2\text{CF}_2\text{SO}_2\text{F}$, 400 MHz, CD_3CN	93
Appendix I2: Gel Permeation Chromatography (GPC) for homo-polymerization run #3 of $\text{CF}_2=\text{FCOCF}_2\text{CF}_2\text{SO}_2\text{F}$ in THF.....	94
Appendix J1: ^{19}F NMR spectrum of homo-polymerization run #4 of $\text{CF}_2=\text{FCOCF}_2\text{CF}_2\text{SO}_2\text{F}$, 400 MHz, CD_3CN	95
Appendix J2: Gel Permeation Chromatography (GPC) for homo-polymerization run #4 of $\text{CF}_2=\text{FCOCF}_2\text{CF}_2\text{SO}_2\text{F}$ in 1, 1, 1, 3, 3, 3-hexafluoroisopropanol (HFIP)	96
Appendix K1: ^{19}F NMR spectrum of homo-polymerization run #5 of $\text{CF}_2=\text{FCOCF}_2\text{CF}_2\text{SO}_2\text{F}$, 400 MHz, CD_3CN CFCl_3	97
Appendix K2: Gel Permeation Chromatography (GPC) for homo-polymerization run #5 of $\text{CF}_2=\text{FCOCF}_2\text{CF}_2\text{SO}_2\text{F}$ in THF.....	98
Appendix L1: ^{19}F NMR spectrum of homo-polymerization run #6 of $\text{CF}_2=\text{FCOCF}_2\text{CF}_2\text{SO}_2\text{F}$, 400 MHz, CD_3CN	99
Appendix L2: Gel Permeation Chromatography (GPC) for homo-polymerization run #6 of $\text{CF}_2=\text{FCOCF}_2\text{CF}_2\text{SO}_2\text{F}$ in THF	100
VITA	101

LIST OF TABLES

Table 1. Fuel Cell Summary	20
Table 2. Test Plan for Homo-Polymerization Methodology Study	34
Table 3. TLC Data for Coupling Reaction Crude Product Mixture	62
Table 4. Polymerization Mw, Yield, and Vinyl end Calculation Data	65

LIST OF FIGURES

Figure 1. Targeted monomer structure.....	18
Figure 2. Targeted polymer structure.....	18
Figure 3. Fuel cell with membrane electrode assembly.....	21
Figure 4. Illustration of MEA on-cathode side of PEMFC.....	22
Figure 5. Illustration of catalyst layer with infused membrane material	24
Figure 6. Structural diffusion mechanism of proton transport.....	24
Figure 7. Proton vehicular transport mechanism	25
Figure 8. Chemical grafting of diazonium zwitterion to carbon support layer.....	26
Figure 9. General structure of Nafion® polymer membrane.....	27
Figure 10. Commercial PFSA ionomer perfluoro-ether side chain comparison	28
Figure 11. Comparison of sulfonic & bis [(perfluoroalkyl)sulfonyl] imide functional groups	30
Figure 12. Targeted monomer structure.....	31
Figure 13. Synthesis plan for target monomer.....	32
Figure 14. Target polymer	33
Figure 15. Synthesis plan for target polymer.....	33
Figure 16. Fluoroalkylation reaction.....	35
Figure 17. Acetylation of 4-hydroxybenzenesulfonic acid sodium salt	38
Figure 18. Chlorination of 4-acetoxybenzenesulfonic acid sodium salt.....	41
Figure 19. Coupling reaction	44
Figure 20. Perfluorobenzoyl peroxide initiator synthesis.....	47
Figure 21. Polymerization of perfluoro 3(oxapent-4-ene) sulfonyl fluoride	50
Figure 22. Souza-design dual manifold high vacuum glassware.....	55

Figure 23. Fluoroalkylation reaction setup 56

Figure 24. Parr 45 mL 4700 pressure vessel with 4310A gage block assembly 65

LIST OF SCHEMES

Scheme 1. PEMFC Half-Cell Reactions	22
Scheme 2. Fluoroalkylation Reaction Mechanism	37
Scheme 3. Acetylation Reaction Mechanism of 4-hydroxybenzenesulfonic acid sodium salt	40
Scheme 4. Reaction Mechanism of Vilsmeier Reagent with 4-Acetoxybenzenesulfonic acid	43
Scheme 5. Coupling Reaction Mechanism	46
Scheme 6. Perfluorobenzoyl Peroxide Initiator Synthesis Reaction Mechanism.....	49
Scheme 7. Homo-polymerization Reaction Mechanism	52

LIST OF ABBREVIATIONS

AFC	Alkaline Fuel Cell
DIEA	Diisopropyl Ethylamine
DMF	N, N-Dimethylformamide
DMFC	Direct Methanol Fuel Cell
DMSO	Dimethylsulfoxide
DOE	Department of Energy
FT-IR	Fourier Transform Infrared Spectroscopy
GC-MS	Gas Chromatography - Mass Spectroscopy
GDF	Gas Diffusion Layer
GE	General Electric
GPC	Gel Permeation Chromatography
MCFC	Molten Carbonate Fuel Cell
MEA	Membrane Electrode Assembly
NMR	Nuclear Magnetic Resonance
PAFC	Phosphoric Acid Fuel Cell
PEMFC	Polymer Electrolyte Membrane Fuel Cell
PFCB	Perfluorocyclobutyl
PFSA	Perfluorosulfonic Acid
PFSI	Perfluorosulfonylimide
PFVE	Perfluorovinyl Ether
ppm	parts per million

PTFE	Polytetrafluoroethylene
SOFC	Solid Oxide Fuel Cell
TLC	Thin Layer Chromatography
TMS	Tetramethylsilane

CHAPTER 1. INTRODUCTION

Preface

The introduction will be divided into two sections. The first section will provide some historical context for this research, highlight the intent of the research, and then move into a dialogue about the various types of fuel cells that are being used today. The discussion will then describe a polymer electrolyte membrane fuel cell (PEMFC). Following this description is a discourse about how a PEMFC works while emphasizing core functional parts of the fuel cell which include the membrane electrode assembly (MEA) and its three critical sub-components: gas diffusion layer (GDF), the catalyst layer, and the polymer electrolyte membrane. The second portion of the introduction will describe the targeted monomer/polymer chemical structure, the synthesis route, and the accompanying analytical characterization for this research.

Research Aims

The focus of my research was the attempted synthesis of 3-diazonium-4-trifluorovinyloxy-(perfluorobutane) benzenesulfonylimide zwitterionic monomer (Figure 1) as well as a methodology study of the polymerization procedure for perfluoro 3-(oxapent-4-ene) sulfonyl fluoride monomer (Figure 2). The resulting polymerization product of the sulfonyl fluoride monomer can be subjected to a series of reactions to yield a diazonium N-(perfluoroalkyl) benzenesulfonamide (PFSI) polymer. For the first project, the monomer was designed with perfluorovinyl ether groups (PFVE), aryl sulfonimide (acid) group, and diazonium functionality. Upon successful polymerization of the new diazonium zwitterion monomer, the

new PFSI polymers, are a suggested replacement for traditionally used Nafion polymer as the electrolyte in PEMFCs.^{1,2}

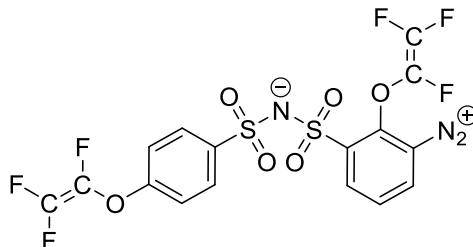


Figure 1. Targeted monomer structure

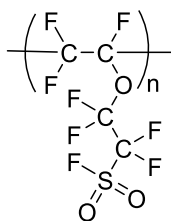


Figure 2. Targeted polymer structure

Fuel Cells

Increased mandates for energy acquisition that alleviate the need for fossil fuel resources has generated heightened curiosity in fuel cells.^{3,4,5} Due to their efficiency, durability, and reliability, fuel cells are prominent contenders for use as mobile energy sources due to efficiency, durability, and reliability.^{3,4,5} The fuel cell was invented by Sir William Robert Grove in 1839, but the first momentous use of the technology came in the 1960s when General Electric (GE) utilized fuel cells as a reserve power generator for the Gemini space missions.^{3,5,6}

Many remarkable alterations were made to PEMFC's in the 1960s, and 70's. An example would be integrating Teflon with the catalyst layer and assimilating DuPont's fully fluorinated

Nafion® membrane.⁵ The federal government began funding research for this technology after an advancement was made that decreased the quantity of transition metal catalyst required for an operational fuel cell.^{5,6}

Progress in areas such as cost diminishment, greater energy output, and better lifespan has augmented the viability of PEMFC's as an alternative energy source.^{3,4,5} Nonetheless, various field applications require alleviated costs and longevity if the technology is to see widespread commercial use.^{5,7} The current lifespan requirement for a fuel cell demands 5,000 hours for automotive applications (cars), 20,000 hours for public transportation (buses), and an excess of 40,000 hours for stationary power generators.^{5,7} This is to be done with only a 10% loss in fuel cell efficiency.^{5,7} More so, the U.S Department of Energy (DOE) aimed to decrease the ordinary cost for a fuel cell to \$45/kW and \$30/kW in 2010 and 2015 respectively.⁵ Even though the aforementioned cost is low enough to compete in the general market place, many performance and reliability issues must be overcome in order to implement fuel cells in the field.⁷

Fuel cells are electrochemical devices that convert chemical energy into electrical power without consumption of hydrocarbon fuels.⁴ Fuel cells are typically organized depending on the electrolyte it uses or the temperature range in which it operates.^{4,8} The different types are:

(1) solid proton exchange membrane or PEMFCs that utilize a polymer electrolyte as the membrane, (2) direct methanol fuel cell which has the same electrolytes as PEMFCs but uses methanol as the fuel, (3) alkaline fuel cells with alkaline electrolyte, (4) phosphoric acid fuel cells with acidic electrolyte, (5) molten carbonate fuel cells that use molten carbonate electrolyte, and (6) solid oxide fuel cells with conducting ceramic ion electrolyte.^{4,8}

Table 1 summarizes the variety of fuel cells as well as their respective electrolyte, operating temperature, fuel used, and most common applications.^{4,8}

Table 1. Fuel Cell Summary. Used with Permission.^{4,8}

<u>Fuel Cell Variant</u>	<u>Electrolyte</u>	<u>Temperature Division</u>	<u>Fuel Used</u>	<u>Fuel Efficiency (Chem. to Elec.)</u>	<u>Application</u>
Polymer Electrolyte Membrane Fuel Cell (PEMFC)	H ⁺ transporting polymer matrix	Low Temp ≈ 50-80°C	H ₂	44-60	Portable, Mobile, Stationary
Direct Methanol Fuel Cell (DMFC)	H ⁺ transporting polymer matrix	Low Temp ≈ 80°C	methanol	-	Portable, Mobile, Stationary
Alkaline Fuel Cell (AFC)	KOH	Low Temp ≈ 60-90°C	H ₂	40-60	Space, Mobile
Phosphoric Acid Fuel Cell (PAFC)	H ₃ PO ₄	Intermediate Temp ≈ 160-220°C	H ₂	55	Distributed power
Molten Carbonate Fuel Cell (MCFC)	Molten mixture of carbonates from alkali metals (K ₂ CO ₃ , Li ₂ CO ₃)	High Temp ≈ 600-700°C	H ₂	60-65	Distributed power generation
Solid Oxide Fuel Cell (SOFC)	Solid oxides (ZrO ₂ , CaO, Y ₂ O ₃)	High Temp ≈ 800-1000°C	H ₂	55-65	Baseload power generation

Polymer Electrolyte Membrane (PEM) Fuel Cells

Typically, PEMFC's contain bipolar plates with gas channels bored through on either side so that the reacting gases (O₂/H₂) can be optimally distributed over the electrode surface.⁶

The MEA consists of a PEM in the middle of the anode and cathode electrodes with a

GDL/catalyst layer on either side as shown in Figure 3 below.⁶

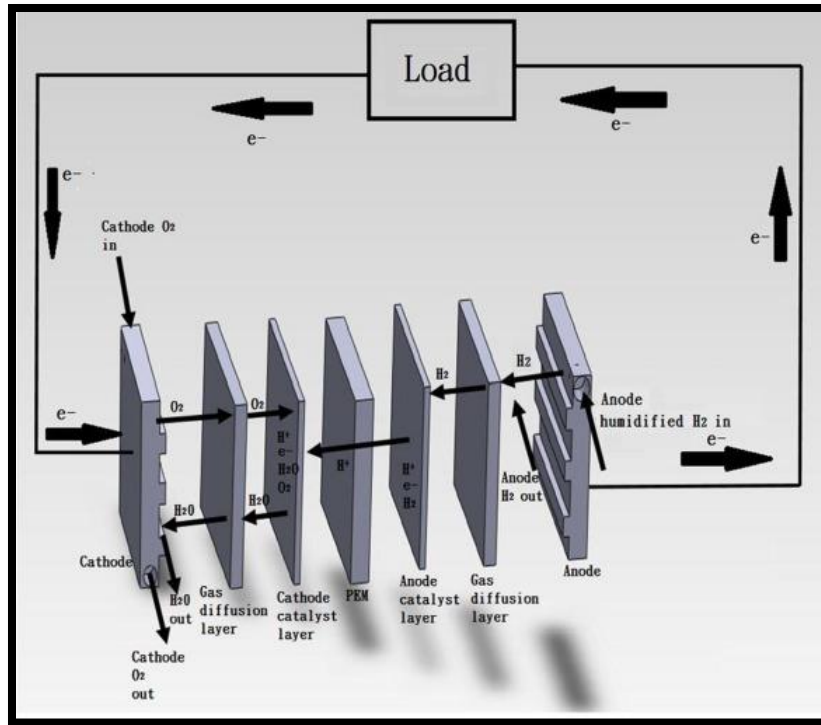
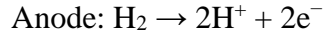


Figure 3. Fuel cell with membrane electrode assembly. Used with permission.⁹

During operation, the hydrogen fuel is introduced to the GDL through the gas channel and then to the anode catalyst layer.^{1,2,6} At the same time, oxygen (O_2) is brought in at the cathode. Oxygen passes the GDL and disperses on the catalyst layer where the oxidation takes place.^{1,2,6} Hydrogen is oxidized to electrons and protons (H^+) at the anode.^{3,4,9} These electrons (e^-) are then used to generate electricity. The polymer membrane only allows protons to pass through.^{3,4,9} On the cathode side, protons, electrons, and oxygen are combined. H_2O is the only by-product of the fuel cell's operation^{3,4,9} The half-cell reactions occurring at the catalyst layer are summarized in Scheme 1 below.



Scheme 1. PEMFC Half-Cell Reactions.²

Membrane Electrode Assembly (MEA)

The MEA (Figure 4) requires the synergistic cooperation of the gas diffusion layer (GDL), PEM, and catalyst layer for the fuel cell to carry out its function.⁶

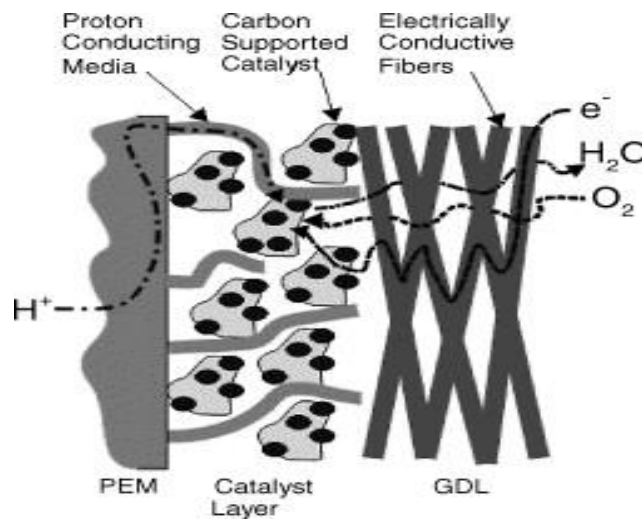


Figure 4. Illustration of MEA on-cathode side of PEMFC. Used with permission.⁶

The GDL carries out three tasks during PEM fuel operation.^{6,9} First, it assures that H_2 and O_2 arrive at the catalyst layer.^{6,9} Second, the GDL serves as an electronic conductor that moves electrons back and forth from the catalyst layer.^{6,9} Third, the GDL ensures that the necessary amount of water is obtained by the polymer membrane and that proper water balance is

maintained.^{6,9} Without water, the electrolyte membrane would become dehydrated by the reacting gases (O_2/H_2).⁹ The electrically conductive fibers of the GDL are most commonly constructed of porous carbon paper/cloth coated with Teflon®.⁶

The catalyst layers generally contain platinum over carbon support layer (Pt/C) that facilitates the half-cell reactions of the electrodes in Scheme 1.^{2,6} The catalyst layer is traditionally prepared by mixing the platinum/carbon components with the electrolyte polymer as a paste to the porous carbon support.¹⁰ This application method results in up to 90 % of the metal being inactive or inaccessible to the polymer membrane.^{10,11} With catalyst loading as little as 0.014 mg/cm^2 reported, other properties of the catalyst layer such as reactant diffusivity, ionic and electrical conductivity, and level of hydrophobicity must be carefully balanced to achieve greater employment of the metal catalyst.⁶

The innermost piece of the MEA, the PEM, is surrounded on either side by a catalyst layer and conducts three critical functions during fuel cell operation.^{4,6,7} First, it is the charge carrier for protons.^{4,6,7} Second, it partitions the reacting gases.^{4,6,7} Third, it serves as an electronic insulator that stops electrons from crossing the anode/cathode boundaries.^{4,6,7} Essentially, the PEM ensures that protons are shuttled from electrode to electrode while averting electrons and partitioning the cathode/anode reactants (O_2/H_2). Figure 5 illustrates how the catalyst layer with infused polymer electrolyte material might interact to facilitate the half-reactions shown in Scheme 1.¹⁰ The black and white dots on the carbon support layer represent platinum that can and cannot participate in fuel cell reactions, respectively.¹⁰ Smaller carbon pores with deposits of the platinum catalyst may be inaccessible to the electrolyte.¹⁰

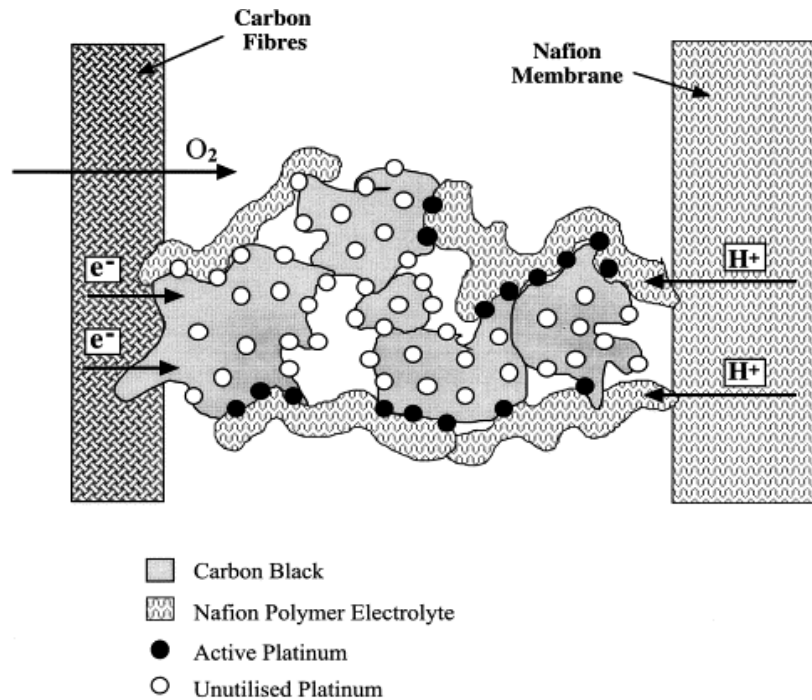


Figure 5. Illustration of catalyst layer with infused membrane material. Used with permission.¹⁰

PEMFC proton transport can be represented as a mixture of the structural diffusion mechanism, also known as Grotthuss or proton hopping, and the vehicular transport mechanism.^{4, 11-12} Structural diffusion can be described as a sequence of proton transfer reactions across a system of hydrogen bound H_2O molecules as shown in Figure 6.¹³ As a hydronium ion (H_3O^+) releases a proton, an adjoining water molecule temporarily adopts this proton forming a new hydronium ion, then the process repeats throughout the system. Each blue arrow in figure 6 indicates the movement or “hopping” of a proton to an adjacent water molecule.

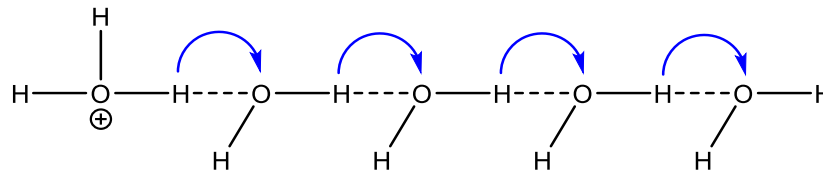


Figure 6. Structural diffusion mechanism of proton transport. Used with permission.¹⁶

The proton vehicular transport is an association of a hydronium ion (H_3O^+) with one (H_5O_2^+) or three (H_9O_4^+) other water molecules through polar interactions as shown in figure 7 below.^{4, 14-15} In the H_9O_4^+ complex, proton movement is initiated by the dissociation of the $\text{H}-\text{O}_\text{D}$ proton with ---O_C , forming the H_5O_2^+ intermediate. The charge is temporarily held by $\text{O}_\text{B}/\text{O}_\text{C}$ which leads to the reorientation of $\text{H}_2\text{O}_\text{A}$ and its consequent hydrogen bonding to O_B . Simultaneously, O_C takes on the positive charge which reforms the H_9O_4^+ complex and the action is cascaded down the network of water molecules.¹⁶

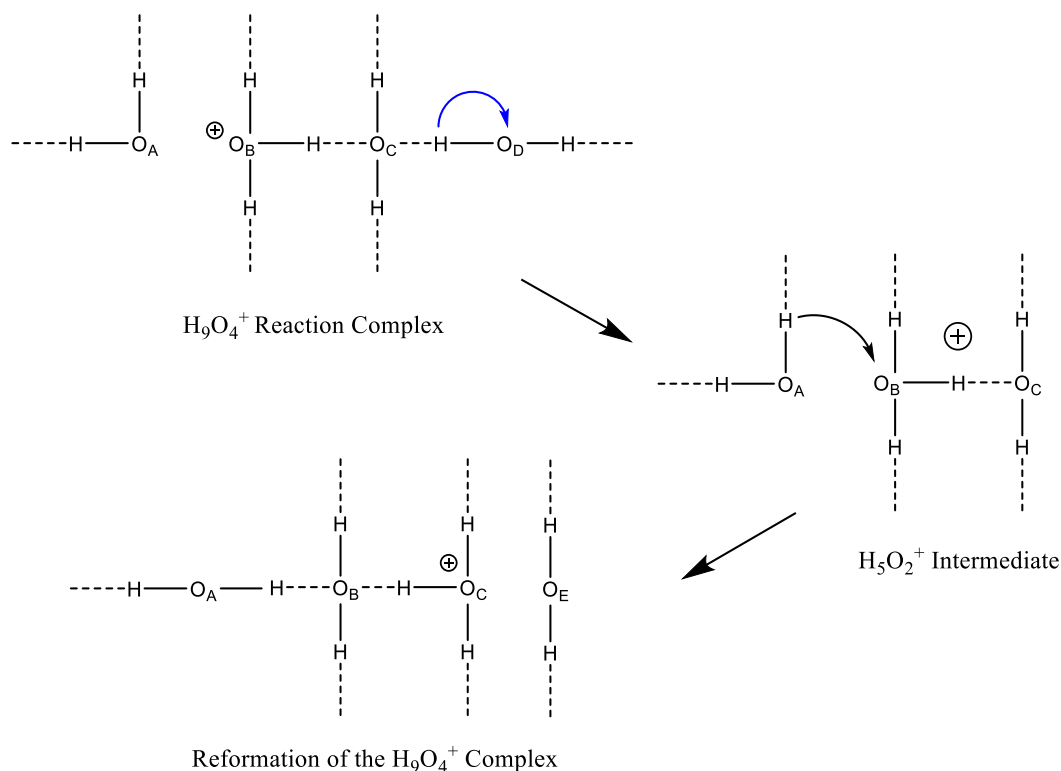


Figure 7. Proton vehicular transport mechanism. Used with permission.¹⁶

The vehicular mechanism is typically employed during low temperature and high humidity operating conditions for PEM fuel cell membranes such as Nafion®.¹⁷ The proton hopping mechanism is generally used to describe conduction under high temperature and low humidity conditions.¹⁷

Proposed MEA System

In our group, a new MEA system has been proposed that will allow a chemical bond to be created between the carbon support layer and the PFSI electrolyte as compared to more traditional methods that rely on the physical mixing of the electrolyte to the carbon support layer.¹⁰ The introduction of a carbon-carbon bond between the PFSI polymer and the carbon layer can be achieved by electrochemical reduction or thermal decomposition of a diazonium group.^{18, 19} Figure 8 shows a general mechanism for how a compound with a diazonium functionality might be grafted onto a carbon support layer.¹⁸

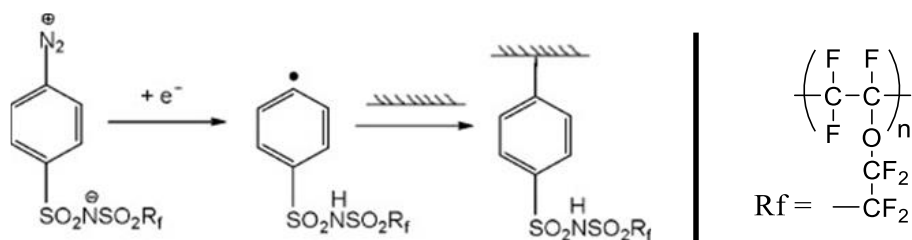


Figure 8. Chemical grafting of diazonium zwitterion to carbon support layer. Used with permission.¹⁸

Polymer Electrolyte Membrane

There are many different types of membranes employed for PEMFCs. They are categorized as perfluorinated ionomers, partially fluorinated polymers, non-fluorinated membranes with aromatic backbone, non-fluorinated hydrocarbons, or acid-base blends based on their structure and physical properties.³ The perfluorinated perfluorosulfonic acid (PFSA) ionomer, Nafion® (Figure 9) developed by DuPont in the early 1970's is one of the most popular polymers used as the electrolyte in PEMFCs.³

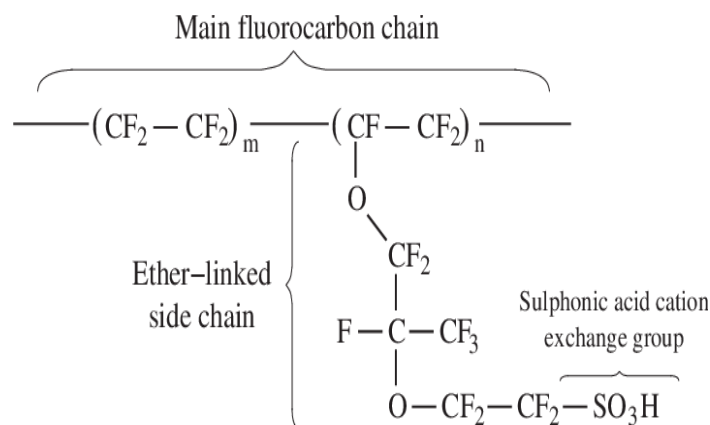


Figure 9. General structure of Nafion® polymer membrane. Used with permission.²⁰

Once considered the “golden standard” in PFSA technology, Nafion® was known for its high proton conductivity when properly hydrated, good mechanical strength and chemical stability, as well as its potential for long lifespan.^{20, 21} Nafion® is reported to have a proton conductivity of 0.08 S cm^{-1} at $25 \text{ }^\circ\text{C}$ and 100% relative humidity.²² Essentially, Nafion® provides a conductivity likened to 1.0M sulfonic acid at the reported conditions.²²

Nafion’s® success led to the development of many PFSA adducts that are commercially available such as those by 3M™, Fumion® membranes by Fumatech, Aciplex® by Asahi Chemical, Flemion® by Asahi Glass Company, Aquivion™ by Solvay Solexis, Fumapem® FS by Fumatech, and GORE by W. L. Gore and Associates.^{22,23} These ionomers have a polytetrafluoroethylene (PTFE) backbone and a perfluoroalkyl-ether pendant side group with a sulfonic acid ($-\text{SO}_3\text{H}$) end. The primary difference between the commercial PFSA products is the length/composition of the perfluoro-ether side chains.^{22, 23} Figure 10 makes structural comparisons for several of the PFSA compounds. Of the PFSA ionomers, Fumion® and Nafion® have the longest ether side chain (LSC). Whereas 3M™, Aciplex®, and Aquivion™ have progressively shorter side chains (SSC).^{22, 23}

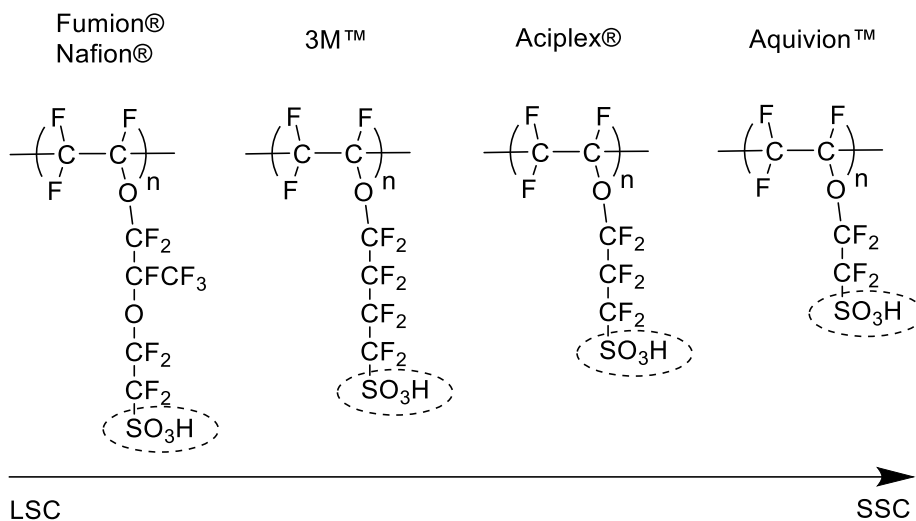


Figure 10. Commercial PFSA ionomer perfluoro-ether side chain comparison. Used with permission.²²

However, PFSA polymers have some limitations. A common problem with Nafion® and other related PFSA ionomers results from insufficient hydration.^{22,24} PFSA ionomers begin to lose hydration at operating temperatures above 80 °C and this effect is exacerbated by temperatures exceeding the boiling point of water (100 °C).^{22,24} Low water content diminishes the electrolytes' ability to conduct protons effectively.^{22,24} At even higher temperatures, the sulfonic acid (-SO₃H) ends on the PFSA polymer chain are suspected of undergoing an intramolecular dehydration reaction to form an anhydride (-SO₂-OSO₂-) which decomposes the acid functionality and consequently reduces the proton conductivity of the membrane.^{24,25} Additionally, due to the application process, PFSA polymers have relatively weak adhesion to the carbon support electrodes that are typically used in fuel cell membrane electrode assembly.¹⁸ This poor binding of the electrolyte to the carbon electrodes leads to a diminished lifetime for both components.²⁶

In more recent years, a body of research has focused on developing materials that have even more advantageous properties than traditional PFSA ionomers. One of such alternatives is a class of materials known as bis[(perfluoroalkyl)sulfonyl] imide ionomers. These imide ionomers generally share a common PTFE backbone and perfluoroalkyl-ether pendant side chains with traditional PFSA ionomers. However, the sulfonic acid group is replaced with a bis[(perfluoroalkyl)sulfonyl] imide. Figure 11 shows a side-by-side comparison of the two functional groups and their resonance structures. It is important to note here that sulfonic acid has a singular resonance structure whereas the Bis[(perfluoroalkyl)sulfonyl] imide group has two sulfonyl groups, indicated by the red and blue arrows, that share in the overall resonance structure of the molecule. Due to these structural characteristics, bis[(perfluoroalkyl)sulfonyl] imide ionomers have exhibited stronger gas-phase acidity compared to PFSA analogues.^{18,27} In fact, in the gas-phase, they are classified as true superacids.²⁷ Additionally, PFSI polymers exhibit greater chemical and electrochemical inertness, improved thermal stability, and less susceptibility to oxidative and dehydration reactions compared to the PFSA class of materials.^{18,24,26,28}

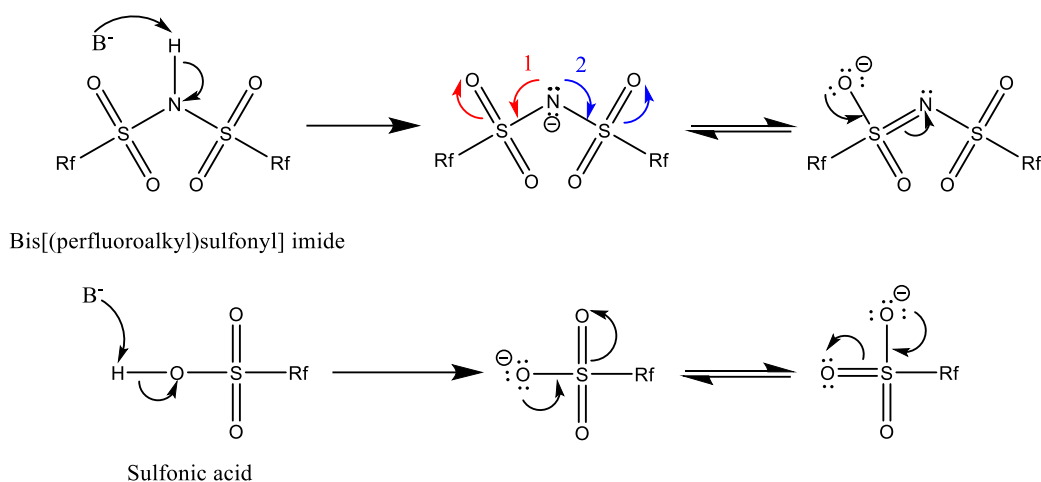


Figure 11. Comparison of sulfonic & bis[(perfluoroalkyl)sulfonyl] imide functional groups

Aim 1: Diazonium N-bis[(perfluoroalkyl) benzenesulfonyl] imide (PFSI) Monomer

The purpose of this research was the total synthesis of a zwitterionic diazonium N-bis[(perfluoroalkyl) benzenesulfonyl] imide monomer (Figure 12). This monomer was designed with a diazonium group to allow chemical grafting onto the carbon support layer of the hydrogen fuel cell, and a bis-sulfonyl imide group that imparts super-acidic proton conductivity. The polymerization of this monomer yields perfluorocyclobutyl (PFCB) polymers that are known for easier polymerization compared to traditional PFSA polymers. This synthesis was designed with nine total steps (Figure 13). The reactions are as follows: 1.) fluoroalkylation (product I), O-acetylation (product II), synthesis of 4-chlorosulfonyl phenyl acetate (product III), the coupling reaction of products (I) & (III) to yield product (IV), O-deacetylation (product V), a second fluoroalkylation reaction (product VI), debromination (product VII), nitration (product VIII), and diazotization reaction to yield the final product (IX).

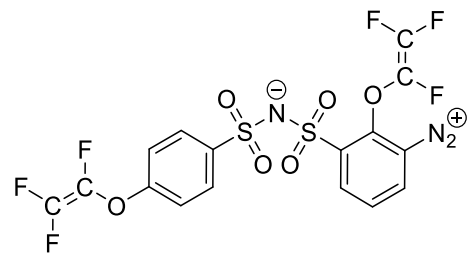


Figure 12. Targeted monomer structure

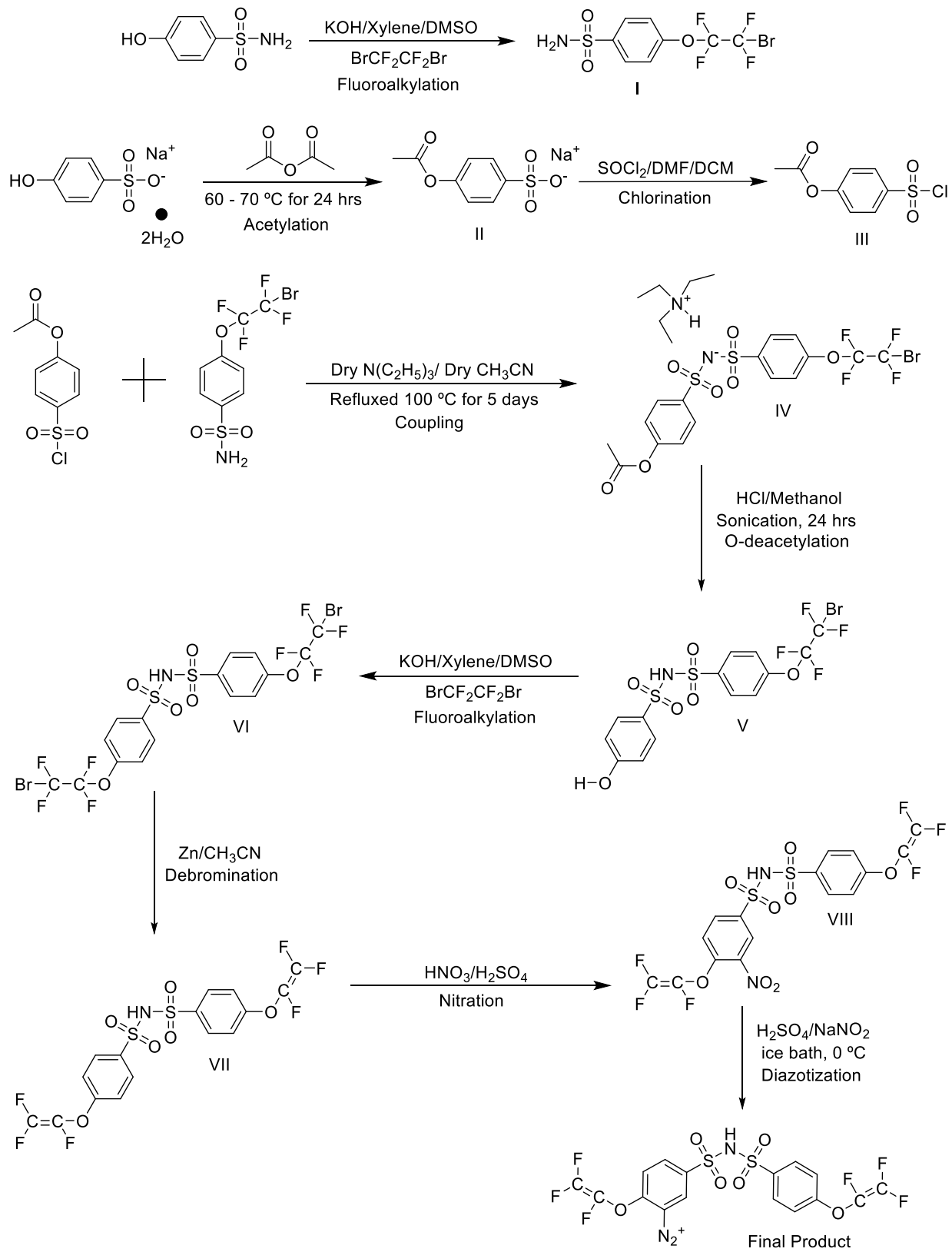


Figure 13. Synthesis plan for target monomer

Aim 2: Methodology study for the homo-polymerization of perfluoro 3-(oxapent-4-ene) sulfonyl fluoride

The purpose of this research was to design and execute a methodology study for the homo-polymerization of the perfluoro 3-(oxapent-4-ene) sulfonyl fluoride monomer (step II in Figure 15). Later research will focus on the chemical modification of this polymer (Figure 14) to incorporate bis-sulfonyl imide and diazonium functionality. However, before proceeding with the synthesis of the modified polymer, a Mw of $\geq 10,000$ Da should be achieved with the initial homopolymerization. To accomplish this, a test series of six polymerizations was devised in which the length of reaction time, amount of monomer, the weight percent of initiator, reactor pressure, temperature, and solvent were systematically varied to determine optimal reaction conditions (Table 2).

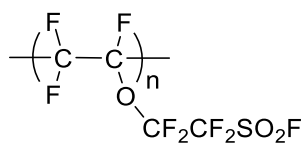


Figure 14. Target polymer

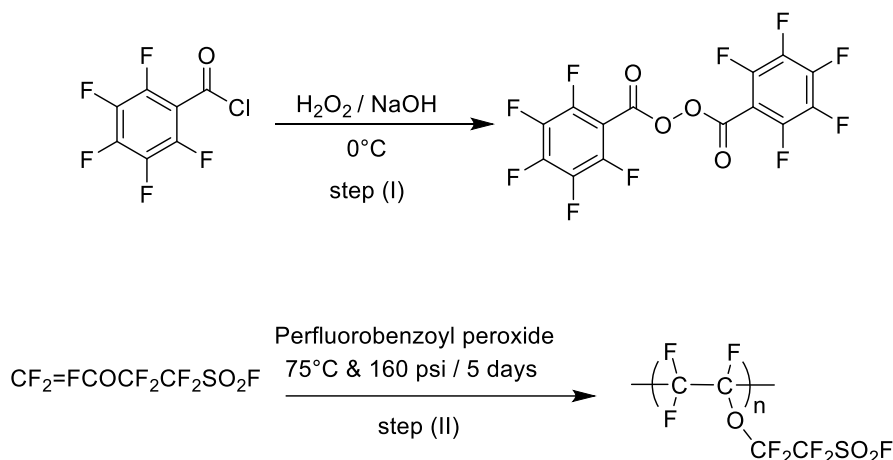


Figure 15. Synthesis plan for target polymer

Table 2. Test Plan for Homo-Polymerization Methodology Study

	Temperature (°C)	Pressure (psi)	Monomer (g)	Initiator (wt % monomer)
Polymerization 1	110	200	2	2
Polymerization 2	75	150	2	2
Polymerization 3	75	150	2	1
Polymerization 4	120	200	2	2
Polymerization 5	150	150	2	2
Polymerization 6	100	150	5	2

CHAPTER 2. RESULTS AND DISCUSSION

Synthesis of 4-(2-bromotetrafluoroethoxy)-benzenesulfonyl amide

4-(2-bromotetrafluoroethoxy)-benzenesulfonyl amide was synthesized by reacting 4-hydroxybenzenesulfonamide with 1,2-dibromotetrafluoroethane in dimethylsulfoxide (DMSO) under N₂ gas protection. Figure 16 shows a summary of the reaction.

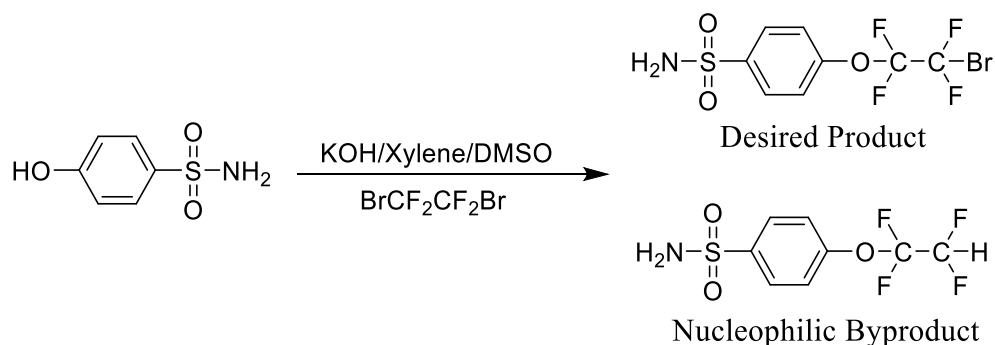


Figure 16. Fluoroalkylation reaction.^{29, 30}

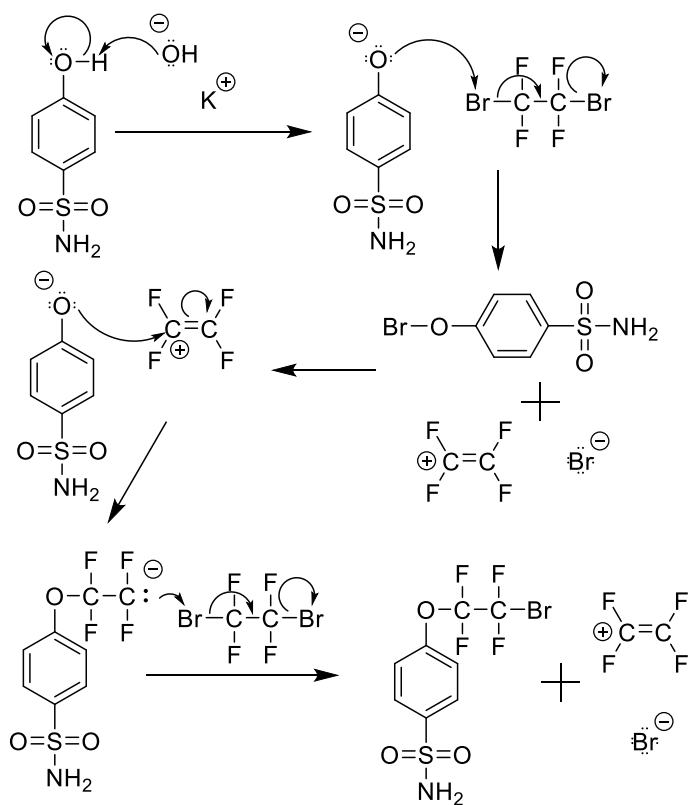
In the first stage of this reaction, KOH acted as a base to deprotonate the hydroxyl proton on the 4-hydroxybenzenesulfonamide. Before the 1,2-dibromotetrafluoroethane was added to the flask, a distillation was performed in which the water formed from the first step was evaporated from the reaction mixture, the xylene azeotropes with water. After the addition of 1,2-dibromotetrafluoroethane to the anhydrous reaction conditions, it took five days to complete the fluoroalkylation. The reaction is thought to proceed through an ionic chain mechanism (Scheme 2).²⁹ The 21.2% yield obtained after liquid-liquid extraction is considered quite low for this reaction. A decent amount of yield could have been lost during the liquid-liquid extraction purification step. DMSO has a relatively high boiling point and separating it from other components in the reaction proved difficult. The crude fluoroalkylation product was placed on ice to freeze the DMSO and lower its solubility in organic solvent. Dichloromethane (1.325

g/mL) was then used to extract the product from the DMSO (1.1 g/mL). However, some of the product could have remained soluble in the inorganic layer with trace amounts of DMSO and avoided collection during the multiple rinse and extraction steps.

When completely anhydrous conditions are not achieved, even trace amounts of moisture can cause a nucleophilic byproduct to be formed where the bromine of the bromotetrafluoroethoxy- group (-OCF₂CF₂Br) is replaced by hydrogen. ¹H NMR (Appendix A1) of the product shows three chemical shifts at 8.03, 7.54, and 6.87 ppm corresponding to the sulfonyl amide protons (-NH₂), and the two sets of aromatic protons (1, 2). However, the ¹⁹F NMR (Appendix A2) shows two sets of peaks which are assigned to the CF₂-Br (-69.27 ppm) and O-CF₂ (-85.52 ppm) fluorine of the desired product as well as the CF₂-H (-88.00 ppm) and O-CF₂ (-137.82 ppm) of the nucleophilic byproduct. The FT-IR (Appendix A3) spectrum for the 4-(2-bromotetrafluoroethoxy)-benzenesulfonyl amide product shows a medium absorption band for the sulfonamide (NH₂) function group at 3360 and 3267 cm⁻¹. The very weak sp² C-H stretching shows absorption bands around 2900 cm⁻¹. Additionally, weak C=C aromatic stretching can be seen at 1589 cm⁻¹. The S=O stretch from the sulfonamide group has strong absorption bands that appear at 1327 and 1149 cm⁻¹. The CF₂ shift range falls between 1000 and 1361 cm⁻¹; the peaks at 1188 and 1095 cm⁻¹ belong to this category.

Scheme 2 highlights the reaction mechanism that begins with deprotonation of the para-hydroxyl group by potassium hydroxide. This phenoxide anion then proceeds to initiate the anionic chain mechanism by extracting a bromine from 1,2-dibromotetrafluoroethane. The second bromine on the same molecule is ejected leaving behind a tetrafluoroethene cation. A second phenoxide molecule comes behind and attacks the tetrafluoroethene cation and the former pi-bond transitions to a lone pair on the terminal CF₂ carbon. With this intermediate, both the

nucleophilic byproduct and the desired product are formed. If water is present, then the lone pair will deprotonate water to yield the byproduct. If conditions are anhydrous enough, a second molecule of 1,2-dibromotetrafluoroethane will be attacked by the lone pair on CF_2 . A bromine is extracted, and a bromine is expelled. This leaves behind a second molecule of the tetrafluoroethene cation which is free to continue this reaction with another phenoxide anion.



Scheme 2. Fluoroalkylation Reaction Mechanism.^{29, 30}

Synthesis of 4-acetoxybenzenesulfonic acid sodium salt

The synthesis of 4-acetoxybenzenesulfonic acid sodium salt required the overnight reaction of 4-hydroxybenzenesulfonate dihydrate with acetic anhydride. Figure 17 shows a summary of the reaction.

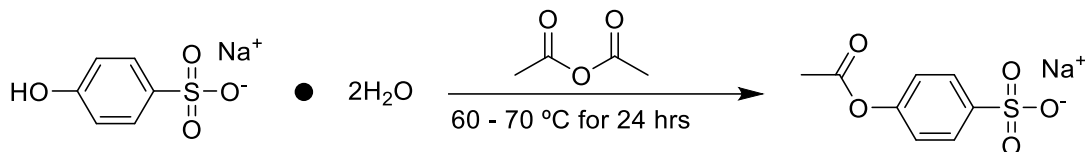


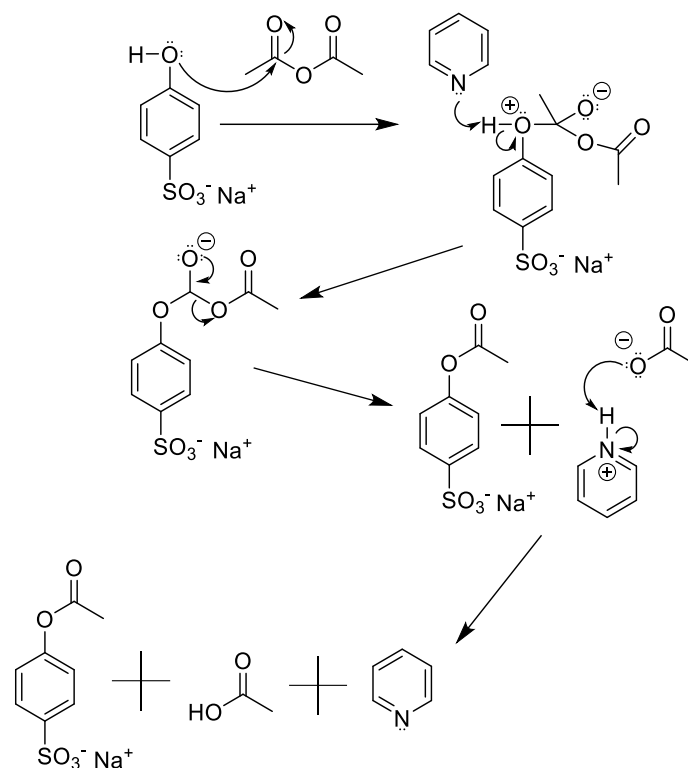
Figure 17. Acetylation of 4-hydroxybenzenesulfonic acid sodium salt.³⁰

Reaction progress can be monitored with TLC. However, we elected to skip this step after a 24-hour reaction time and move directly to the purification steps. Due to the very basic conditions of the coupling reaction in the synthesis plan, it becomes necessary to protect the hydroxyl group of the 4-hydroxybenzenesulfonate dihydrate with an acetyl group to prevent deprotonation. Deprotonation would create an alkoxide anion that could function as a nucleophile and react with the chlorosulfonyl groups on other 4-(chlorosulfonyl) phenyl acetate molecules. The second purification step required suspending the crude product in ethyl acetate with stirring while heating. This was necessary to remove any trace amounts of acetic anhydride in the product after the co-evaporation steps with toluene. The purity and structure of the compound was assessed with ¹H NMR. The yield for this reaction was 83.7 %, which is comparable to the reported literature value of 80.0 %.³¹

The proton NMR (Appendix B1) of the final product shows three distinct sets of peaks. The two doublets at 7.94 and 7.33 ppm are associated with the aromatic protons. Whereas the tall singlet at 2.41 ppm belongs to the (-CH₃) of the newly attached acetyl group. The carbon-13

NMR (Appendix B2) was run without proton decoupling. Therefore, the three peaks each with an approximate integration of 1.0 with chemical shifts at 172 (A), 152 (B), and 140 (C) ppm belong to the carbonyl carbon, the C-O bonded carbon of the aromatic ring, and the S-O bonded carbon of the aromatic ring, respectively. The doublets at 127 (D) and 122 (E) ppm belong to the aromatic carbons. The upfield quartet at 20.6 (F) ppm belongs to the (-CH₃) carbon of the acetate group, the quartet is a result of splitting by the three hydrogens attached to the carbon. The IR spectrum (Appendix B3) for this product produced the typical weak aromatic sp² C-H stretching around 2900 cm⁻¹. Additionally, the medium C=O absorption band from the carbonyl group on the acetyl group can be seen at 1747 cm⁻¹, and very weak band at 1589 cm⁻¹ can be attributed to the C=C aromatic stretching. The two strongest peaks on this spectrum at 1219 cm⁻¹ and 1180 cm⁻¹ are attributed to the S=O stretching of the sulfonic acid group and the C-O stretching, respectively.

This reaction proceeds through a nucleophilic addition/elimination reaction as shown in scheme 3. The mechanism begins with a nucleophilic attack of the hydroxyl group on one of carbonyl carbons of the acetic anhydride. Pyridine is utilized as the catalyst, which deprotonates the hydroxyl group alleviating the positive charge on that oxygen. The electrons giving rise to the negative charge on the oxygen of the acetic anhydride return to their original position as a pi-bond. This kicks off an acetate anion as a leaving group; the result is formation of an acetate protecting group on the former hydroxide group. The acetate anion and the protonated pyridine cation are in an acid-base equilibrium with one another.



Scheme 3. Acetylation Reaction Mechanism of 4-hydroxybenzenesulfonic acid sodium salt.³¹⁻³³

Synthesis of 4-(chlorosulfonyl) phenyl acetate

The purpose for the synthesis of 4-(chlorosulfonyl) phenyl acetate was to replace the sodium salt of the 4-acetoxybenzenesulfonic acid sodium salt compound with a chlorine atom. In the following step of the synthesis plan, the 4-(2-bromotetrafluoroethoxy)-benzenesulfonyl amide compound from step (I) needs to be coupled (step (IV)) with the product of this reaction. By attaching a chloride to the sulfonyl group, this creates a good leaving group for the nucleophilic addition-elimination reaction taking place in step (IV) of the synthesis plan. Figure 18 shows a summary of the reaction.

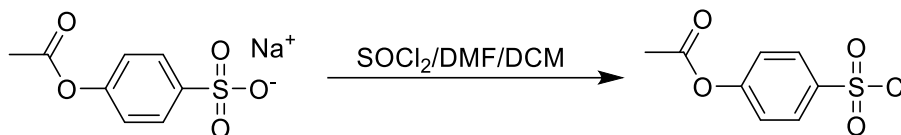


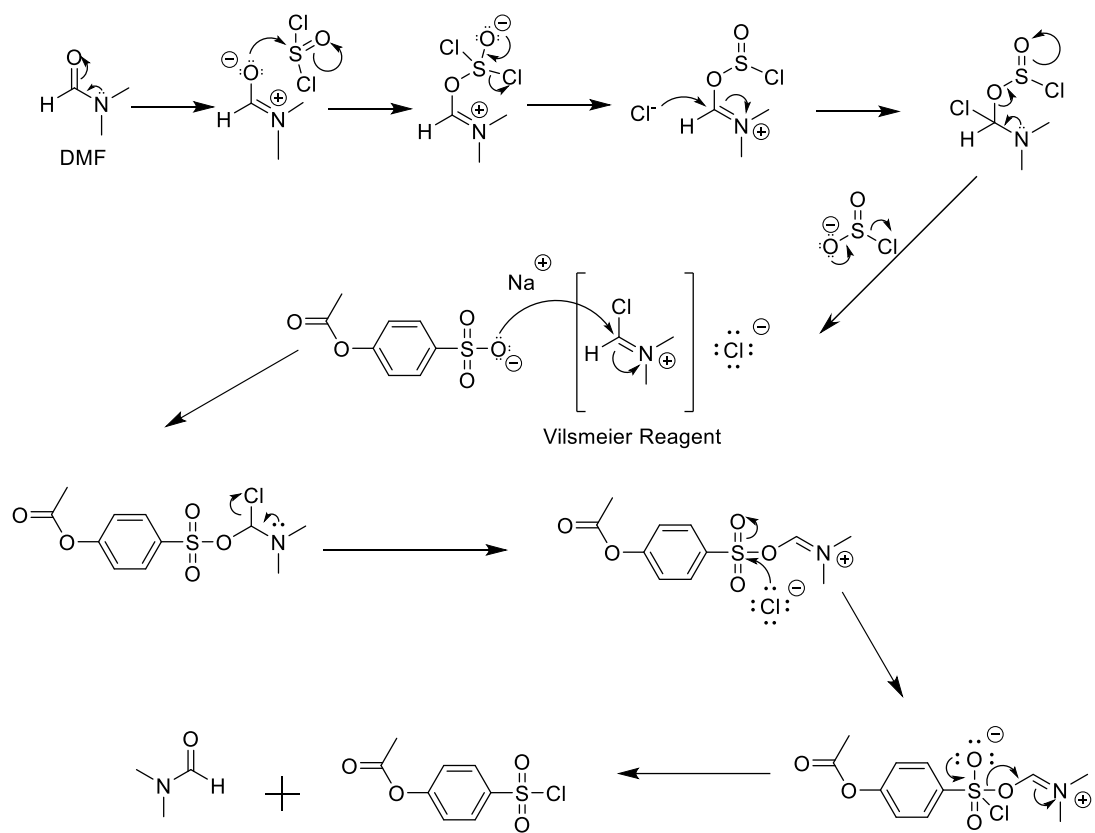
Figure 18. Chlorination of 4-acetoxybenzenesulfonic acid sodium salt.

After synthesis, two co-evaporations of the crude product with toluene were carried out to remove any unreacted thionyl chloride/dimethylformamide (DMF). The dichloromethane was used to perform a solid-liquid extraction. The 4-(chlorosulfonyl) phenyl acetate product was extracted with dichloromethane from starting material 4-chlorosulfonic acid sodium salt solid. A two-solvent (hexane and dichloromethane) room temperature recrystallization was then utilized to obtain the pure 4-(chlorosulfonyl) phenyl acetate product. The “insoluble solvent” hexanes were added to the reduced dichloromethane filtrate, until the product precipitated out of solution. A yield of 81.6 % was obtained for this reaction.

The ^1H NMR (Appendix C1) for the final product exhibited three distinct peaks. At 8.20 and 7.59 ppm there are two doublets that represent the aromatic protons of the benzene ring. The tall singlet at 2.35 ppm that integrates to three protons belongs to the (-CH₃) group of the acetyl group. The IR spectrum (Appendix C2) for the same compound produced the typical weak aromatic sp² C-H stretching around 3000 cm⁻¹. The C=C stretching from the benzene ring shows a weak absorption band around 1585 cm⁻¹. Additionally, a medium absorption band can be seen at 1759 cm⁻¹, belonging to the C=O stretch of the carbonyl bond. The strong peaks at 1377 and 1199 cm⁻¹ belong to the S=O stretching of the sulfonyl chloride. Lastly, the C-O stretch causes the strong absorption band at 1161 cm⁻¹. The gas chromatogram (Appendix C3) shows three peaks in total for this compound. The peak at 4.10 minutes belongs to the solvent, the peak at 10.21 minutes is most likely an impurity, and the peak at 10.58 minutes belongs to the 4-

(chlorosulfonyl) phenyl acetate product ($M_w = 234.66$ g/mol). From the mass spectroscopy spectrum (Appendix C3), the parent/molecular ion peak is visible at 234 m/z and the base peak at 43 m/z. The 4-(chlorosulfonyl) phenyl acetate appears to have a small amount of impurity present in the mixture.

When thionyl chloride is used with catalytic amounts of DMF, an electrophilic chloroiminium cation known as the Vilsmeier reagent is formed (Scheme 4).³⁴⁻³⁸ To form the Vilsmeier reagent, DMF transitions to a zwitterionic resonance species that performs a nucleophilic attack on the sulfur center of thionyl chloride. As this intermediate breaks down, a chlorine anion is kicked off as a leaving group. This anion then performs a nucleophilic attack on the iminium carbon alleviating the positive charge on the nitrogen. The lone pair on the nitrogen then reforms the same resonance structure that kicks SO_2Cl off as a leaving group. The SO_2Cl is an unstable molecule that quickly devolves into SO_2 and Cl^- . The chlorine anion now serves as a counterion to the newly formed iminium intermediate also known as the Vilsmeier reagent. The charged oxygen of the sulfonic acid group conducts a nucleophilic attack on the iminium carbon of the Vilsmeier reagent alleviating the positive charge on the nitrogen. Next, the iminium cation reforms kicking a chlorine anion off as a leaving group. In the following step a chlorine anion performs a nucleophilic addition in which DMF is regenerated and the sulfonyl chloride product is formed.



Scheme 4. Reaction Mechanism of Vilsmeier Reagent with 4-Acetoxybenzenesulfonic acid.³⁴⁻³⁸

Coupling reaction of 4-(2-bromotetrafluoroethoxy)-benzenesulfonyl amide with 4-chlorosulfonyl phenyl acetate

The purpose of this reaction was to couple the 4-(2-bromotetrafluoroethoxy)-benzenesulfonyl amide product from step (I) with the 4-chlorosulfonyl phenyl acetate synthesized in step (III). Figure 19 shows a summary of the reaction.

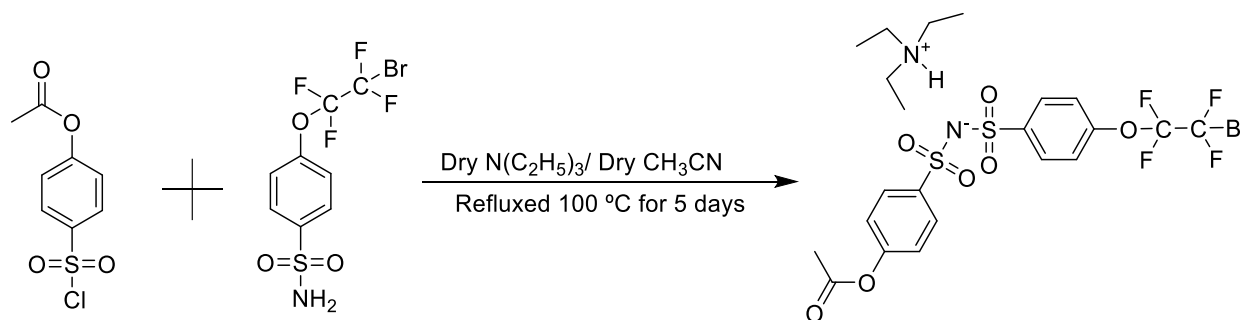
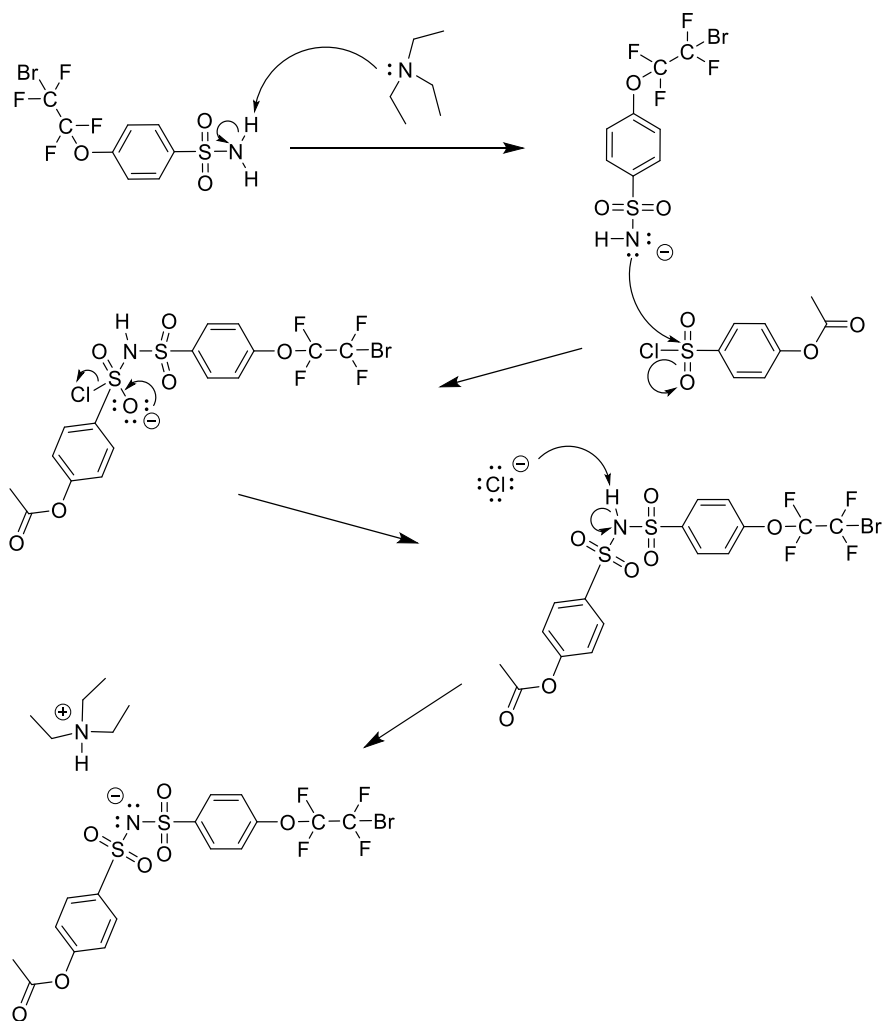


Figure 19. Coupling reaction.

The reaction was carried out in acetonitrile with triethylamine as the catalyst under anhydrous conditions to avoid any nucleophilic byproducts. The reaction was stopped after refluxing at 100 °C for five days and a ¹⁹F NMR was ran on the crude product mixture to assess the status of the reaction. It appears some unreacted 4-(2-bromotetrafluoroethoxy)-benzenesulfonyl amide, the coupling product of the benzenesulfonyl amide nucleophilic byproduct with 4-chlorosulfonyl phenyl acetate, and the coupling product of 4-(2-bromotetrafluoroethoxy)-benzenesulfonyl amide with 4-chlorosulfonyl phenyl acetate are present in the reaction mixture. According to the ¹⁹F NMR spectrum (Appendix D1), the reaction did not complete after 5 days. Comparing the ¹⁹F NMR spectrum of the fluoroalkylation product (Appendix A2) with the ¹⁹F NMR spectrum of the crude coupling product (Appendix D1) leads to speculation that only a small percentage of the desired coupling product was formed. The

chemical shifts at -88.03 and -137.6 ppm (Appendix D1) are assigned to the (-CF₂-CF₂-H) group of the nucleophilic coupling byproduct. This is synonymous with the chemical shifts at -88.00 and -137.8 ppm of the original benzenesulfonyl amide nucleophilic byproduct (Appendix A2). The peaks at -69.11 and -75.93 ppm (Appendix D1) belong to unreacted 4-(2-bromotetrafluoroethoxy)-benzenesulfonyl amide. The peaks at -75.29 and -85.54 ppm (Appendix D1) are suspected to be from the desired coupling product of 4-(2-bromotetrafluoroethoxy)-benzenesulfonyl amide with 4-chlorosulfonyl phenyl acetate.

The proposed reaction mechanism for the coupling reaction (Scheme 5) begins with triethylamine deprotonating the sulfonyl amide group. The negatively charged amide then proceeds with a nucleophilic attack on the sulfonyl chloride group forming the bis-sulfonyl amide compound. A chlorine anion is eliminated and in the next step deprotonated the bis-sulfonyl amide leaving it negatively charged. The protonated triethylamine then forms an amine salt with the bis-sulfonyl amide anion.



Scheme 5. Coupling Reaction Mechanism.³⁹

This synthesis is typically complete after a five-day reaction period. However, from the ^{19}F NMR data it appears as if the reaction required more time. The unusually slow reaction of 4-(2-bromotetrafluoroethoxy)-benzenesulfonyl amide with 4-chlorosulfonyl phenyl acetate could be due to the electron withdrawing group on the benzenesulfonyl amide reactant. The bromotetrafluoroethoxy is a strong electron withdrawing group that can slow the nucleophilic addition reaction of the sulfonyl amide group with the sulfonyl chloride moiety. Since the reaction was not complete, TLC data was inconclusive and none of the attempted mobile phase solvents (Table 3) provided good separation of the components. This is most likely due to too

many components present in the crude product to achieve a separation of ≥ 0.30 between all the compounds. For future syntheses of 4-(2-bromotetrafluoroethoxy)-benzenesulfonyl amide, it would be advantageous to perform a separation of the nucleophilic byproduct from the desired fluoroalkylation product before use in the coupling reaction. This would essentially eliminate the fluoroalkylation nucleophilic byproduct from the coupling reaction. Therefore, a TLC mobile phase solvent would only need to be developed for separating unreacted 4-(2-bromotetrafluoroethoxy)-benzenesulfonyl amide from its coupling product with 4-chlorosulfonyl phenyl acetate.

Synthesis of perfluorobenzoyl peroxide [(2,3,4,5,6-pentafluorobenzoyl) 2,3,4,5,6-pentafluorobenzenecarboperoxoate]

Perfluorobenzoyl peroxide [(2,3,4,5,6-pentafluorobenzoyl) 2,3,4,5,6-pentafluorobenzenecarboperoxoate] has been reported in literature to successfully initiate the free-radical polymerization of monomers very similar in structure to the perfluoro 3(oxapent-4-ene) sulfonyl fluoride monomer.⁴⁰ Therefore, this compound was utilized in the polymerization methodology study laid out in Table 2 of the previous chapter. Figure 20 shows a summary of the initiator synthesis.

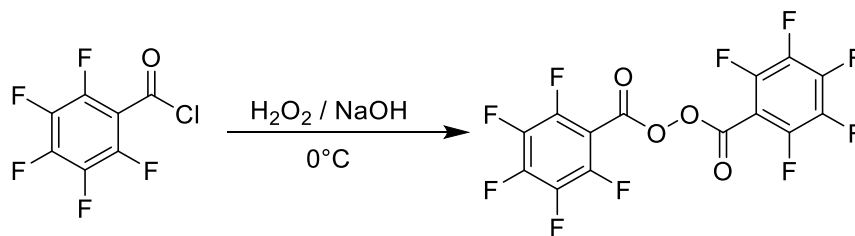
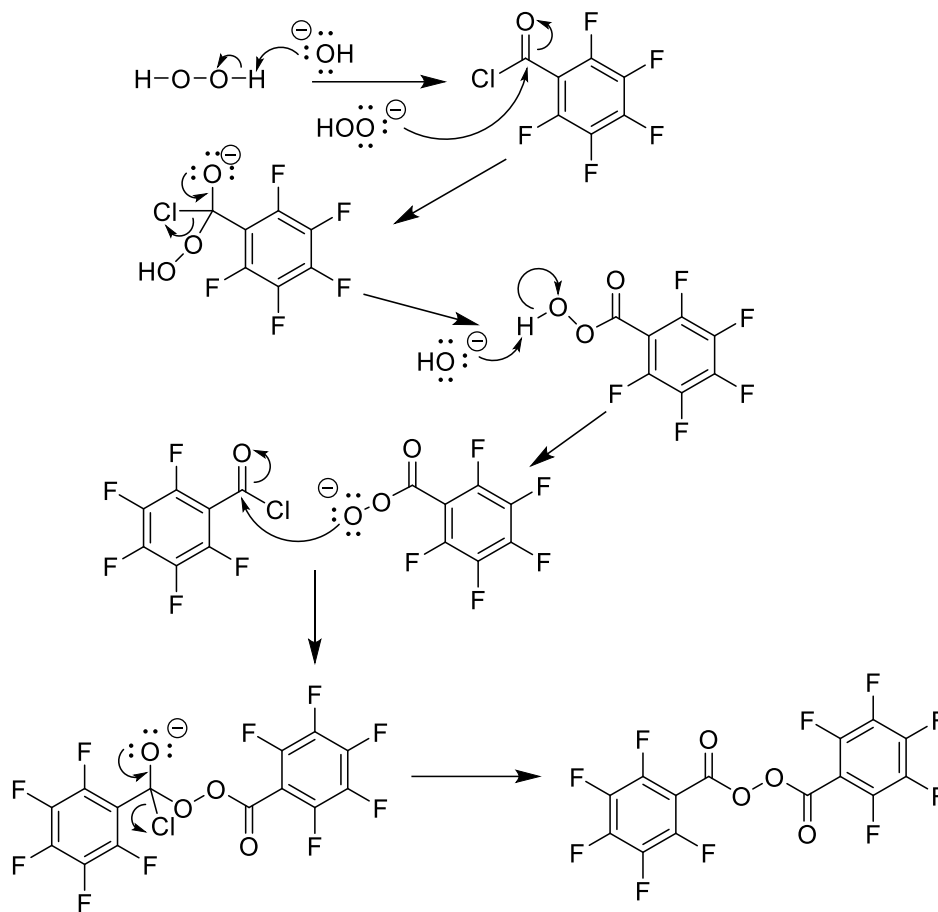


Figure 20. Perfluorobenzoyl peroxide initiator synthesis

This peroxide is suspected of being more miscible with the monomer as opposed to a non-fluorinated organic peroxide. The synthesis begins with the deprotonation of hydrogen peroxide (H_2O_2) by sodium hydroxide (NaOH). Most common laboratory reactions are exothermic and evolve heat as the reaction progresses to completion. Peroxides are generally heat sensitive, and if the reaction were to become too hot, the H_2O_2 could decompose to H_2O and O_2 . Therefore, the synthesis was conducted in an ice bath. Similarly, pentafluorobenzoyl chloride was added slowly over the course of 10 – 15 minutes to the reaction mixture to ensure that the heat of reaction was carefully controlled. Chloroform and methanol were used in a 1:2 ratio respectively for the re-crystallization of the initiator from the crude product. Chloroform was used first since pentafluorobenzoyl peroxide has good solubility in this solvent. However, the initiator peroxide is only slightly miscible in the methanol and induces crystallization upon addition. This compound had a measured melting point of 78.8 – 79.9 °C and around a 56 % yield which is comparable to the reported literature value of 78 – 79 °C and 60 % yield.⁴⁰⁻⁴¹ The ^{19}F NMR (Appendix E1) for the synthesized compound exhibits chemical shifts at -136.6 (4F), -146.2 (2F), and -160.4 (4F) ppm (2:1:2 integration ratio) belonging to the ortho, para, and meta fluorine, respectively. The FT-IR spectrum (Appendix E2) shows the typical C=O stretching at 1786 cm^{-1} and C=C stretching at 1651 cm^{-1} . The C-O stretch in this spectrum is quite weak but does appear at 1057 cm^{-1} . The C-F aromatic stretching has a strong absorption band at 1157 cm^{-1} and C-F stretch has peaks at 991, 910, and 806 cm^{-1} . The reaction mechanism for this reaction (Scheme 6) begins with the deprotonation of hydrogen peroxide by NaOH . The peroxy-anion performs a nucleophilic addition-elimination reaction on the pentafluorobenzoyl chloride with a chloride anion as the leaving group. The resulting hydro-peroxide is then deprotonated by

NaOH. This peroxy-anion performs a nucleophilic addition-elimination reaction on a second molecule of pentafluorobenzoyl chloride forming the final product.



Scheme 6. Perfluorobenzoyl Peroxide Initiator Synthesis Reaction Mechanism.⁴²

Homo-polymerization of Perfluoro 3(oxapent-4-ene) sulfonyl fluoride

This methodology study was designed to determine the optimal combination of pressure, weight percent of initiator, and temperature needed to yield a high molecular weight polymer (> 10,000 Da) with the perfluoro 3(oxapent-4-ene) sulfonyl fluoride monomer. Figure 21 shows a summary of the polymerization reaction.

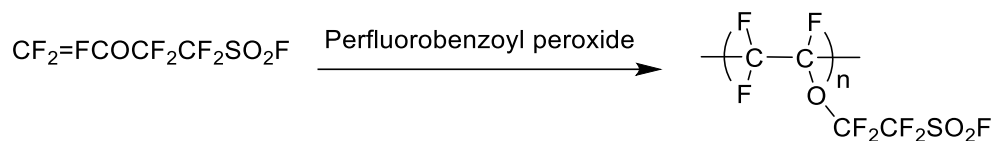


Figure 21. Polymerization of perfluoro 3(oxapent-4-ene) sulfonyl fluoride

To determine the relative extent of polymerization, a vinyl end NMR calculation was used on the ^{19}F NMR spectra.⁴³ This calculation is the arithmetic average of the three vinyl end fluorine molecules of the polymer product. According to this calculation, Polymerization 6 (Table 3) was suspected to have the highest molecular weight. The higher the ratio (vinylic fluorine ^{19}F integration values to number of vinylic fluorine on polymer backbone), the greater the extent of polymerization. The ^{19}F NMR of the unreacted monomer (Appendices F1 & F2) has a chemical shift at 45.7 (A) ppm corresponding to the sulfonyl fluoride at the end of the ether pendant side chain of the fluoroethylene backbone. The peaks at -83.0 (B) and -111.2 (C) ppm belong to the two respective (-CF₂) groups on the ether side chain. The peaks at -111.6 (D), -120 (E), and -136 (F) ppm belong the vinylic fluorine. From a comparison of the ^{19}F NMR monomer spectrum with the six ^{19}F NMR spectra (Appendices G1, H1, I1, J1, K1, & L1) from the polymerization products, it is evident that a distinct broadening of the peaks occurs as well as a general distortion of the ^{19}F NMR baseline. This is of course only a qualitative characteristic of the spectra which is why the vinyl fluorine end group calculation is utilized to get some

quantitative sense for the extent of polymerization. Polymerizations 1, 2, 3, 4, 5, and 6 have yields of 26.9, 44.9, 35.9, 11.6, 16.6, and 33.1% respectively. The reported literature yield for this type of reaction was approximately 30 - 50%.⁴⁰

The mechanism of polymerization (Scheme 7) begins with the heat induced heterolytic peroxide bond cleavage of pentafluorobenzoyl peroxide to create two primary radicals in a process known as initiation. A primary radical then facilitates the heterolytic bond cleavage of a monomer molecule to create a secondary radical. This secondary radical then goes on to bond with another monomer molecule in a free radical chain reaction known as propagation. To build high molecular weight polymers, propagation should occur until all the monomer in the reaction is consumed. At the end of a growing chain, either bimolecular or primary termination describes the event that ends propagation. Bimolecular termination is when a growing polymer chain binds with another growing polymer chain. This type of termination is ideal for creating higher molecular weight polymers. Primary termination is when a primary radical binds with a growing chain. Primary termination typically leads to lower molecular weight polymer species (e.g., dimers, trimers, oligomers).

CHAPTER 3. EXPERIMENTAL

General Considerations

NMR Spectroscopy

All proton and fluorine nuclear magnetic resonance (NMR) spectra were generated with a Jeol JNM-ECP-ECP 400 MHz Fourier-Transform NMR spectrometer. The chemical shifts were measured on a scale of parts per million (ppm) using high-frequency position conversion. Coupling constants are referred to as J values with units of Hertz (Hz). The resonance splitting patterns are labeled as singlet (s), doublet (d), triplet (t), quartet (q), and multiplet (m). All NMR samples were prepared with a concentration of 1-2 mmol sample per liter of deuterated solvent. For ^1H NMR, the standardized reference material used was tetramethyl silane (TMS), for ^{19}F NMR, trichlorofluoromethane (CFCl_3) gas.

Gas Chromatography-Mass Spectroscopy

All gas chromatography-mass spectroscopy (GC-MS) samples were prepared with a concentration of 1 mg sample per 1 mL acetone and analyzed on a Shimadzu GCMS-QP2010 Plus Instrument.

Infrared Spectroscopy

All infrared spectra were generated using a Shimadzu IR Prestige-21FTIR Instrument. Compounds were analyzed by placing just enough finely powdered sample to cover the lens of the attenuated total internal reflectance accessory. An instrument scan from 4000 cm^{-1} to 450 cm^{-1} was then performed. Each peak of interest on the IR-spectra corresponds to a wavelength (cm^{-1})

and a subjective description of peak intensity such as very strong (vs), strong (s), medium (m), weak (w), and very weak (vw).

Gel Permeation Chromatography

All gel permeation chromatography were generated using one of the following setups. The first consists of an EcoSEC GPC system from TOSOH. This column set consists of the following three columns: two Tosoh TSKgel SuperMultiporeHZ-M; 4.6×150 mm; 4 μm; and a TSKgel SuperMultiporeHZ-M guard. The operating flow rate was set to 0.35 ml/min for both the reference cell and the sample cell. The column temperature and detector temperature were set at 40 °C and the sample injection volume was 10 uL. Polymer solutions were prepared in THF to make a final concentration of about 1.5 mg/mL. The samples were dissolved and filtered through a 0.2 μm pore size PTFE filters into autosampler vials. The second setup consists of a Polymer Laboratories 5 μm HFIPgel, Guard + HFIPgel Mixed column setup. The flow rate was set to 1.0 mL/min and the column temperature/detector temperature were set at 45 °C. Sample injection volume was 50 μL, and samples were prepared in HFIP to make a final concentration of 1.0 – 2.0 mg/mL.

Souza-Design Dual Manifold High Vacuum Line System

Many processes throughout this work such as low-pressure distillation and drying of reagents were conducted using a dual manifold glass high vacuum line such as the one shown in Figure 22. One of the manifolds was used exclusively as the vacuum line; the other to push gas through a reaction vessel. This system utilizes Teflon™/polytetrafluoroethylene (PTFE) high vacuum stopcocks to start/stop the flow of gases/pressure in and out of the apparatus. The device also contains a liquid nitrogen trap that condenses corrosive or volatile vapors attempting to

escape the device and enter the diffusion pump. Additionally, the device contains a mechanical Welch vacuum pump used to reach the desired dynamic vacuum range of 10^{-4} to 10^{-7} torr, and a built-in separation system.

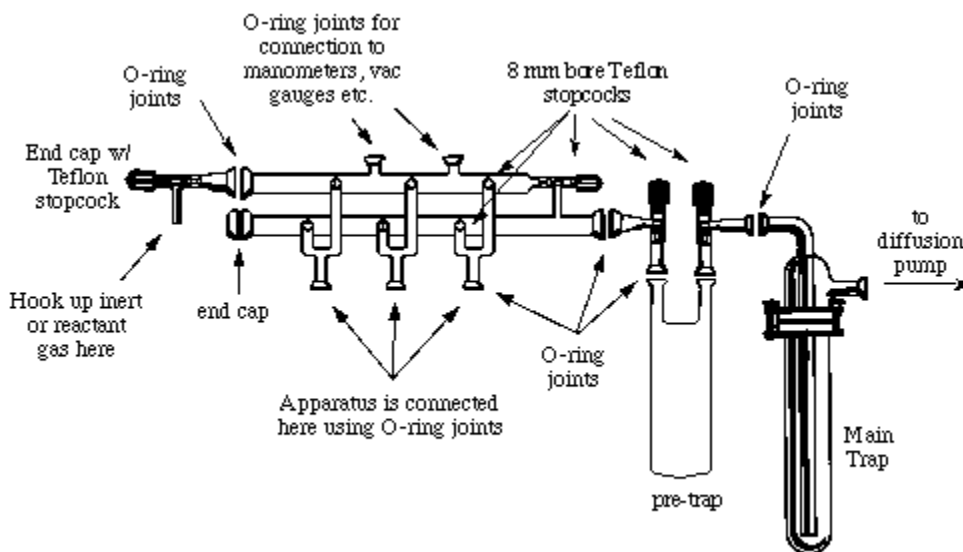


Figure 22. Souza-design dual manifold high vacuum glassware. Used with permission.⁴⁶

Experimental Practice

Several of the starting reagents in the following experimental procedures such as pentafluorobenzoyl peroxide (CAS# 2251-50-5), perfluoro(3-oxapent-4-ene)sulfonyl fluoride monomer (CAS# 29514-94-1), hydrogen peroxide 30% wt solution in water (CAS: 7722-84-1), 4-hydroxybenzenesulfonamide (CAS# 1576-43-8), sodium 4-hydroxybenzenesulfonate dihydrate (CAS# 10580-19-5), and acetic anhydride (CAS# 108-24-7) were purchased commercially and used per manufacturer recommendation unless advised alternatively. Hygroscopic compounds were kept in a nitrogen-purged glovebox until ready for use. Any dried reagents were done so using a Schlenk flask, the Souza-design dual manifold high vacuum system, and activated

molecular sieves. All reactions were carried out in common laboratory glassware unless stated otherwise. All thin layer chromatography was performed with silica gel 60 F₂₅₄ plates cut to 4 cm x 8 cm. A thin pencil line was drawn parallel to the 4 cm side of the plate approximately 1 cm from the bottom of the plate.

Synthesis of 4-(2-bromotetrafluoroethoxy)-benzenesulfonyl amide

For a typical procedure, in a nitrogen-purged glovebox, 3.0 g (17.32 mmol) of 4-hydroxybenzenesulfonyl amide, 1.15 g KOH (0.0205 mol), 15 mL of dried DMSO, and 1.5 mL of dried xylene was added to a 50 mL 3-neck round bottom flask with a stir bar. Rubber septa were placed on the two outside openings of the round-bottom flask. Then the flask was moved from the glovebox to a fume hood and completed a setup like Figure 23.

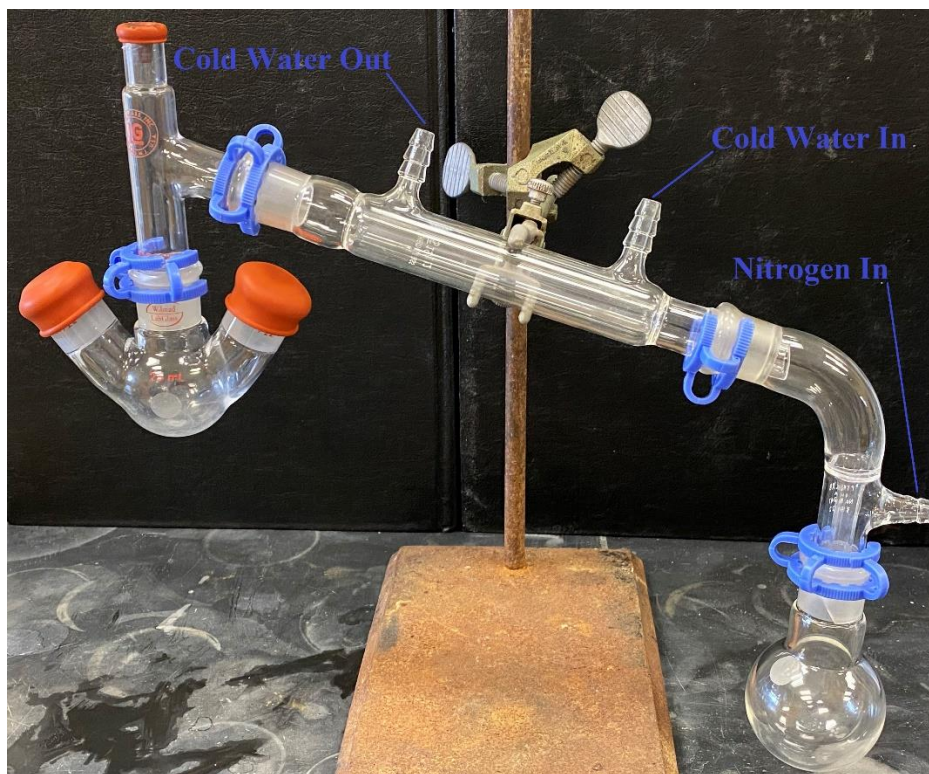
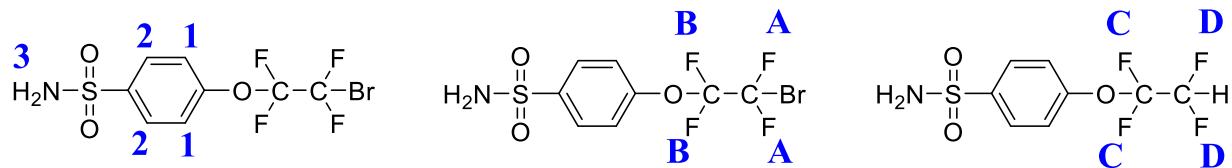


Figure 23. Fluoroalkylation reaction setup.

Care was taken to minimize time that the contents of the flask were exposed to open atmosphere. Reaction was heated to 60 °C for 10 hours under nitrogen gas protection (or overnight). The mixture was then heated to 120 °C under vacuum to distill the xylene/water azeotrope formed. After distillation was completed, the reaction temperature was re-adjusted to 35 °C with nitrogen gas protection restored. Next, 2.3 mL of dibromotetrafluoroethane (BrCF₂CF₂Br, 0.0193 mol) was added slowly to the flask. The reaction was run for seven days at 35 °C under nitrogen gas and stirring while monitoring the reaction progress with ¹⁹F NMR. Product collected included 4-(2-bromotetrafluoroethoxy)-benzenesulfonyl amide and the hydrolysis side product.

Liquid-liquid extraction & concentration of purified product

The crude fluoroalkylation product was placed in an ice bath until most of the ice melted. The product was then carefully moved to a separatory funnel. 20 mL of dichloromethane was then added to the separatory funnel; care was taken not to disturb the crude product at this point. The DMSO was frozen due to the ice bath and appeared in both the inorganic/organic layers. The organic layer (dichloromethane) was removed from the separatory funnel and placed in a second separatory funnel. The organic layer was then washed 2X's with 20 mL aliquots of ice-cold DI water. Once the majority of the DMSO was removed, the organic layer was dried over anhydrous sodium sulfate, relocated to a 100 mL round-bottom flask, and then placed on rotary evaporator (~ 40 °C) until all the volatiles were removed. The percent yield for this reaction was 21.2 %. The ratio of fluoroalkylation product to hydrolysis impurity was determined to be 4:1, respectively.



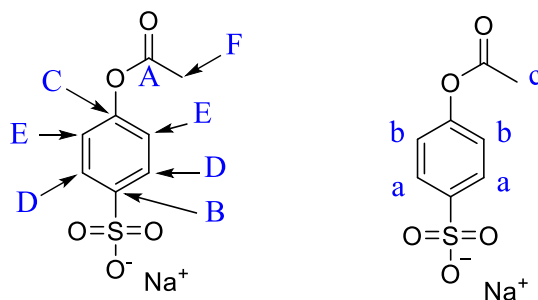
$^1\text{H NMR}$ (**A1**) (400 MHz; CD_3COCD_3): ppm δ_1 :8.03 (2H, d), δ_2 : 7.54 (2H, d), δ_3 : 6.87 (2H, s)

$^{19}\text{F NMR}$ (**A2**) (400 MHz; CD_3COCD_3): ppm δ_A : -69.27 (2F, d), δ_B : -85.52 (2F, d), δ_C : -88.0 (2F, d), δ_D : -137.8 (2F, t)

IR ($\nu_{\text{max}}/\text{cm}^{-1}$) (**A3**): 3360.00 m & 3267.41 m (N-H), 2962.66 vw, 2924.09 vw, & 2854.65 vw (sp^2 C-H), 1589.34 vw (C=C), 1327.03 s & 1149.57 vs (S=O), 1188.15 s & 1095.57 vs (C-F).

Synthesis of 4-acetoxybenzenesulfonic acid sodium salt

In a typical procedure, 2.0 g of sodium 4-hydroxybenzenesulfonate dihydrate (8.61 mmol) was added to a 50 mL round bottom flask along with a stir bar, 14 mL acetic anhydride, and 1.0 mL pyridine. The flask was fitted with a cool water condenser and heated to 60 – 70 °C overnight with stirring. Reaction progress was monitored with TLC once the mixture was cooled to room temperature. The crude product (4-acetoxy-benzenesulfonate) was then concentrated to a white solid using a rotary evaporator. The crude product was co-evaporated with 3-4, 25 mL aliquots of toluene using a rotary evaporator. The solid product was suspended in 50 mL of ethyl acetate. With stirring, this solution was heated to 80 °C with an oil bath. While still warm, the solution was poured over pre-wet vacuum filter paper to collect the solid. Additionally, the collected product was washed with another 30 – 40 mL of room temperature ethyl acetate. The percent yield for this reaction was 83.7 %.



¹H NMR (**B1**) (400 MHz; D₂O): ppm δ_a: 7.94 (2H, d), δ_b: 7.33 (2H, d), δ_c: 2.41 (3H, s)

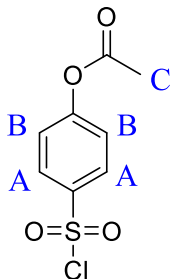
¹³C NMR (**B2**) (400 MHz; D₂O): ppm δ_A: 172.9 (1C), δ_B: 152.4 (1C), δ_C: 140.6 (1C), δ_D: 127.5 (2C) δ_E: 122.4 (2C), δ_F: 20.6 (1C)

IR (ν_{max}/cm⁻¹) (**B3**): 2924 vw & 2854 vw (sp² C-H), 1747 m (C=O), 1589 vw (C=C), 1219 s (S=O), 1180 vs (C-O).

Synthesis of 4-chlorosulfonyl phenyl acetate

In a typical procedure, 0.8 g (3.45 mmol) of 4-acetoxysulfonic acid sodium salt was suspended in 7 mL of thionyl chloride in a 50 mL round-bottom flask with a stir bar. 2-3 drops (disposable transfer pipette) of dimethylformamide (DMF) were added, and the mixture was refluxed at ~ 75 °C for 1 hour with stirring. The resulting residue was co-evaporated with two 25 mL aliquots of toluene using a rotary evaporator. The product was then suspended in 10 mL of dichloromethane and stirred at room temperature for about 30 minutes. This suspension was filtered using vacuum filtration and the filtrate collected in a separate clean round-bottom flask. The filtrate was then reduced to approximately 1/5 of its original volume using a rotary evaporator. To the reduced filtrate, hexanes (~ 8 – 15 mL) was added dropwise with stirring at room temperature until 4-chlorosulfonyl phenyl acetate precipitated out of solution. The

precipitate was collected and dried via vacuum filtration. The percent yield for this reaction was 81.6 %.



$^1\text{H NMR}$ (**C1**) (400 MHz; CD_3COCD_3): ppm- δ_{A} : 8.20 (2H, d), δ_{B} : 7.59 (2H, d), δ_{C} : 2.35 (3H, s)

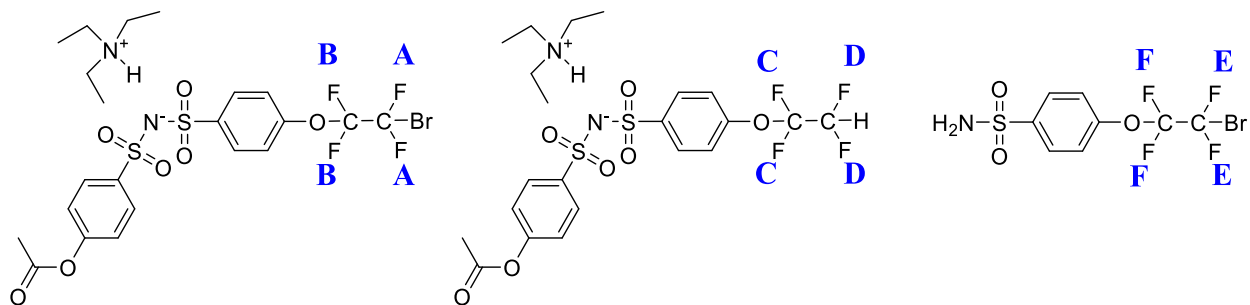
IR ($\nu_{\text{max}}/\text{cm}^{-1}$) (**C2**): 3097 vs & 3051 vs (sp^2 C-H), 1759 m (C=O), 1585 w (C=C), 1377 s & 1199 s (S=O), 1161 vs (C-O).

MS (**C3**) (M^+ , 100%): 234, 192, 157, 93, 65, 43.

Coupling Reaction of 4-chlorosulfonyl phenyl acetate with 4-(2-bromotetrafluoroethoxy)-benzenesulfonyl amide

In a typical procedure, all glassware used in this procedure was dried for 24 hours in a 200 °C oven. Additionally, 20 mL acetonitrile and 3 mL of diisopropyl ethylamine (DIEA) were dried for 24 hours over activated molecular sieves. In a dry and nitrogen purged glove box, 0.367 g (1.04 mmol) of 4-(2-bromotetrafluoroethoxy)-benzenesulfonyl amide, 0.245 g (1.04 mmol) of 4-chlorosulfonyl phenyl acetate, and a stir bar was added to a 100 mL 3-neck round-bottom flask fit with 2 rubber septa on the outside openings. 20 mL of dry acetonitrile and 3 mL of DIEA were injected into the flask under anhydrous conditions. Care was taken to minimize time that the contents of the flask were exposed to open atmosphere while transporting the reaction flask

from glove box to fume hood. The mixture was refluxed at 82 °C for 5 days with stirring under nitrogen gas protection. Separation of the crude product required the use of TLC to determine the best mobile phase solvent for purification via column chromatography.



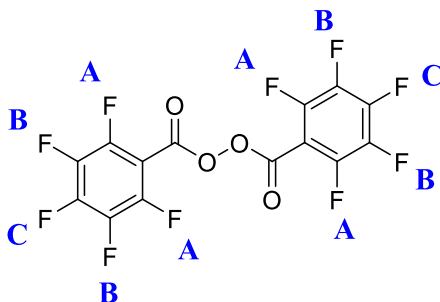
¹⁹F NMR (**D1**) (400 MHz; CD₃COCD₃) ppm- δ_A: -75.29 (2F, d), δ_B: -85.54 (2F, d), δ_C: -88.03 (2F, d), δ_D: -137.64 (2F, d), δ_E: -69.11 (2F, d), δ_F: -75.93 (2F, d)

Table 3. TLC Data for Coupling Reaction Crude Product Mixture

<u>Ratio & Solvent Blend</u>	<u>No. of spots</u>	<u>Crude Product R_f values</u>	<u>Reference material R_f value</u>
4:1, tert-butyl methyl ether (TBME):hexane	3	0.93, 0.88, 0.57	0.57
3:1, ethyl acetate (EA):hexane	2	0.86, 0.80	0.61
2:1, EA:hexane	2	0.98, 0.88	0.62
2:1, hexane:EA	2	0.58, 0.48	0.15
1:1, EA:hexane	3	0.96, 0.81, 0.76	0.23
100% hexane	1	0.06	0.06
4:1, hexane:EA	2	0.19, 0.15	0.07
3:1, methanol:hexane	1	0.88	0.87
4:1, EA:hexane	2	0.98, 0.90	0.69
3:1, EA:hexane	2	0.96, 0.90	0.69
1:1, diethyl ether:hexane	4	0.43, 0.40, 0.31, 0.09	0.12
3:1, diethyl ether:hexane	4	0.75, 0.71, 0.62, 0.33	0.33
100% TBME	2	0.98, 0.74	0.74
100% diethyl ether	1	0.82	0.54
1:1, TBME:chloroform	4	0.71, 0.67, 0.60, 0.24	0.29
3:1, dichloromethane:chloroform	3	0.39, 0.24, 0.05	0.10
1:1, Acetonitrile:water	1	0.98	0.96
dichloromethane:hexane	2	0.27, 0.16	0.06
3:1, chloroform:methanol	3	0.98, 0.89, 0.86	0.68
1:1, dichloromethane:chloroform	3	0.25, 0.18, 0.04	0.05
5:1, TBME:hexane	1	0.85	0.53
3:1, dichloromethane:hexane	3	0.48, 0.20, 0.06	0.11
5:1, dichloromethane:hexane	2	0.39, 0.26	0.07
5:1, chloroform:hexane	3	0.11, 0.05, 0.02	0.02
2:1, chloroform:hexane	3	0.09, 0.05, 0.02	0.03
5:2:1, dichloromethane:TBME:hexane	2	0.76, 0.69	0.25
1:1:1, dichloromethane:TBME:hexane	3	0.66, 0.62, 0.53	0.24
2:1:1, dichloromethane:TBME:hexane	3	0.73, 0.65, 0.11	0.2
3:3:1, chloroform:dichloromethane:methanol	2	0.76, 0.68	0.47

Synthesis of perfluorobenzoyl peroxide [(2,3,4,5,6-pentafluorobenzoyl) 2,3,4,5,6-pentafluorobenzenecarboxylate]

In a typical procedure, 5 mL of a 4 M sodium hydroxide (NaOH) solution was prepared by dissolving 0.804 g (0.0201 mol) of solid NaOH pellets in 5 mL of DI water (H₂O). Then, 0.61 mL of the 4 M NaOH and 3 mL of hydrogen peroxide (H₂O₂, 30 wt% solution in water) was placed into a clean 50 mL round-bottom flask with a stir bar. Using a dropping funnel, 0.62 mL (1 g/4.33 mmol) of perfluorobenzoyl chloride was added to the mixture over the course of 10-15 minutes while stirring the mixture over an ice bath. To maintain the alkalinity of the solution, some of the remaining 4 M NaOH was added to the reaction mixture to acquire a pH of around \approx 11 per pH paper. The reaction was refluxed for 1 hour at 0°C before the crude product was collected by vacuum filtration. In a separate clean vessel, chilled chloroform was added to the crude product until the solid just dissolved (\sim 1.5 mL). The mixture was then recrystallized with methanol (\sim 3.0 mL). A second vacuum filtration was carried out to collect the final product. The percent yield for this reaction was 55.7 %.



¹⁹F NMR (**E1**) (400 MHz; CD₃COCD₃) ppm- δ_A : -136.57 (2F, d), δ_B : -160.35 (1F, t), δ_C : -146.16 (2F, d).

Melting Point: 78.8 – 79.9 °C

IR ($\nu_{\text{max}}/\text{cm}^{-1}$) (**E2**): 1786 m (C=O), 1651 w (C=C), 1157 s (C-F aromatic), 1057 vw (C-O), 991 vs, 910 s, and 806 s (C-F).

Homo-Polymerization of perfluoro-3(oxapent-4-ene) sulfonyl fluoride Monomer

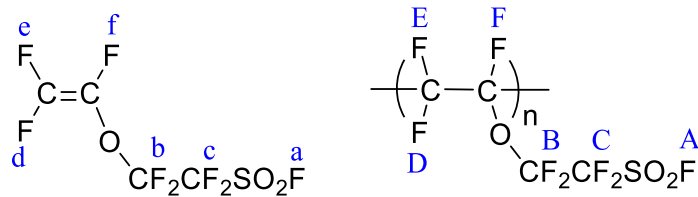
This methodology study was conducted per Table 2 outlined in Chapter 1. For each run, freshly distilled perfluoro-3(oxapent-4-ene) sulfonyl fluoride monomer, perfluorobenzoyl peroxide, and a stir bar were added to the Parr stainless steel reactor before pressurizing and heating to the indicated value. The reactor was purged three times with argon gas before pressurizing the unit for the polymerization. A Parr 45 mL 4700 pressure vessel with 4310A gage block assembly (Figure 24) was used for all six polymerization reactions along with a magnetic stir bar. If the indicated temperature for the respective run was ≤ 100 °C, then an oil bath was used to heat the reaction for the duration. However, if the specified temperature for that run was ≥ 100 °C, then a sand bath was used. All six reactions were cooked over a period of five days. After each polymerization run was completed, the crude product was placed on a Kugelrohr apparatus for 48 hours at 145 - 150 °C to remove excess monomer and initiator. ^{19}F NMR and gel permeation chromatography (GPC) were used to characterize the polymers.

Table 4. Polymerization Mw, Yield, and Vinyl end Calculation Data

Run	M _w	¹⁹ F NMR/GPC (Appendices)	Vinylic Fluorine Calculation	Polymerization Yield
Polymerization 1	600	G1 & G2	$(0.82+0.50)/3 = 0.44$	26.9%
Polymerization 2	1234	H1 & H2	$(0.61+0.26)/3 = 0.29$	44.9%
Polymerization 3	1743	I1 & I2	$(1.82+0.68)/3 = 0.83$	35.9%
Polymerization 4	428	J1 & J2	$(2.19+0.84)/3 = 1.01$	11.6%
Polymerization 5	2,303	K1 & K2	$(2.43+0.76)/3 = 1.06$	16.6%
Polymerization 6	3,735	L1 & L2	$(2.85+0.86)/3 = 1.24$	33.1%



Figure 24. Parr 45 mL 4700 pressure vessel with 4310A gage block assembly. Used with permission.⁴⁷



Monomer: ^{19}F NMR (**F1**) (400 MHz; CD_3CN) ppm- δ_a : 45.7 (1F, s), δ_b : -83.0 (2F, m), δ_c : -111.2 (2F, m), δ_d : -111.6 (1F, dd), δ_e : -120 (1F, dd), δ_f : -136 (1F, dd).

Polymerization Run #1: ^{19}F NMR (**G1**) (400 MHz; CD_3CN) ppm- δ_A : 46.1 (1F, m), δ_B : -77.1 (2F, m), δ_C : -111.1 (2F, m), δ_D : -114.8 (1F, m), δ_E : -114.8 (1F, m), δ_F : -135.6 (1F, m).

GPC (**G2**): M_w : 600 and Polydispersity index (M_w/M_n): 2.14

Polymerization Run #2: ^{19}F NMR (**H1**) (400 MHz; CD_3CN) ppm- δ_A : 46.0 (1F, m), δ_B : -77.1 (2F, m), δ_C : -111.0 (2F, m), δ_D : -114.9 (1F, m), δ_E : -114.9 (1F, m), δ_F : -135.6 (1F, m).

GPC (**H2**): M_w : 1,234 and Polydispersity index (M_w/M_n): 3.03

Polymerization Run #3: ^{19}F NMR (**I1**) (400 MHz; CD_3CN) ppm- δ_A : 46.1 (1F, m), δ_B : -76.8 (2F, m), δ_C : -111.1 (2F, m), δ_D : -115.1 (1F, m), δ_E : -115.1 (1F, m), δ_F : -136.6 (1F, m).

GPC (**I2**): M_w : 1,743 and Polydispersity index (M_w/M_n): 1.86

Polymerization Run #4: ^{19}F NMR (**J1**) (400 MHz; CD_3CN) ppm- δ_A : 46.1 (1F, m), δ_B : -77.1 (2F, m), δ_C : -111.1 (2F, m), δ_D : -115.9 (1F, m), δ_E : -115.9 (1F, m), δ_F : -135.9 (1F, m).

GPC (**J2**): M_w : 438 and Polydispersity index (M_w/M_n): 1.71

Polymerization Run #5: ^{19}F NMR (**K1**) (400 MHz; CD_3CN) ppm- δ_A : 46.0 (1F, m), δ_B : -77.0 (2F, m), δ_C : -111.0 (2F, m), δ_D : -115.5 (1F, m), δ_E : -117.6 (1F, m), δ_F : -136.5 (1F, m).

GPC (**K2**): Mw: 2,303 and Polydispersity index (Mw/Mn): 1.39

Polymerization Run #6: ^{19}F NMR (**L1**) (400 MHz; CD_3CN) ppm- δ_{A} : 46.1 (1F, m), δ_{B} : -77.2

(2F, m), δ_{C} : -110.9 (2F, m), δ_{D} : -115.5 (1F, m), δ_{E} : -117.6 (1F, m), δ_{F} : -136.3 (1F, m).

GPC (**L2**): Mw: 3,735 and Polydispersity index (Mw/Mn): 1.50

CHAPTER 4. CONCLUSIONS

For project 1, Steps I through III of the synthesis plans (Figure 13) were successfully carried out in the lab. 4-(2-bromotetrafluoroethoxy)-benzenesulfonyl amide (step I) was synthesized with a 21.2 % yield which is considered low for this reaction. A significant portion of the yield was most likely lost during the liquid-liquid extraction purification steps. 4-acetoxybenzenesulfonic acid sodium salt (step II) was synthesized with an 83.7 % yield. 4-(chlorosulfonyl) phenyl acetate (step III) was synthesized with an 81.6 % yield. The coupling reaction of 4-(2-bromotetrafluoroethoxy)-benzenesulfonyl amide product from (step I) with 4-(chlorosulfonyl) phenyl acetate synthesized (step III) was attempted but not successful. ^{19}F NMR was conducted on the crude coupling product but, it was determined that the reaction did not complete due to slow reaction kinetics and the formation of nucleophilic byproducts.

The project 2 methodology study was designed to explore the optimal conditions required to yield a polymer with a molecular weight of $\geq 10,000$ Da from the perfluoro 3(oxapent-4-ene) sulfonyl fluoride monomer. Polymerization runs 1-6 obtained yields of 26.9, 44.9, 35.9, 11.60, 16.6, and 33.1 %, respectively. Similarly, the weight average molecular weight (M_w) for polymerization runs 1-6 were 600, 1,234, 1,743, 428, 2,303, and 3,735, respectively. We are still trying to get the accurate M_w of the polymer #6 due to its solubility issues. The best results (run #6) were obtained when the reaction was carried out for five days around 100 °C at 150 psi with 2 wt % initiator, and 5 g of monomer. The significant difference in M_w between polymerization 6 and all the other polymerization runs indicate that the starting amount of the monomer (concentration) needs to be increased to build higher molecular weight polymers. Based on the results of this study it is recommended that the reaction conditions include 2 wt % initiator and remain at 100 °C and 150 psi for five days with higher concentration of monomer.

REFERENCES

1. Zhou, J.; Tao, Y.; Chen, X.; Chen, X.; Fang, L.; Wang, Y.; Sun, J.; Fang, Q. Perfluorocyclobutyl-based polymers for functional materials. *Mater. Chem. Front.* **2019**, 3:1280-1301.
2. Bi, L.; Hong, J.; Li, S.; Zhu, Z.; Zhu, Y. Post-functionalization of perfluorocyclobutyl aryl ether polymers with a novel perfluorosulfonated side chain precursor. *J. Polym. Res.* **2019**, 26:1-9
3. Smitha, B.; Sridhar, S.; Kahn, A.A. Solid polymer electrolyte membranes for fuel cell applications-a review. *J. Membrane Science.* **2005**, 259: 10-26.
4. Peighambardoust, S.J.; Rowshanzamir, S.; Amjadi, M. Review of the proton exchange membranes for fuel cell applications. *Inter. J. Hydrogen Energy.* **2010**, 35: 9349-9384.
5. Wang, Y.; Chen, K.S.; Mishler, J.; Cho, S.C.; Adroher, X.C. A review of polymer electrolyte membrane fuel cells: Technology, applications, and needs on fundamental research. *Applied Energy.* **2011**, 88: 981-1007.
6. Litster, S.; McLean, G. PEM fuel cell electrodes. *J. Power Sources.* **2004**, 130: 61-76.
7. Wu, J.; Xiao, Z.Y.; Martin, J.J.; Wang, H.; Zhang, J.; Shen, J.; Wu, S.; Merida, W. A review of PEM fuel cell durability: degradation mechanisms and mitigation strategies. *J. Power Sources.* **2008**, 184: 104-119.
8. de-Troya, J. J.; Alvarez, C.; Fernandez-Garrido, C. Analysing the possibilities of using fuel cells in ships. *Int. J. Hydrog. Energy.* **2016**, 41: 2853- 2866.

9. Wu, H.W. A review of recent development: Transport and performance modeling of PEM fuel cells. *Applied Energy*. **2016**, 165: 81-106.
10. Thompson, S. D.; Jordan, L. R.; Forsyth, M. Platinum electrodeposition for polymer electrolyte membrane fuel cells. *Electrochim. Acta*. **2001**, 46: 1657-1663.
11. S. Srinivasan, O.A. Velev, A. Parthasarathy, D.J. Manko, Appleby, space electrochemical research and technology (SERT) 1991, NASA Conference Publication 3125, April 9–10, **1991**.
12. Devanathan, R.; Venkatnathan, A.; Rousseau, R.; Dupuis, M.; Frigato, T.; Gu, W.; Helms, V. Atomistic Simulation of Water Percolation and Proton Hopping in Nafion Fuel Cell Membrane. *The Journal of Physical Chemistry B* **2010**, 114 (43): 13681–13690.
13. Kusoglu, A.; Weber, A. Z. New Insights into Perfluorinated Sulfonic-Acid Ionomers. *Chem. Rev.* **2017**: 987-1104.
14. Lawler, R.; Caliendo, C.; Ju, H.; Kim, J. Y.; Lee, S. W.; Jang, S. S. Effect of the Side-Chain Length in Perfluorinated Sulfonic and Phosphoric Acid-Based Membranes on Nanophase Segregation and Transport: A Molecular Dynamics Simulation Approach. *The Journal of Physical Chemistry B* **2020**, 124 (8): 1571–1580.
15. Liu, L.; Chen, W.; Li, Y. An Overview of the Proton Conductivity of Nafion Membranes through a Statistical Analysis. *Journal of Membrane Science* **2016**, 504: 1–9.
16. Agmon, N. The Grotthuss Mechanism. *Chemical Physics Letters* **1995**, 244 (5): 456–462.
17. Wei, J. *Polymer-Based Multifunctional Nanocomposites and Their Applications*; Elsevier, 2019.

18. Mei, H.; VanDerveer, D.; DesMarteau, D. D. Synthesis of diazonium (perfluoroalkyl) benzenesulfonylimide zwitterions. *J. Fluor. Chem.* **2013**, 145: 35-40.
19. Allongue, P.; Delamar, M.; Desbat, B.; Fagubaume, O.; Hitmi, R.; Pinson, J.; Saveant, J.M. Covalent Modification of Carbon Surfaces by Aryl Radicals Generated from the Electrochemical Reduction of Diazonium Salts. *J. Am. Chem. Soc.* **1997**, 119: 201-207.
20. Shah, A. A.; Ralph, T. R.; Walsh, F. C. Modeling and Simulation of the Degradation of Perfluorinated Ion-Exchange Membranes in PEM Fuel Cells. *J. Electrochem. Soc.* **2009**, 156: B465-B484.
21. Zhang, Y.; Ting, J.W.Y.; Rohan, R.; Cai, W.; Li, J.; Xu, G.; Chen, Z.; Lin, A.; Cheng, H. Fabrication of a proton exchange membrane via blended sulfonamide functionalized polyamide. *J. Material Science.* **2014**, 49: 3442-3450.
22. Nakajima, T. and Groult, H., n.d. *Advanced fluoride-based materials for energy conversion*. Elsevier, pp.326-345.
23. Thomas, B. H.; Shafer, G.; Ma, J. J.; Tu, M.-H.; DesMarteau, D. D. Synthesis of 3,6-Dioxo- Δ^7 -4-Trifluoromethyl Perfluorooctyl Trifluoromethyl Sulfonimide: Bis[(Perfluoroalkyl)Sulfonyl] Superacid Monomer and Polymer. *Journal of Fluorine Chemistry.* **2004**, 125 (8): 1231–1240.
24. Hassani, M. O.; Germain, A.; Brunel, D.; Commeyras, A. Thermal Stability of Perfluoroalkanesulfonic Acids and Their Anhydrides. New and Easy Approach to RFSO₂ORF Esters. *Tetrahedron Letters.* **1981**, 22 (1): 65–68.

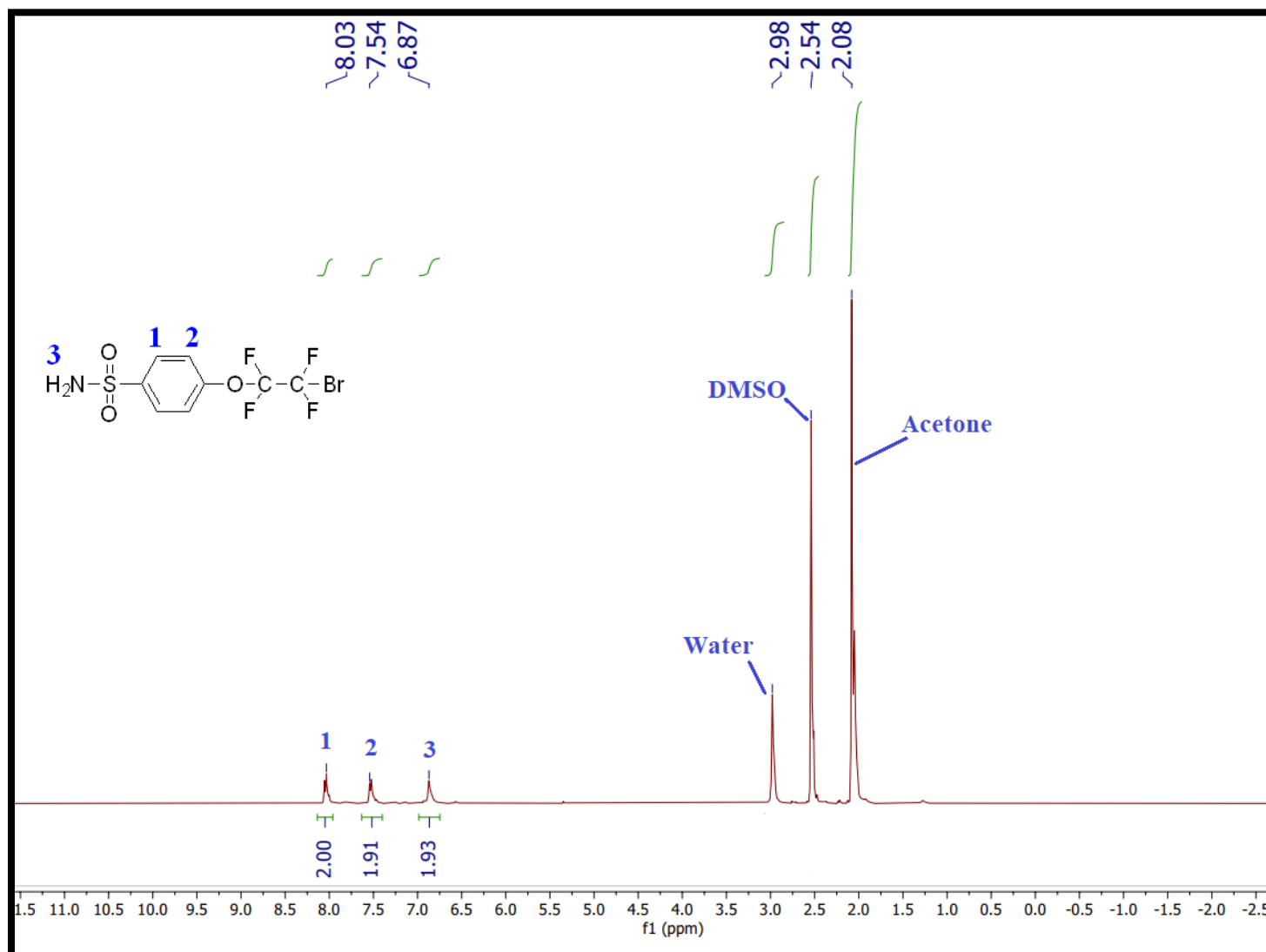
25. Savett, S. C.; Atkins, J. R.; Sides, C. R.; Harris, J. L.; Thomas, B. H.; Creager, S. E.; Pennington, W. T.; DesMarteau, D. D. A Comparison of Bis[(Perfluoroalkyl)Sulfonyl]Imide Ionomers and Perfluorosulfonic Acid Ionomers for Applications in PEM Fuel-Cell Technology. *Journal of The Electrochemical Society* **2002**, *149* (12).
26. Koppel, I. A.; Taft, R. W.; Anvia, F.; Zhu, S.-Z.; Hu, L.-Q.; Sung, K.-S.; DesMarteau, D. D.; Yagupolskii, L. M.; Yagupolskii, Y. L. The Gas-Phase Acidities of Very Strong Neutral Bronsted Acids. *Journal of the American Chemical Society*. **1994**, *116* (7): 3047–3057.
27. DesMarteau, D. D. Novel Perfluorinated Ionomers and Ionenenes. *Journal of Fluorine Chemistry* **1995**, *72* (2): 203–208.
29. Rico, I.; Wakselman, C. Condensation of 1,2-Dibromotetrafluoroethane with Various Potassium Thiophenoxides and Phenoxides. *Journal of Fluorine Chemistry* **1982**, *20* (6), 759–764.
30. Li, J.; Qiao, J. X.; Smith, D.; Chen, B.-C.; Salvati, M. E.; Roberge, J. Y.; Balasubramanian, B. N. A Practical Synthesis of Aryl Tetrafluoroethyl Ethers via the Improved Reaction of Phenols with 1,2-Dibromotetrafluoroethane. *Tetrahedron Letters* **2007**, *48* (42), 7516–7519.
31. Smith, N.; Bonnefous, C.; Payne, J.; Hoffman, T.; Wash, P.; Hassig, C.; Scranton, S. Inhibitors of Histone Deacetylase for the Treatment of Disease. <https://patentscope.wipo.int/search/en/detail.jsf?docId=WO2007067994> (accessed May 8, 2021).

32. https://organicchemistrydata.org/hansreich/resources/electron_pushing/#ep-acetylation-alcohol (accessed May 14, 2021).
33. Anbu; Nagarjun; Jacob; Kalaiarasi; Dhakshinamoorthy. Acetylation of Alcohols, Amines, Phenols, Thiols under Catalyst and Solvent-Free Conditions. *Chemistry* **2019**, *1* (1), 69–79.
34. Hazen, G. G.; Bollinger, F. W.; Roberts, F. E.; Russ, W. K.; Seman, J. J.; Staskiewicz, S. 4-Dodecylbenzenesulfonyl Azides. *Organic Syntheses* **2003**, 144–144.
35. Humljan, J.; Gobec, S. Synthesis of N-Phthalimido β -Aminoethanesulfonyl Chlorides: the Use of Thionyl Chloride for a Simple and Efficient Synthesis of New Peptidosulfonamide Building Blocks. *Tetrahedron Letters* **2005**, *46* (23), 4069–4072.
36. Bosshard, H. H.; Mory, R.; Schmid, M.; Zollinger, H. Eine Methode Zur Katalysierten Herstellung Von Carbonsäure- Und Sulfosäure-Chloriden Mit Thionylchlorid. *Helvetica Chimica Acta* **1959**, *42* (5), 1653–1658.
37. Wirth, D. D. In *E-EROS encyclopedia of reagents for organic synthesis*; Wiley: Hoboken, 2017; Vol. 1, pp 1–4.
38. Montalbetti, C. A. G. N.; Falque, V. Amide Bond Formation and Peptide Coupling. *Tetrahedron* **2005**, *61* (46), 10827–10852.
39. Lakrou, S.; K'tir, H.; Amira, A.; Berredjem, M.; Aouf, N.-E. A Simple and Eco-Sustainable Method for the Sulfonylation of Amines under Microwave-Assisted Solvent-Free Conditions. *RSC Adv.* **2014**, *4* (31), 16027–16032.

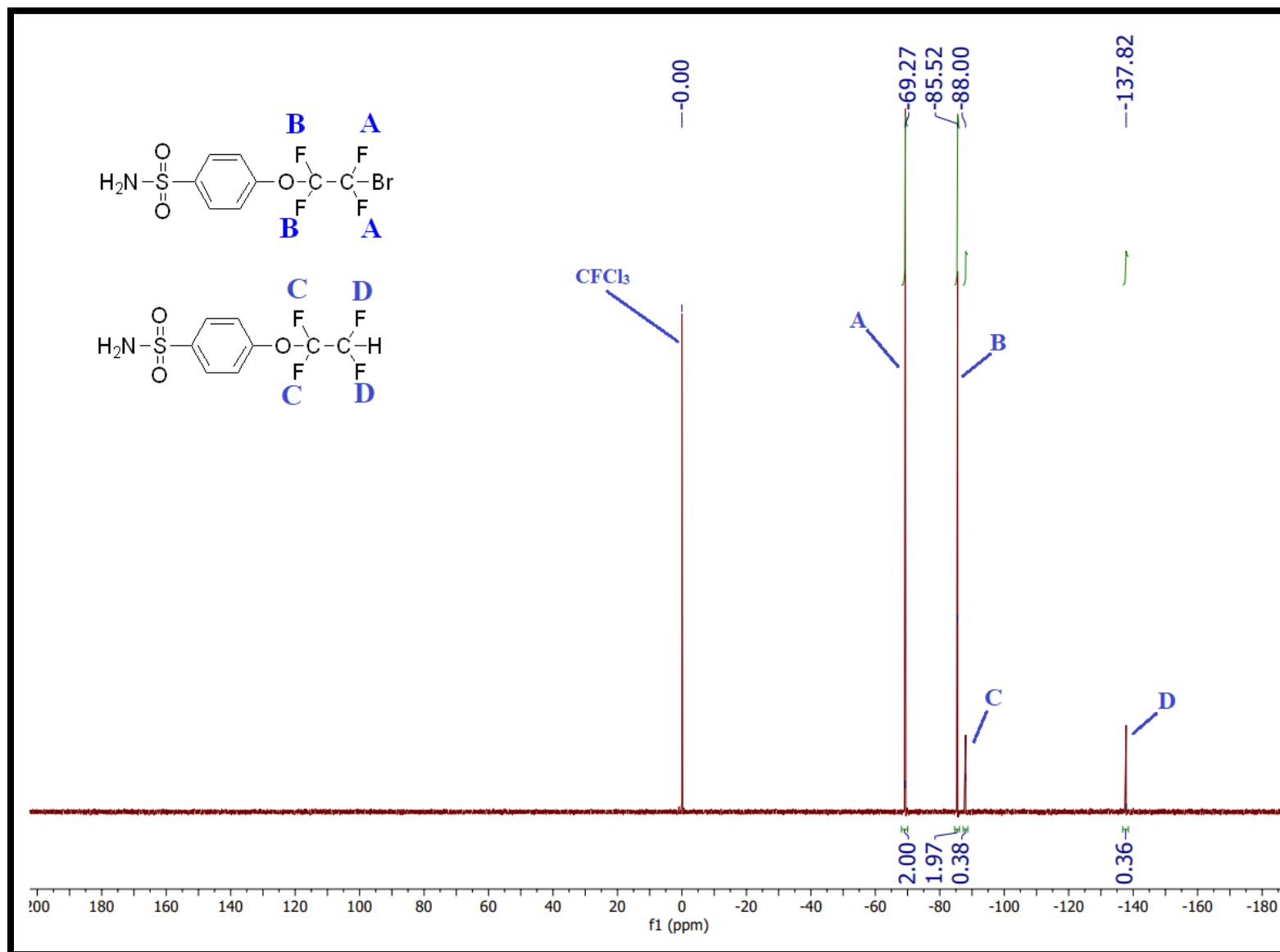
40. Flach, A. M.; Johnson, F. E.; Cabasso, I. Synthesis and Characterization of Fluorinated Polyionomers. Part I: Polyperfluoro-Sulfonylethoxy Propylene Vinyl Ether Sulfonimides Containing Aryl Sulfonic Acids. *Polymer Chemistry* **2013**, *4* (11), 3370.
41. Burdon, J.; Campbell, J. G.; Tatlow, J. C. Aromatic Polyfluoro-Compounds. Part XLIV. Bis(Pentafluorobenzoyl) Peroxide. *Journal of the Chemical Society C: Organic* **1969**, No. 5, 822–823.
42. Karty J.; *Organic Chemistry, Principles and Mechanism*, 1st ed., W. W. Norton and Company, New York –London, 2014, pp 1011-1027.
43. <https://www.sigmaaldrich.com/US/en/technical-documents/protocol/analytical-chemistry/nuclear-magnetic-resonance/polymer-analysis-by> (accessed Jun 10, 2021).
44. Odian, G. *Principles of polymerization*, 4th ed.; John Wiley & Sons: Hoboken, NJ, 2004.
45. Yamazaki, S.; Sawada, H. Chapter 1. Fluorinated Peroxides as Initiators of Fluorinated Polymers. *Fluorinated Polymers: Synthesis, Properties, Processing and Simulation* 1–21.
46. Toreki, R. The Glassware Gallery: Schlenk Lines and Vacuum Lines
<http://www.ilpi.com/inorganic/glassware/vacline.html> (accessed Apr 5, 2021).
47. Series 4700 General Purpose Pressure Vessels, 22 & 45 mL.
<https://www.parrinst.com/products/non-stirred-pressure-vessels/series-4700/> (accessed Jun 8, 2021).

APPENDICES

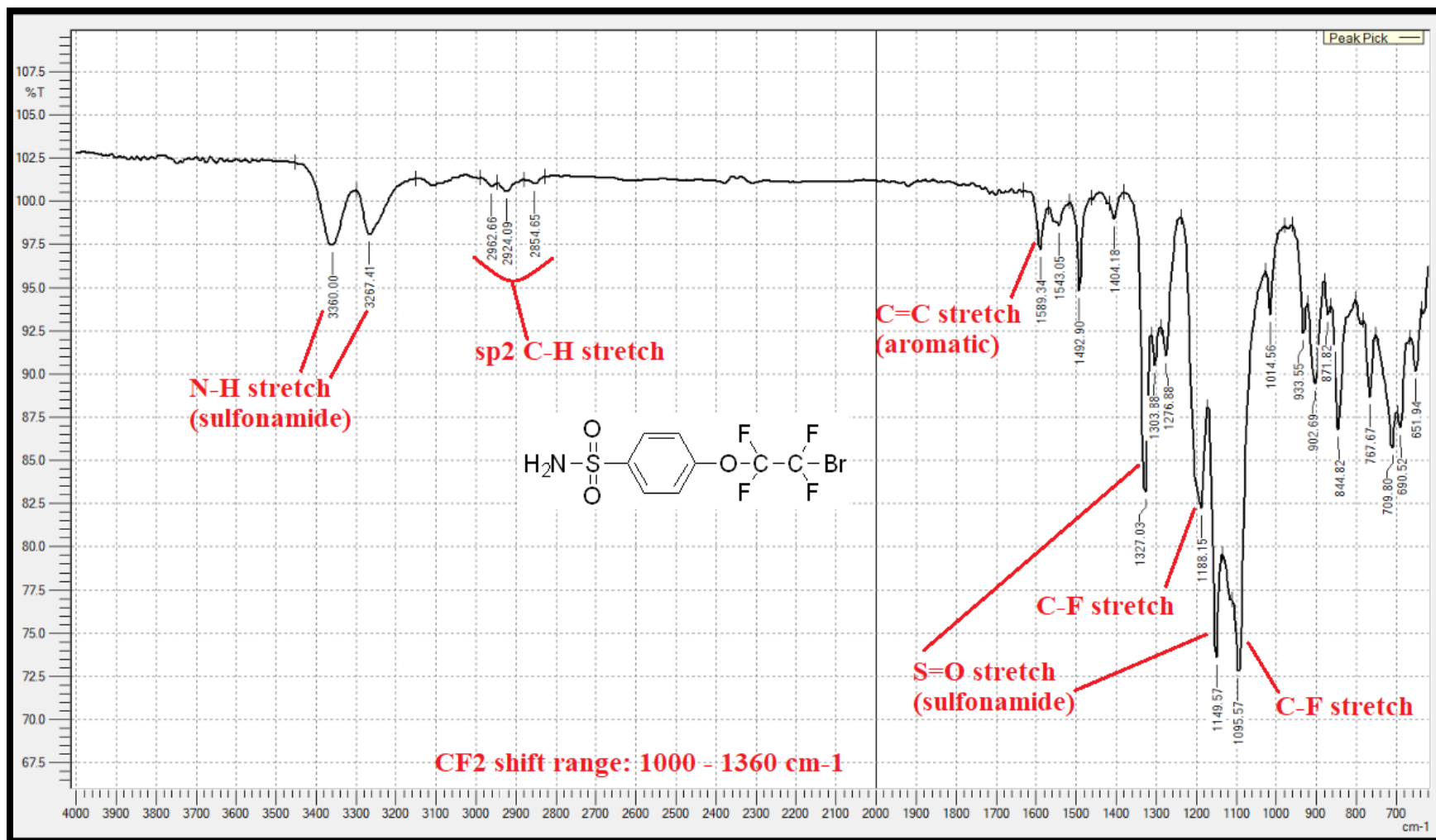
Appendix A1: ^1H NMR spectrum of 4-(2-bromotetrafluoroethoxy)-benzenesulfonyl amide, 400 MHz, CD_3COCD_3



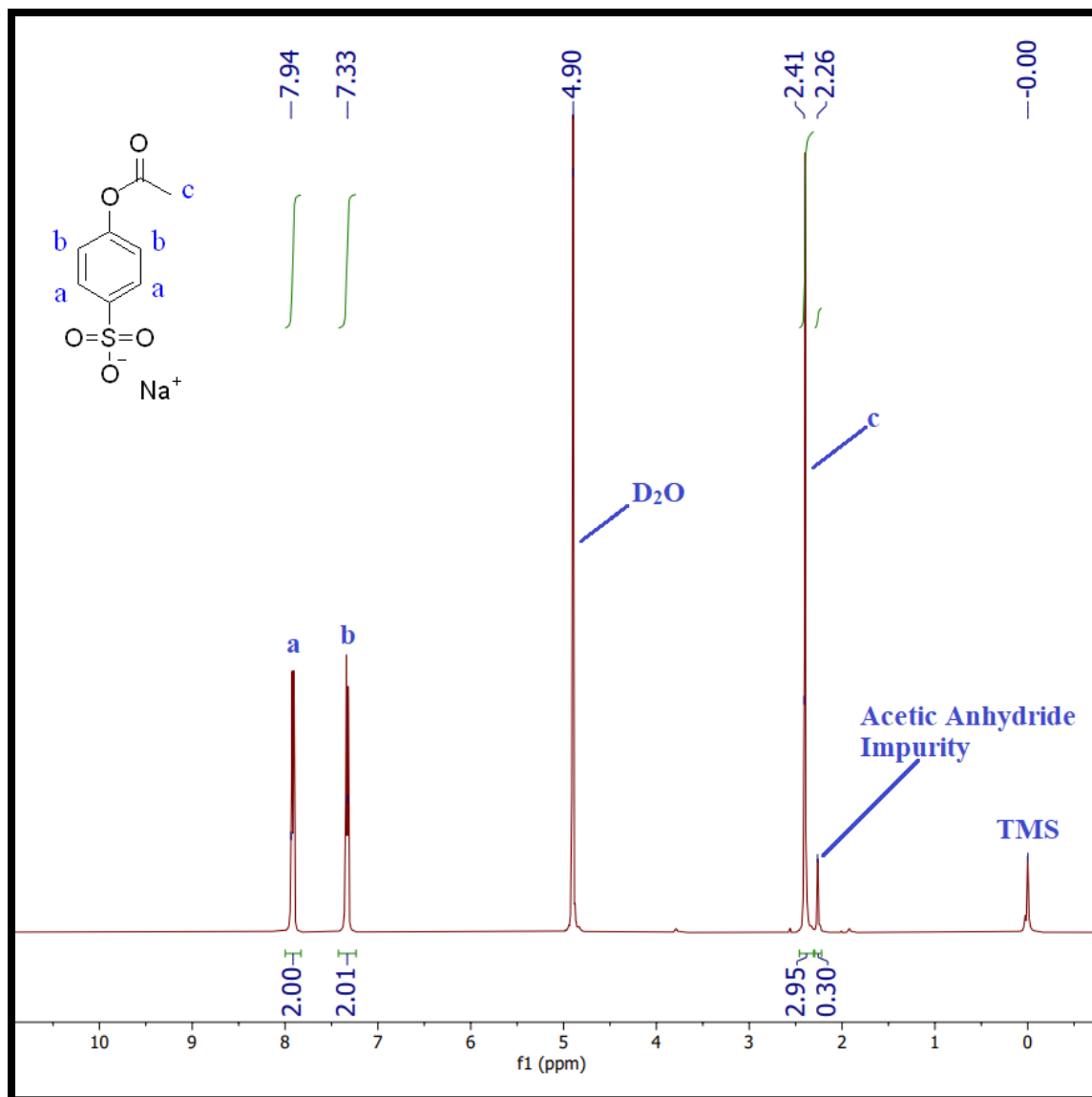
Appendix A2: ^{19}F NMR spectrum of 4-(2-bromotetrafluoroethoxy)-benzenesulfonyl amide, 400 MHz, CD_3COCD_3



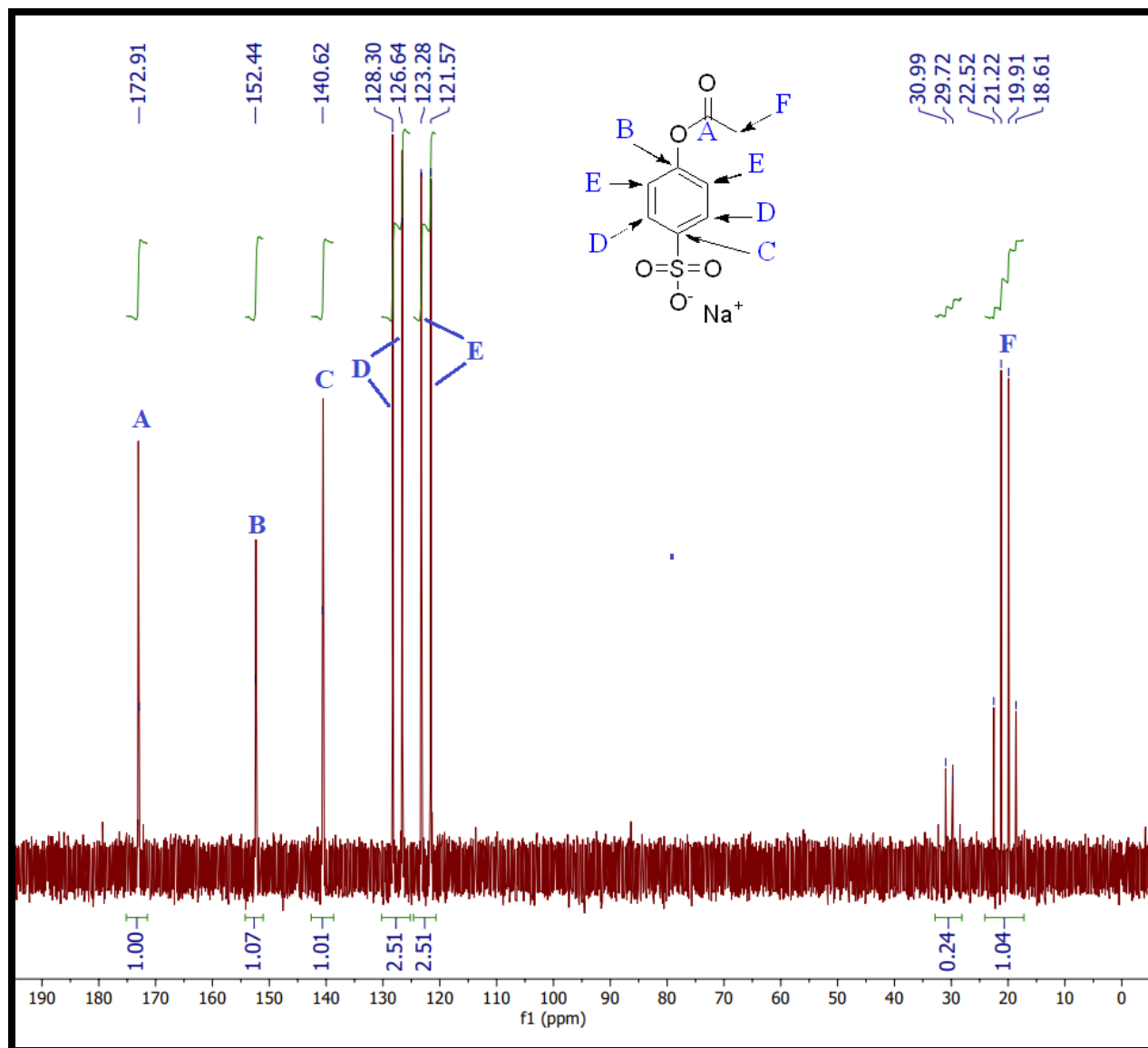
Appendix A3: FT-IR spectrum of 4-(2-bromotetrafluoroethoxy)-benzenesulfonyl amide



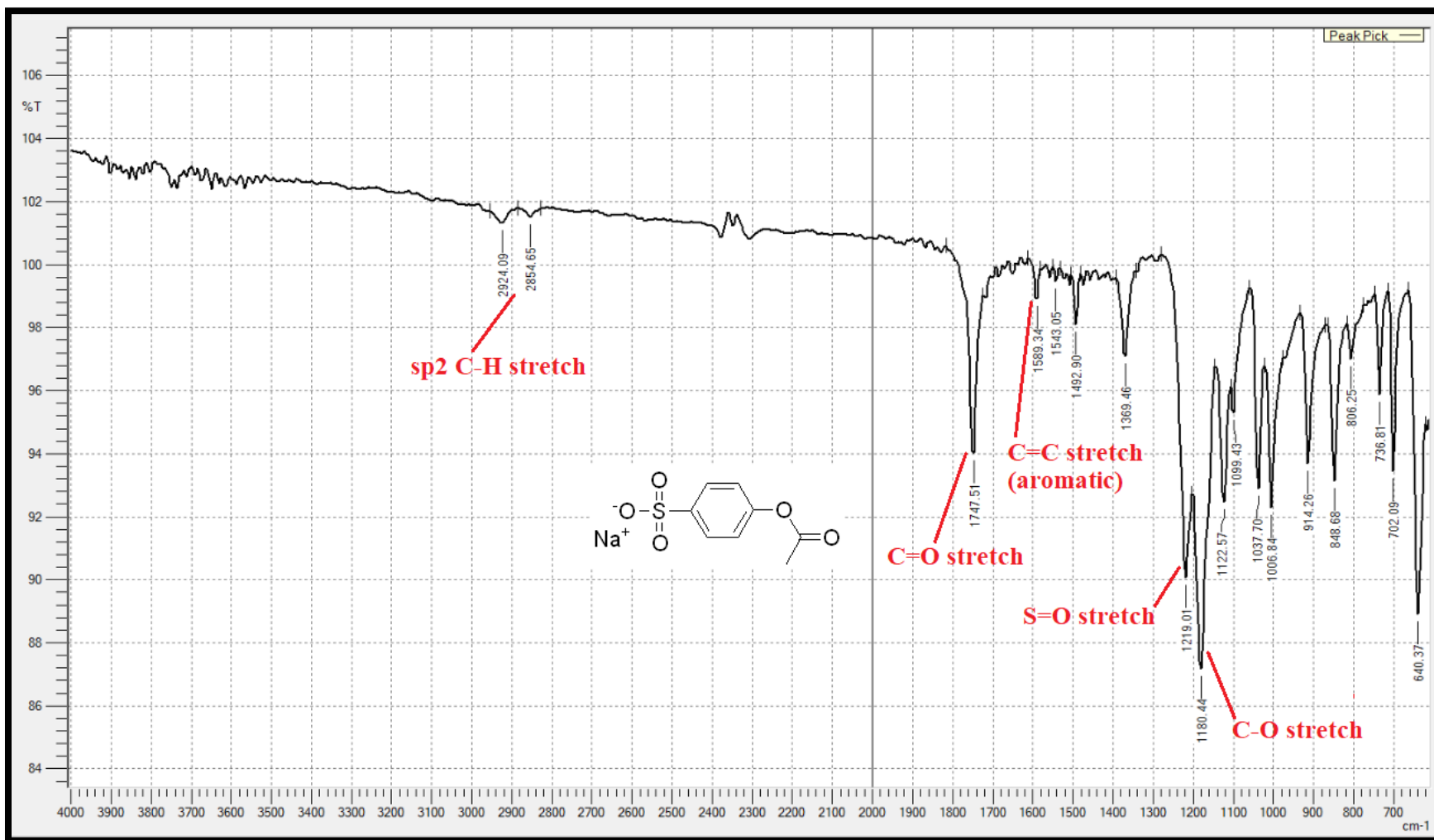
Appendix B1: ^1H NMR spectrum of 4-acetoxybenzenesulfonic acid sodium salt, 400 MHz, D_2O



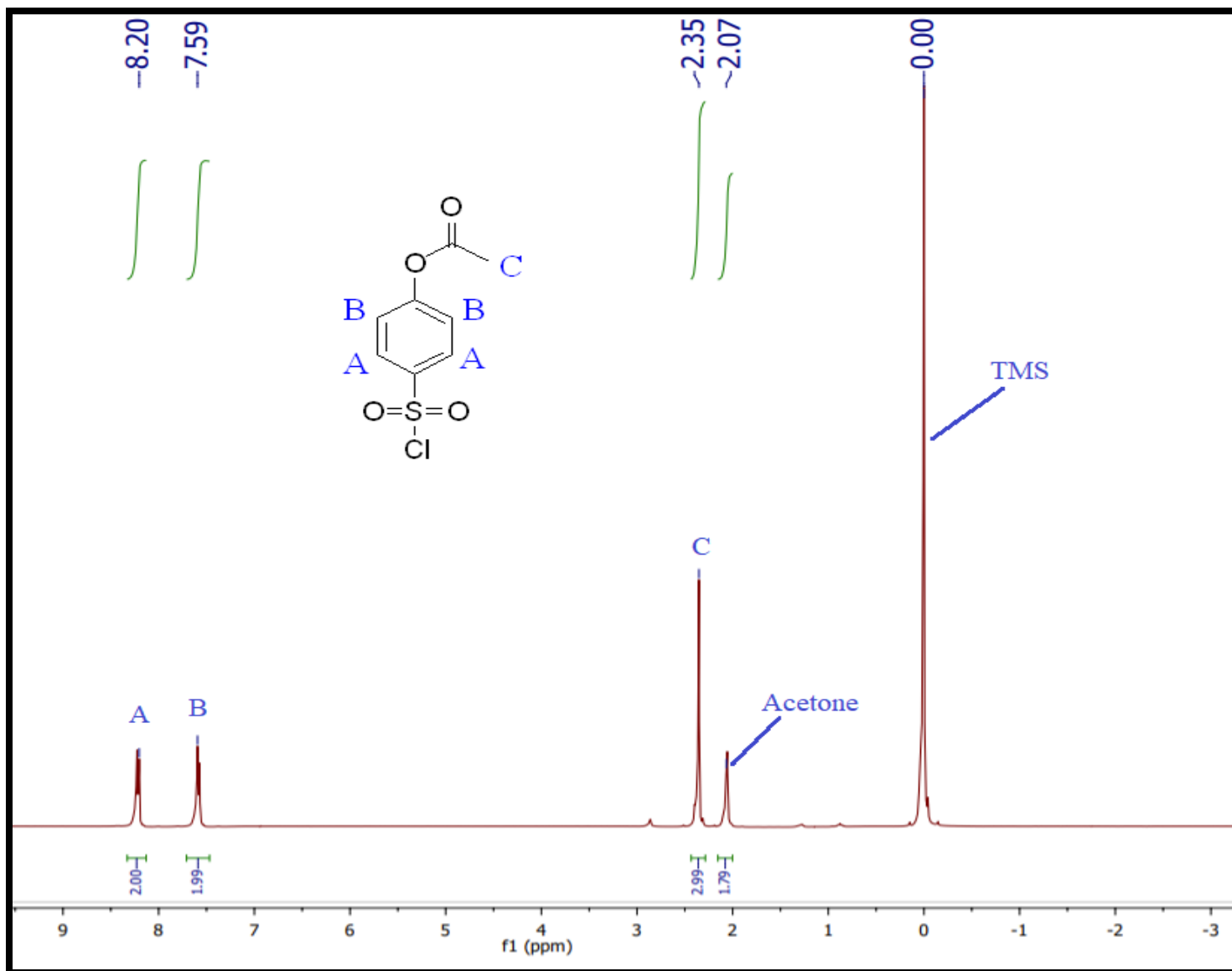
Appendix B2: ^{13}C NMR spectrum of 4-acetoxysulfonic acid sodium salt, 400 MHz, D_2O



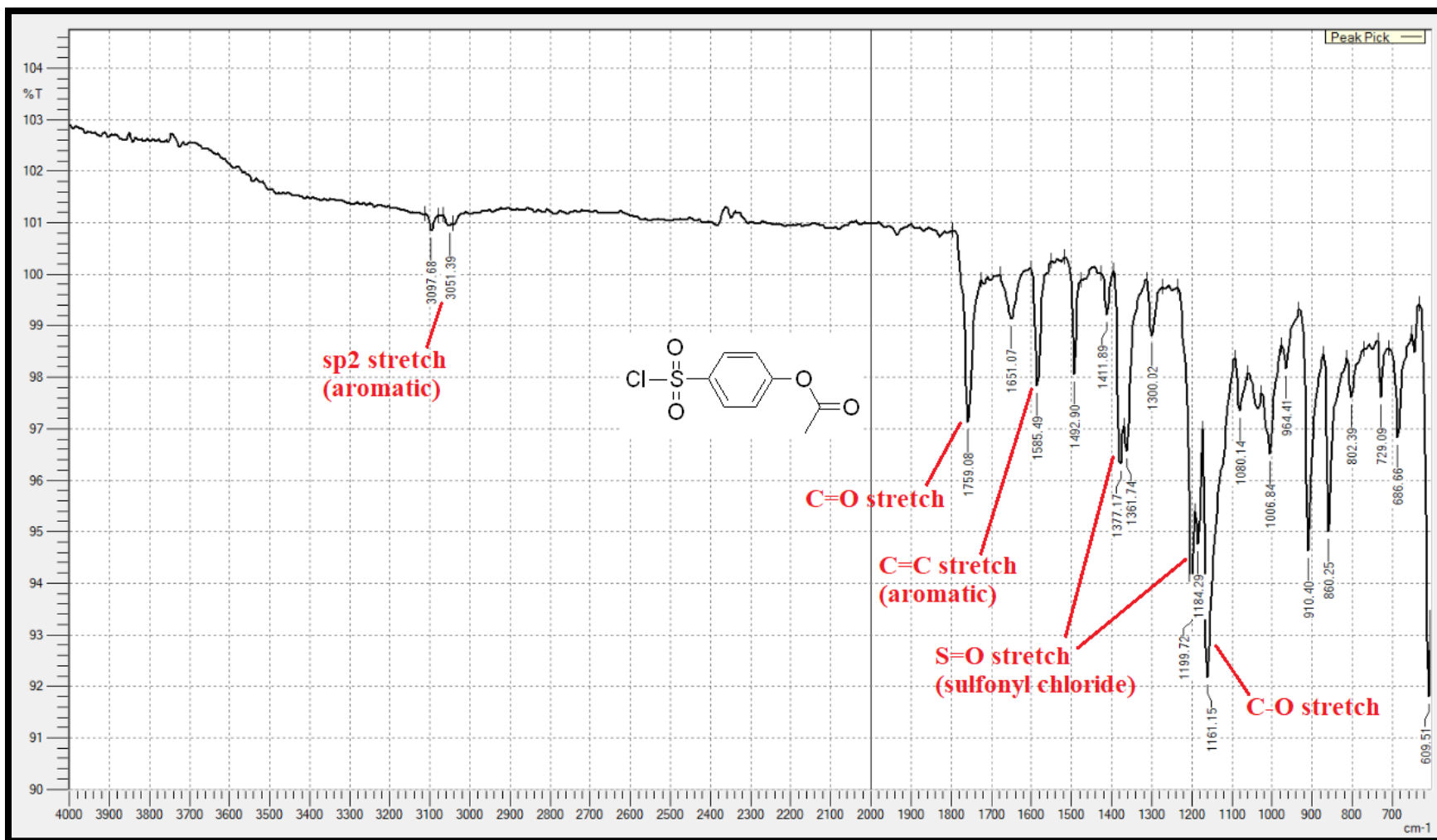
Appendix B3: FT-IR Spectrum of 4-acetoxybenzenesulfonic acid sodium salt



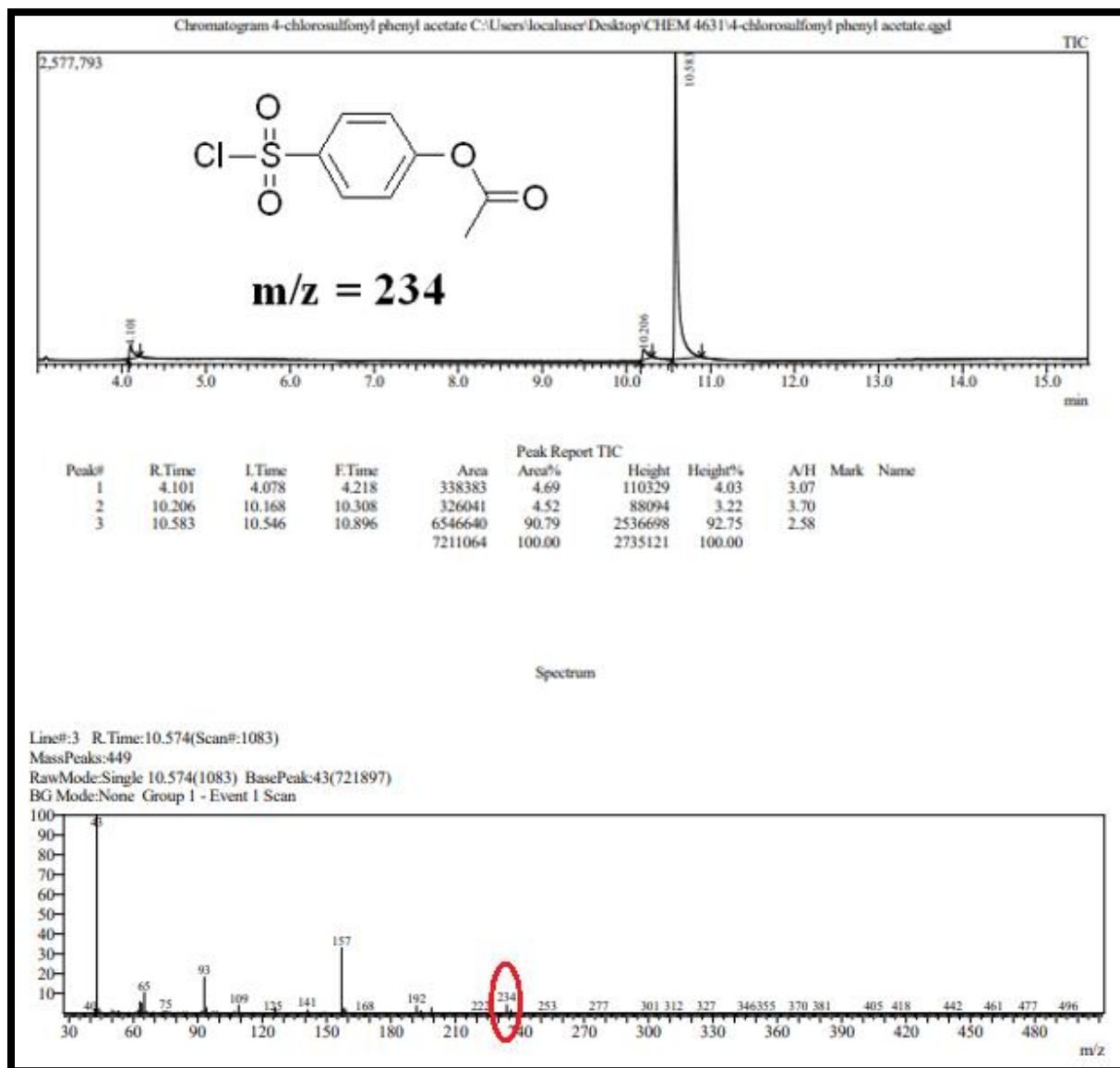
Appendix C1: ^1H NMR spectrum of 4-(chlorosulfonyl) phenyl acetate, 400 MHz, CD_3COCD_3



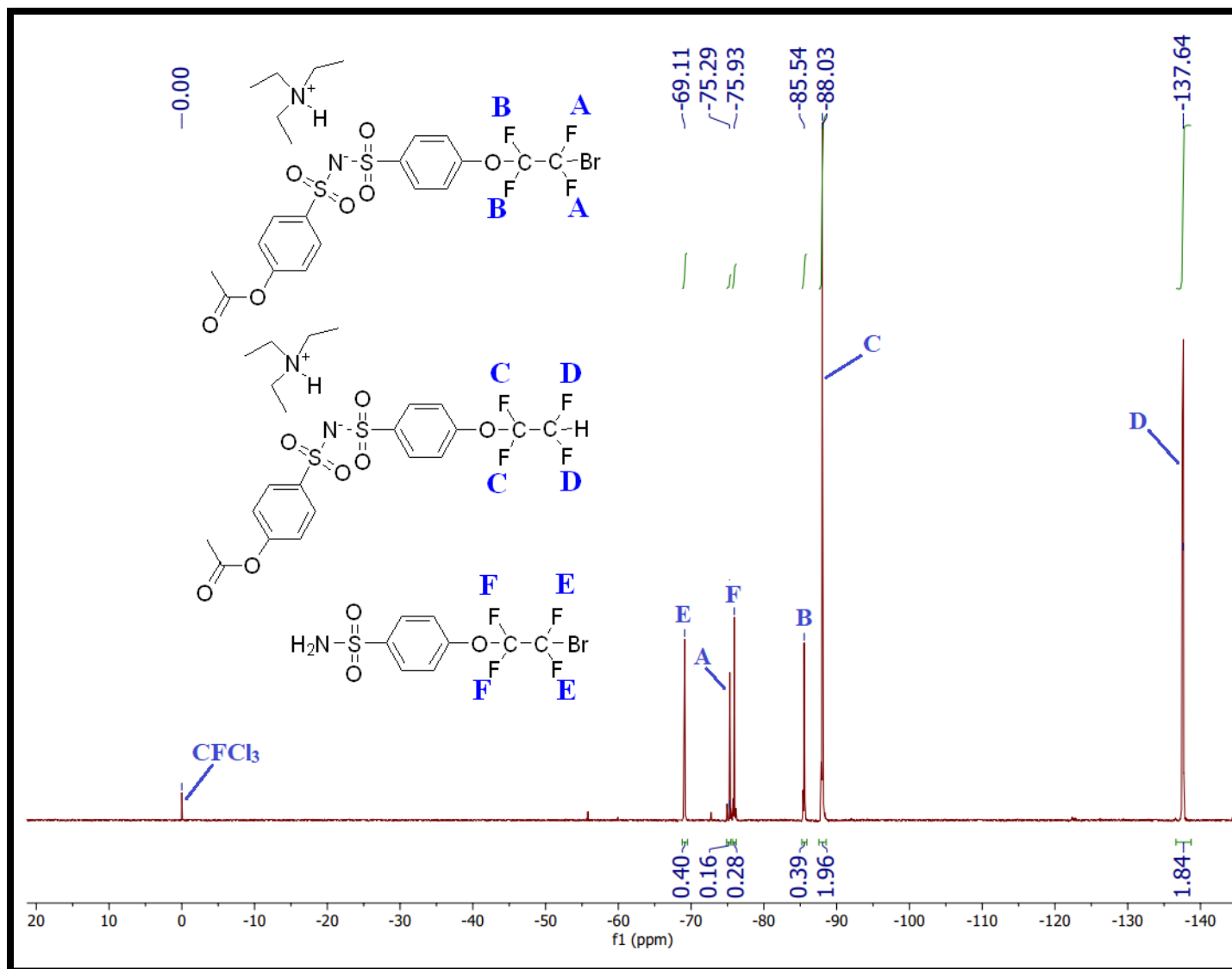
Appendix C2: FT-IR spectrum of 4-(chlorosulfonyl) phenyl acetate



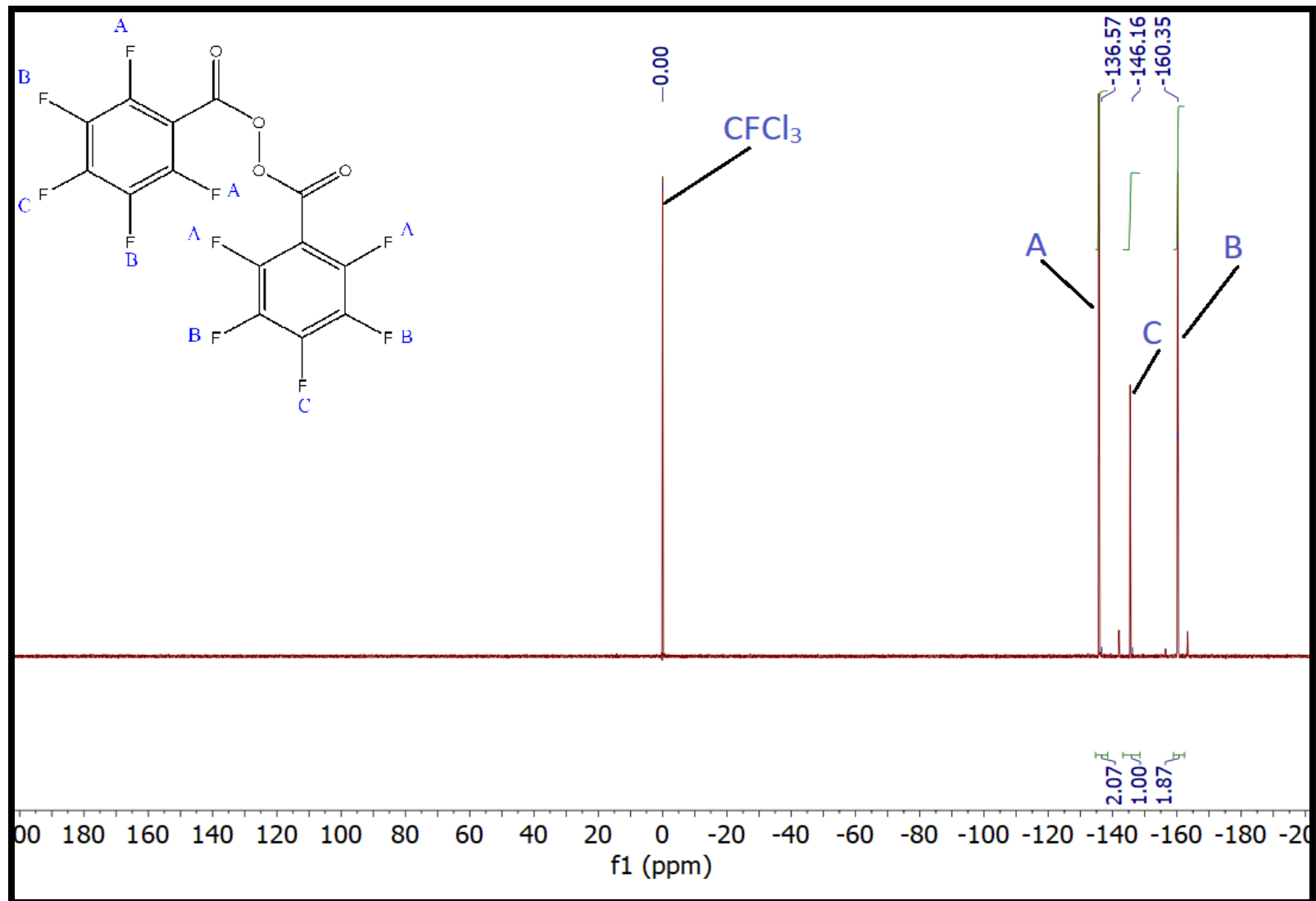
Appendix C3: GC-MS Chromatogram of 4-(chlorosulfonyl) phenyl acetate



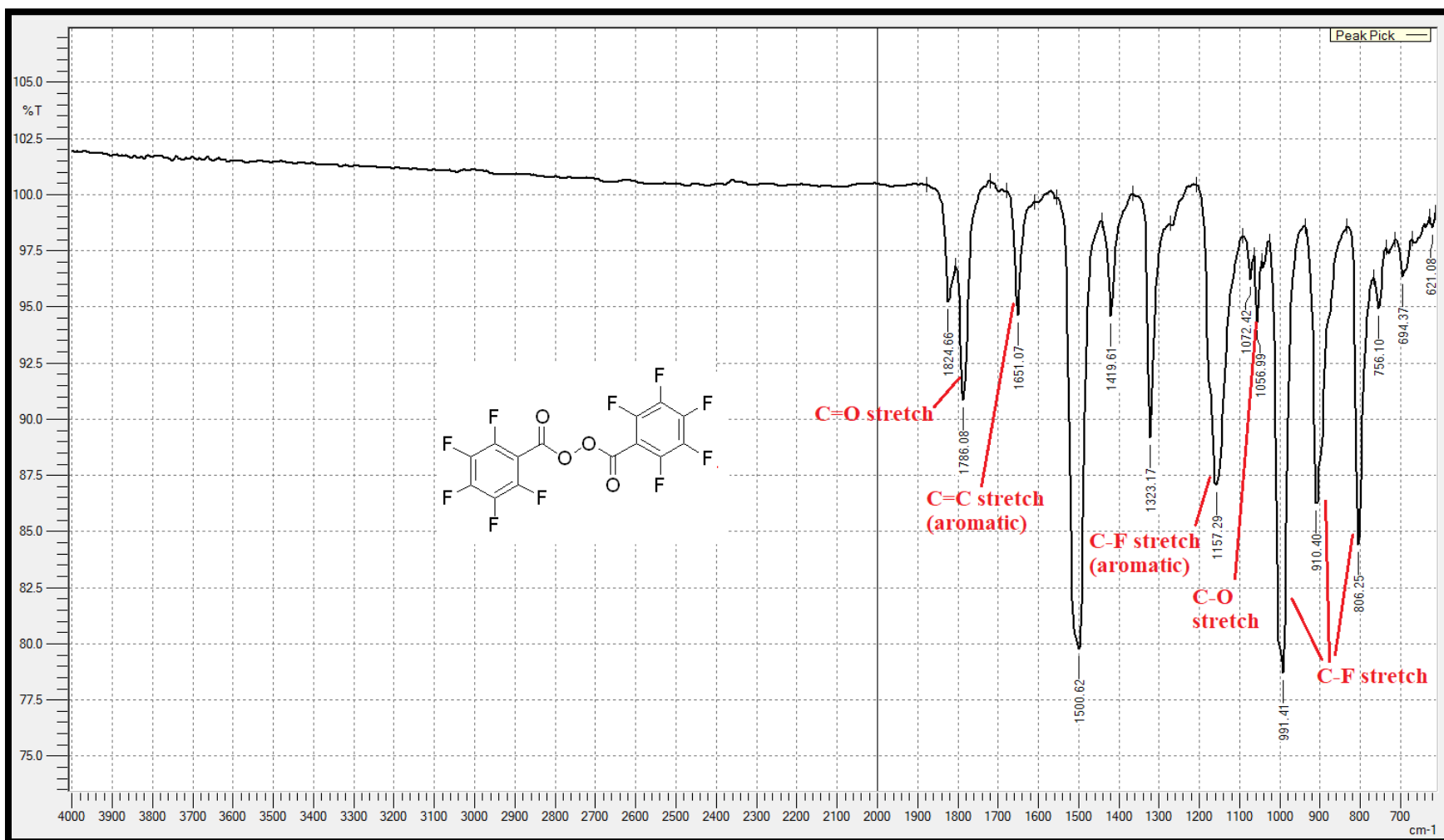
Appendix D1: ^{19}F NMR spectrum of Coupling Reaction of 4-(chlorosulfonyl) phenyl acetate with 4-(2-bromotetrafluoroethoxy)benzenesulfonyl amide, 400 MHz, CD_3COCD_3



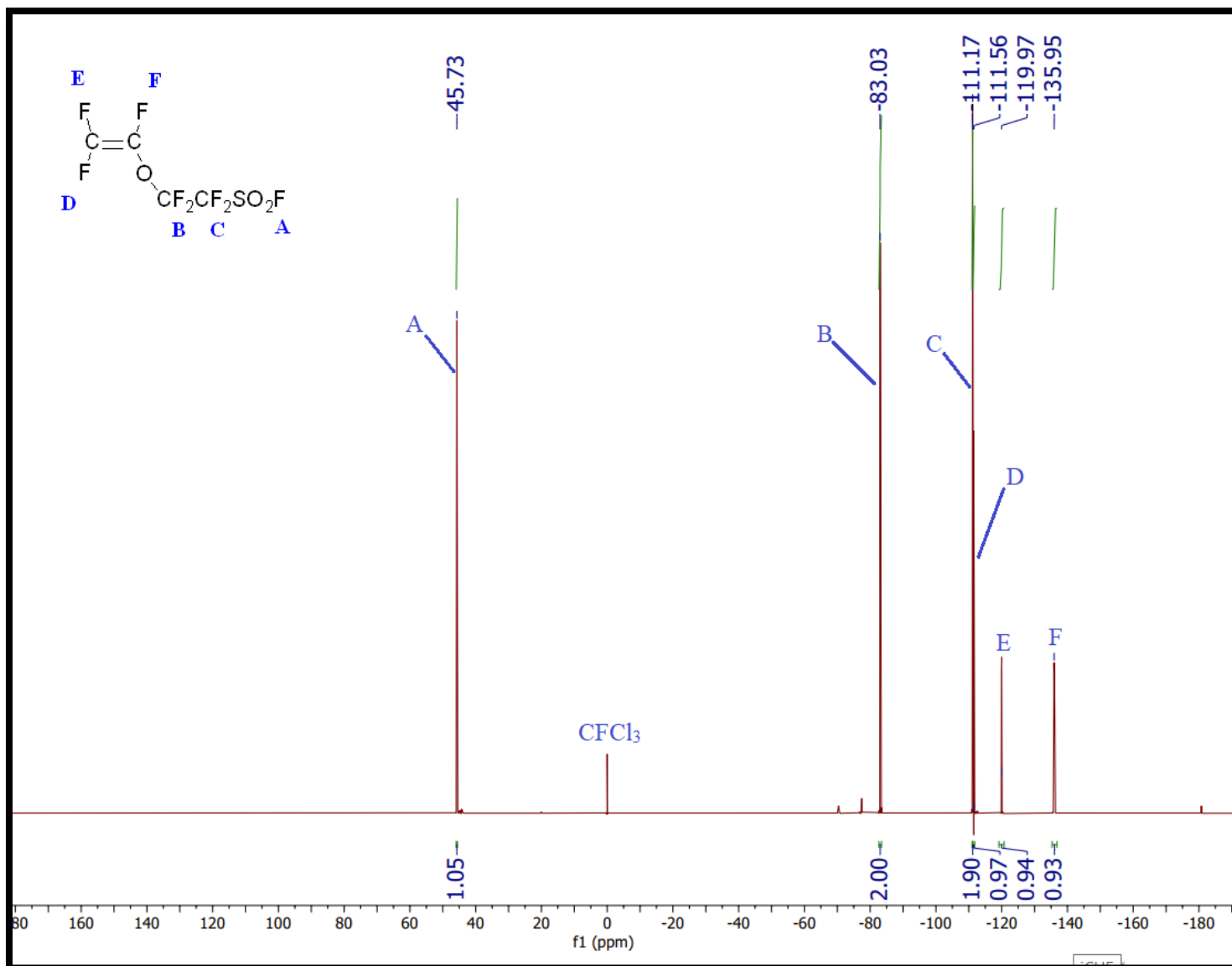
Appendix E1: ^{19}F NMR spectrum of (2,3,4,5,6-pentafluorobenzoyl) 2,3,4,5,6-pentafluorobenzenecarboperoxoate, 400 MHz, CD_3COCD_3



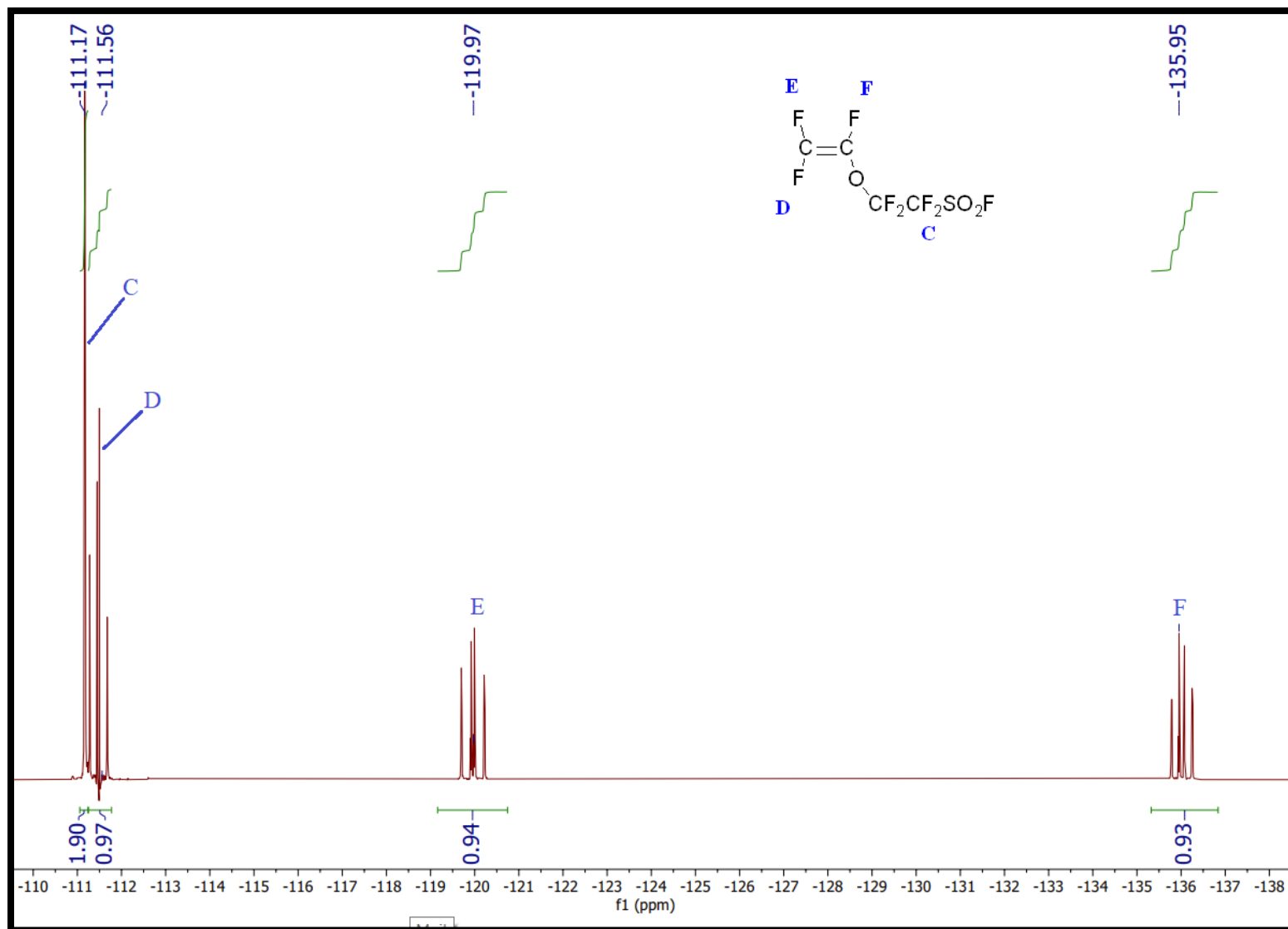
Appendix E2: FT-IR spectrum of (2,3,4,5,6-pentafluorobenzoyl) 2,3,4,5,6-pentafluorobenzenecarboxperoxyate



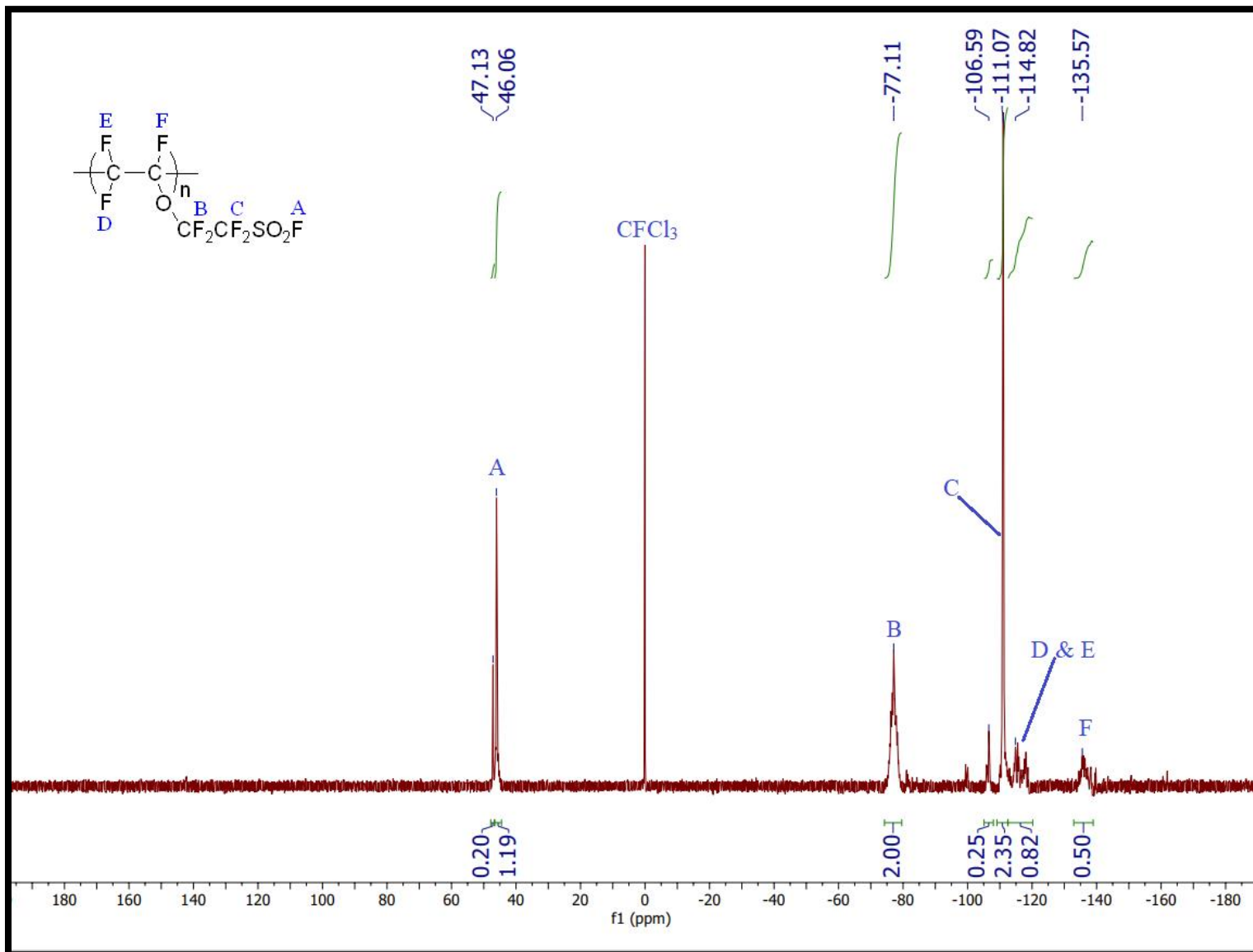
Appendix F1: ^{19}F NMR spectrum of perfluoro 3(oxapent-4-ene) sulfonyl fluoride monomer, 400 MHz, CD_3COCD_3



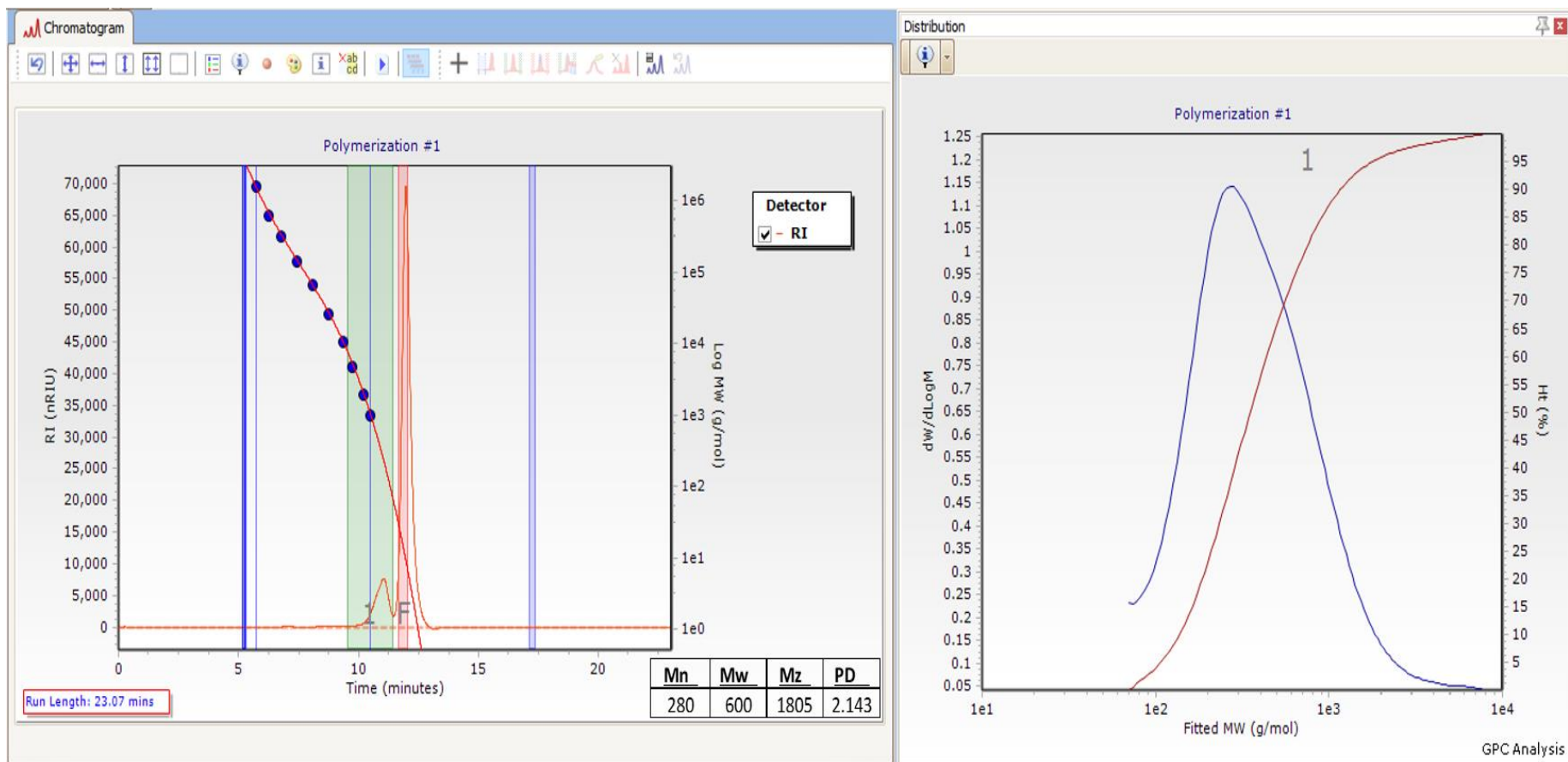
Appendix F2: (Expanded region -110 to -137 ppm) ^{19}F NMR spectrum of perfluoro 3(oxapent-4-ene) sulfonyl fluoride monomer, 400 MHz, CD_3COCD_3



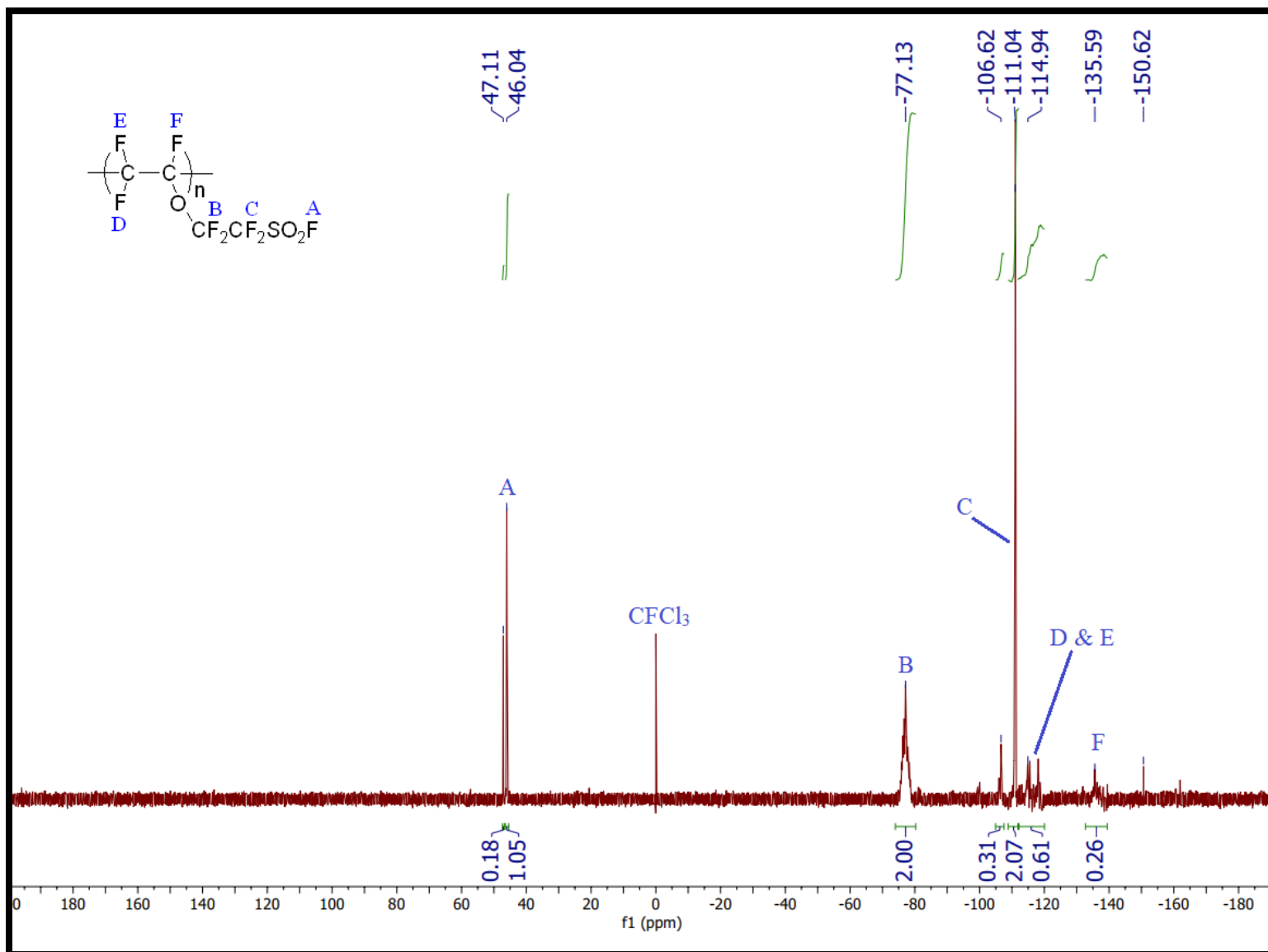
Appendix G1: ^{19}F NMR spectrum of homo-polymerization run #1 of $\text{CF}_2=\text{FCOCF}_2\text{CF}_2\text{SO}_2\text{F}$, 400 MHz, CD_3CN



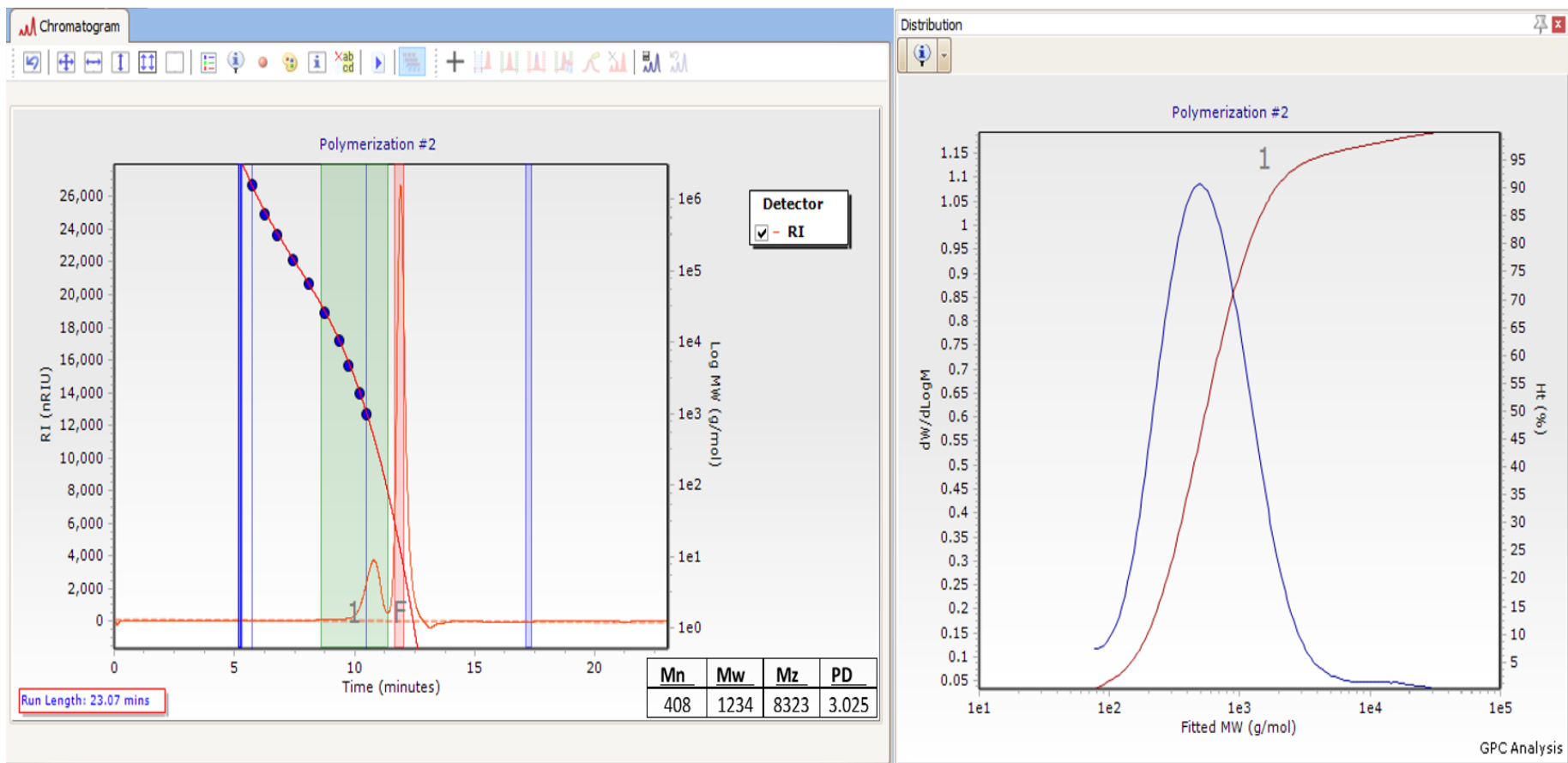
Appendix G2: Gel Permeation Chromatography (GPC) for homo-polymerization run #1 of $CF_2=FCOCF_2CF_2SO_2F$ in 1, 1, 1, 3, 3, 3-hexafluoroisopropanol (HFIP)



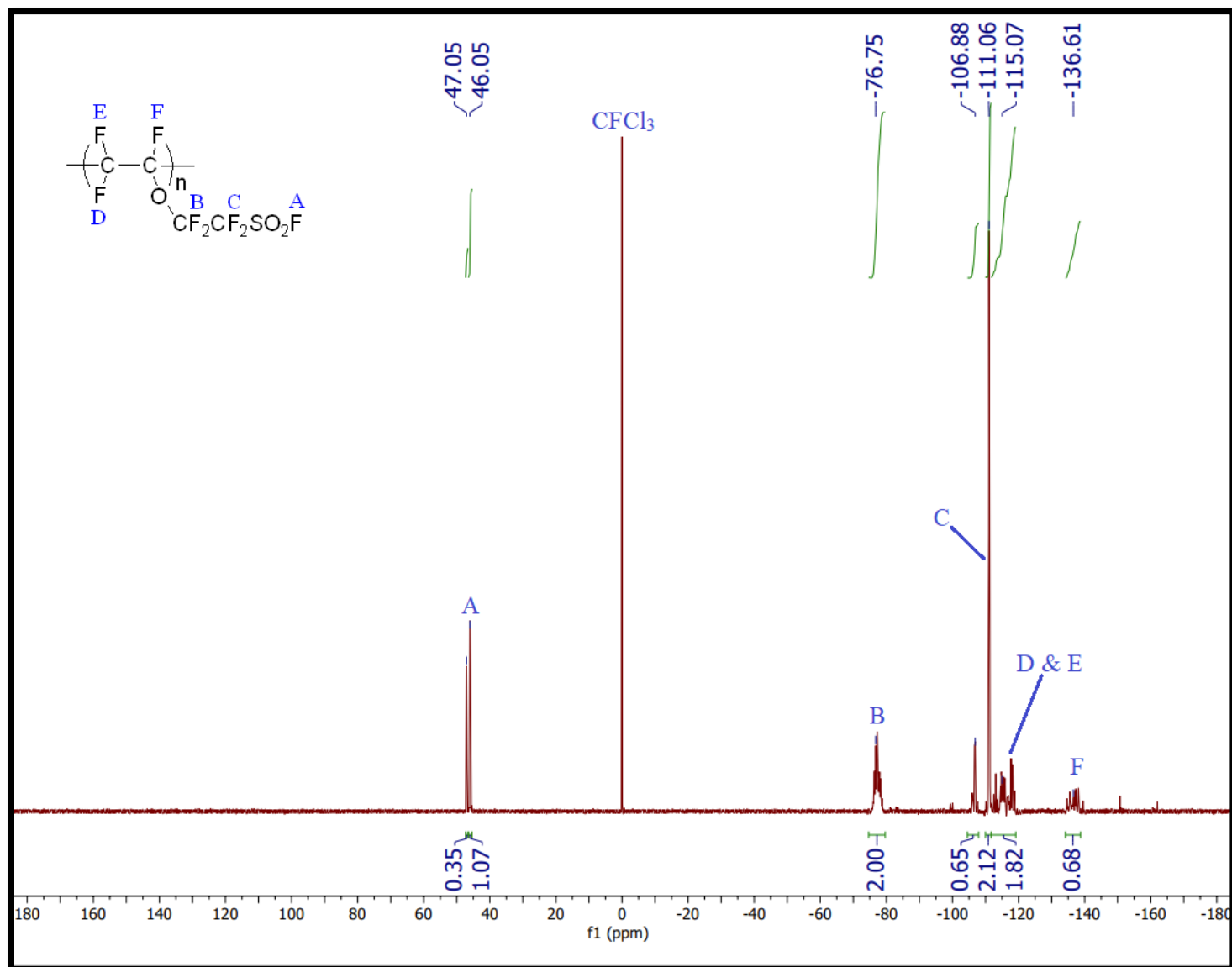
Appendix H1: ^{19}F NMR spectrum of homo-polymerization run #2 of $\text{CF}_2=\text{FCOCF}_2\text{CF}_2\text{SO}_2\text{F}$, 400 MHz, CD_3CN



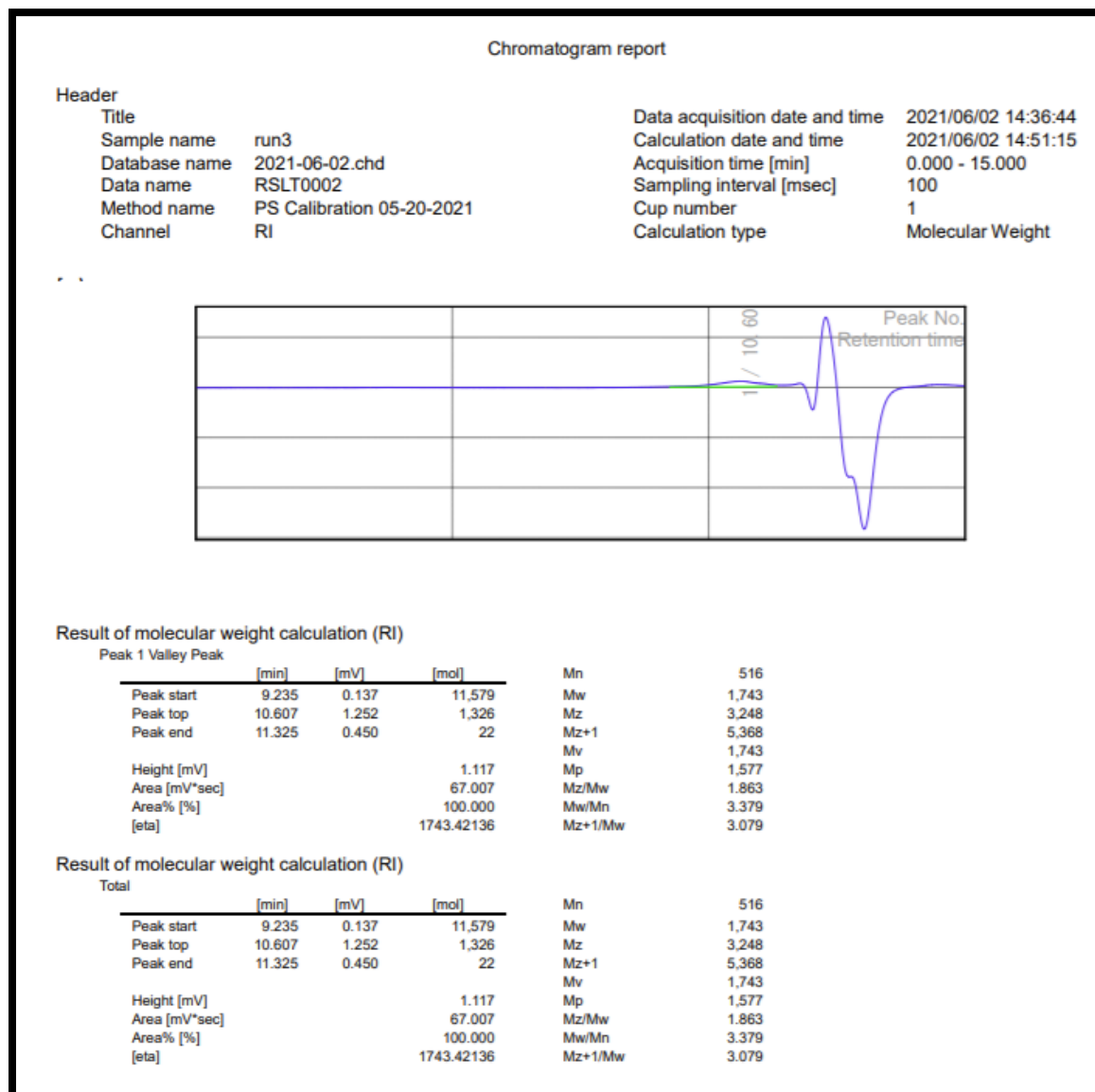
Appendix H2: Gel Permeation Chromatography (GPC) for homo-polymerization run #2 of $CF_2=FCOCF_2CF_2SO_2F$ in 1, 1, 1, 3, 3, 3-hexafluoroisopropanol (HFIP)



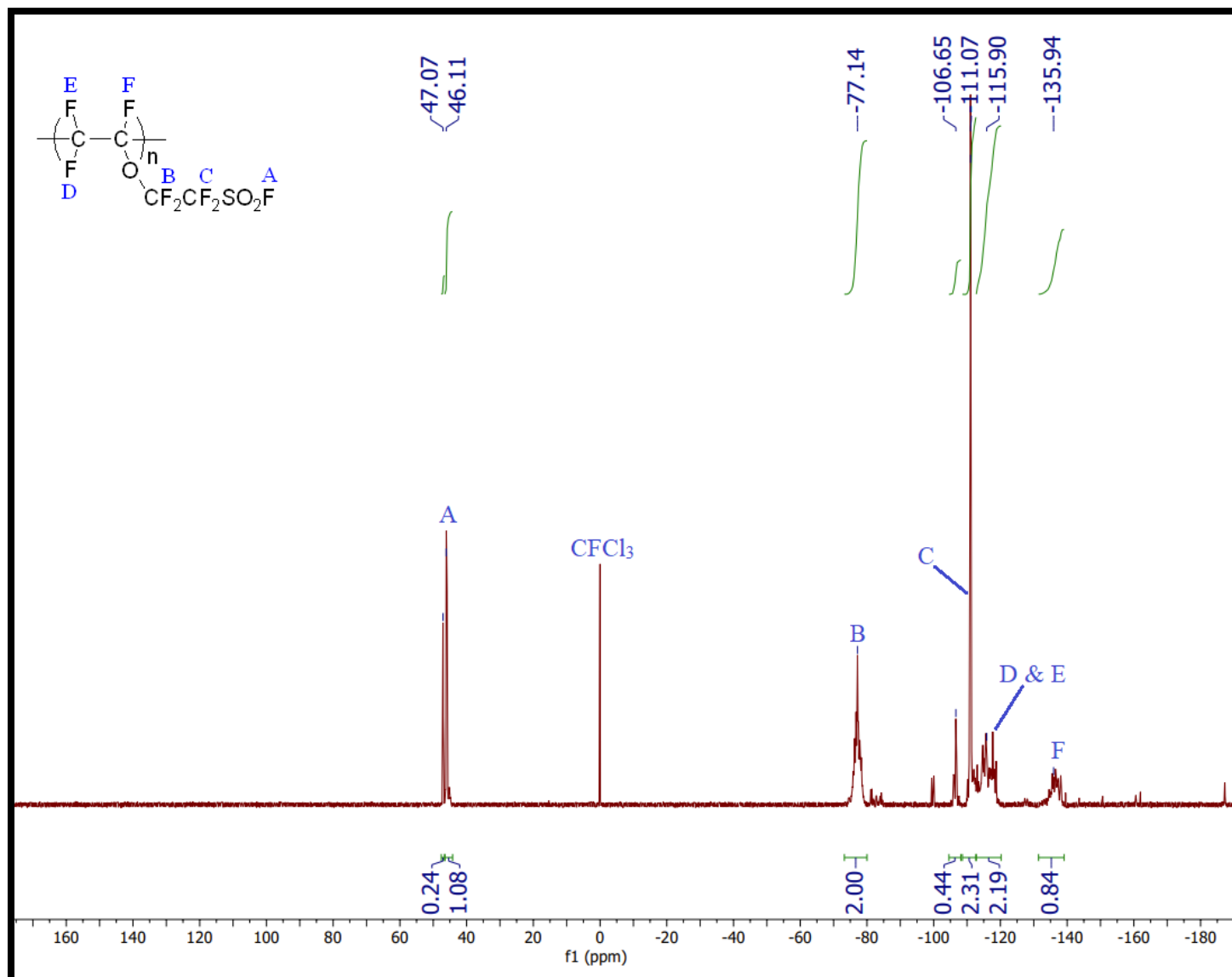
Appendix II: ^{19}F NMR spectrum of homo-polymerization run #3 of $\text{CF}_2=\text{FCOCF}_2\text{CF}_2\text{SO}_2\text{F}$, 400 MHz, CD_3CN



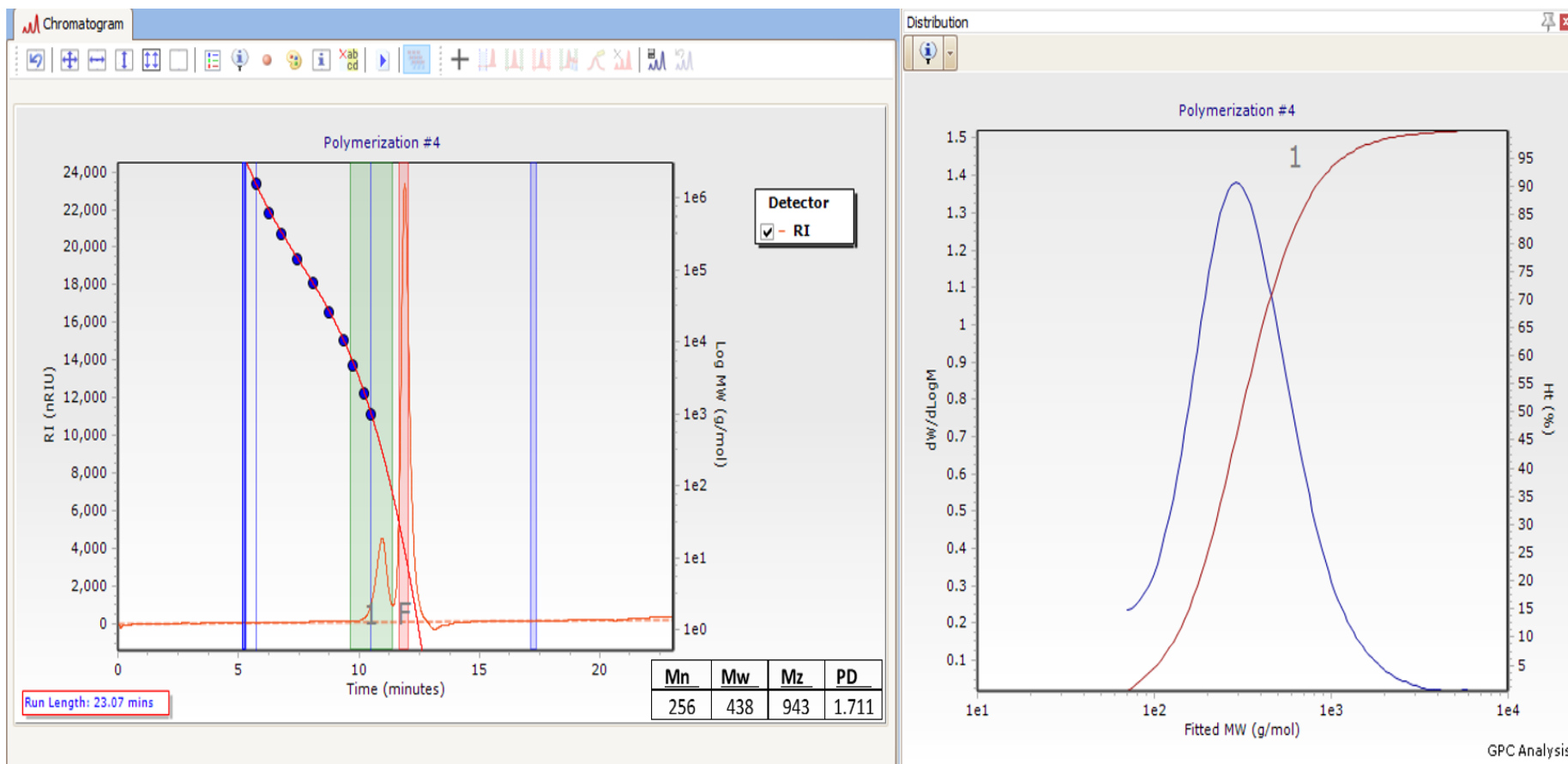
Appendix I2: Gel Permeation Chromatography (GPC) for homo-polymerization run #3 of $CF_2=FCOCF_2CF_2SO_2F$ in THF



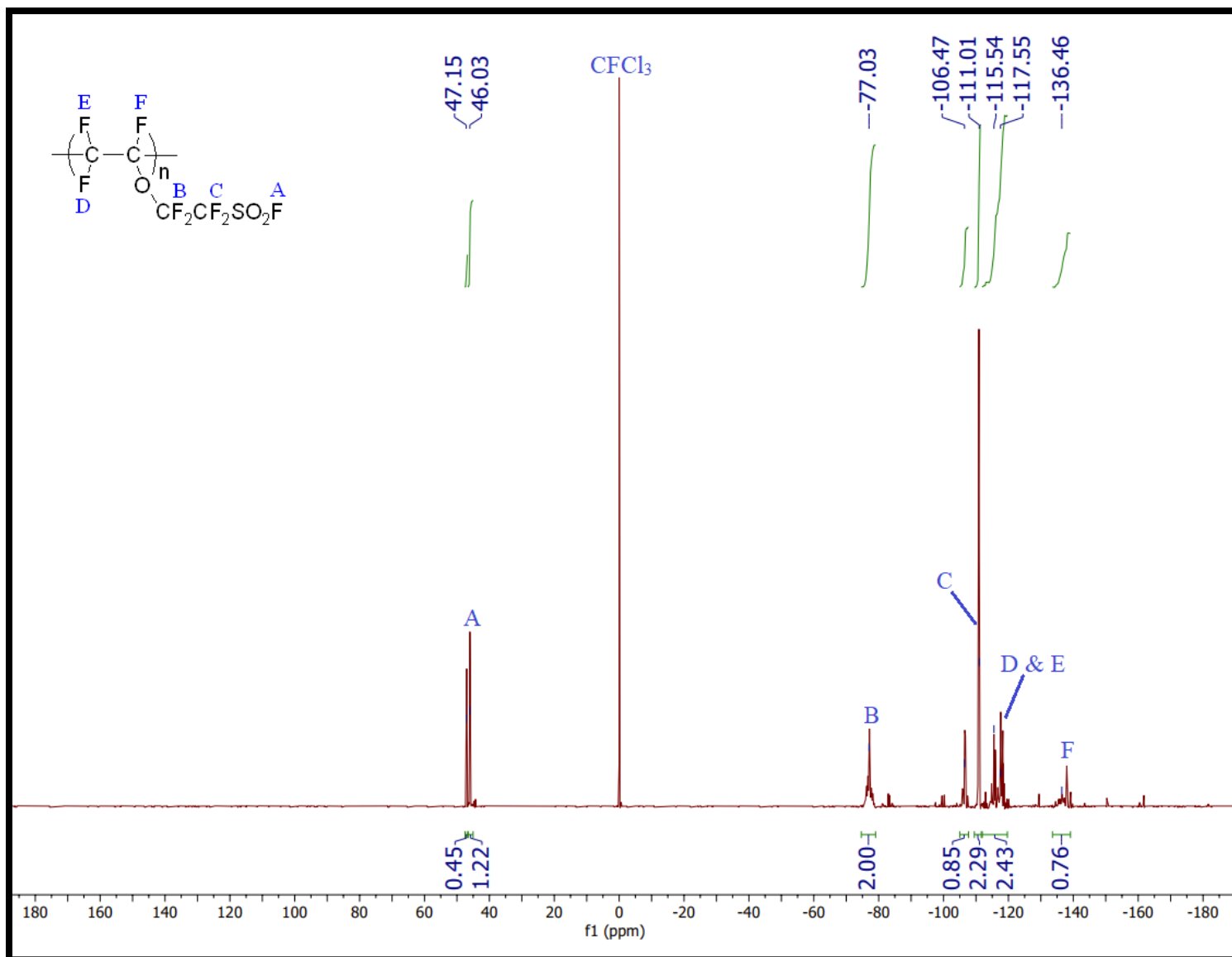
Appendix J1: ^{19}F NMR spectrum of homo-polymerization run #4 of $\text{CF}_2=\text{FCOCF}_2\text{CF}_2\text{SO}_2\text{F}$, 400 MHz, CD_3CN



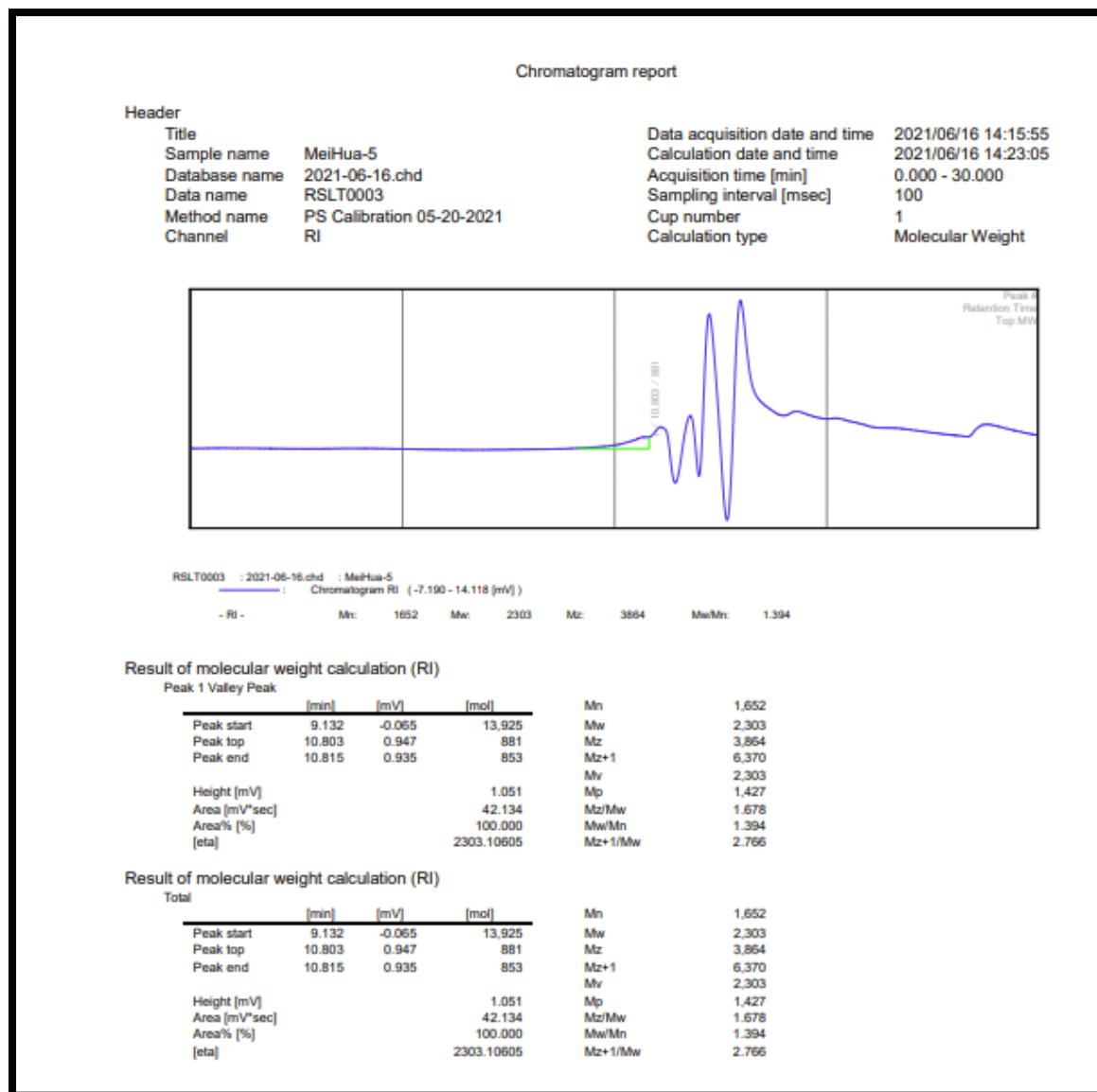
Appendix J2: Gel Permeation Chromatography (GPC) for homo-polymerization run #4 of $CF_2=FCOCF_2CF_2SO_2F$ in 1, 1, 1, 3, 3, 3-hexafluoroisopropanol (HFIP)



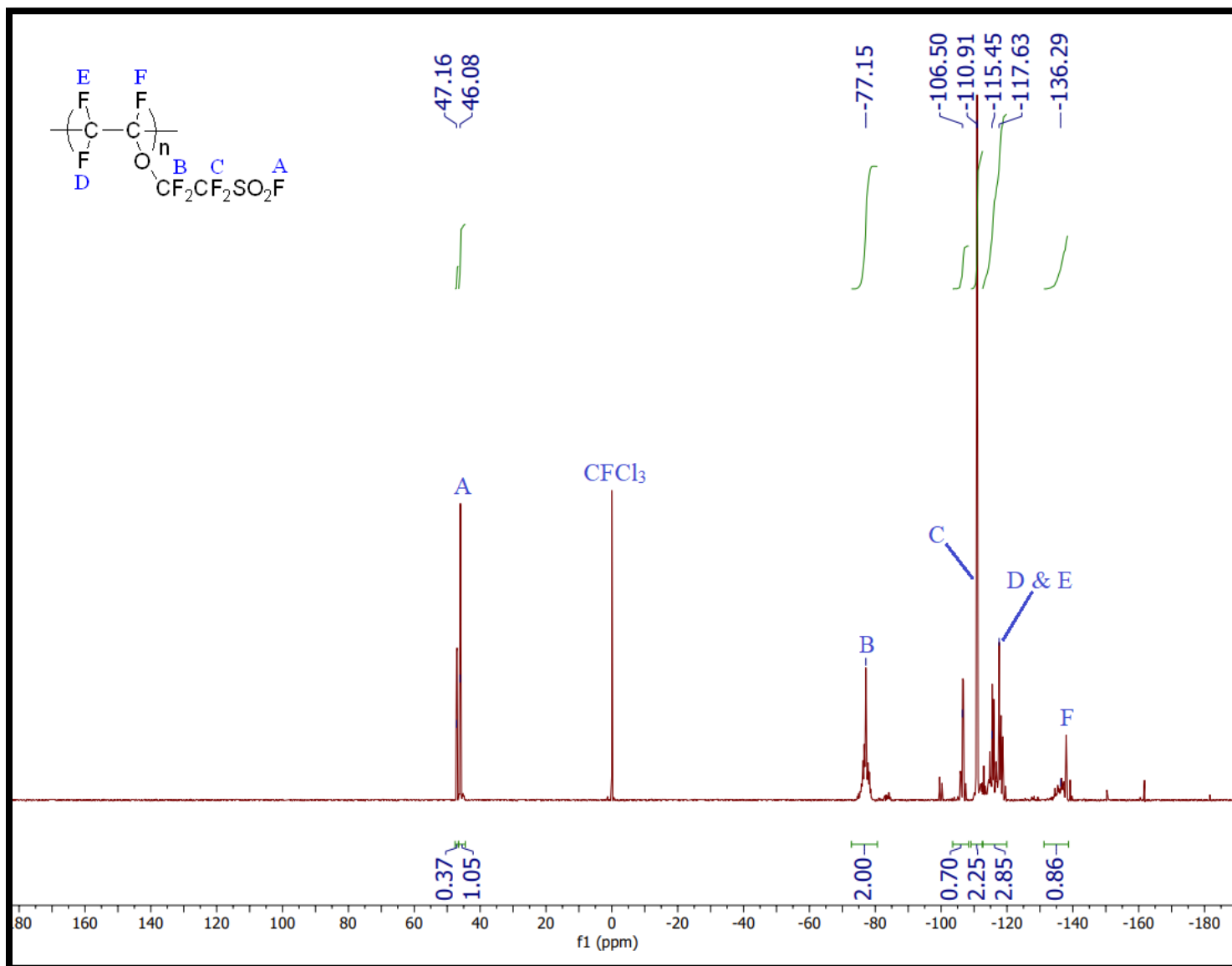
Appendix K1: ^{19}F NMR spectrum of homo-polymerization run #5 of $\text{CF}_2=\text{FCOCF}_2\text{CF}_2\text{SO}_2\text{F}$, 400 MHz, CD_3CN CFCl_3



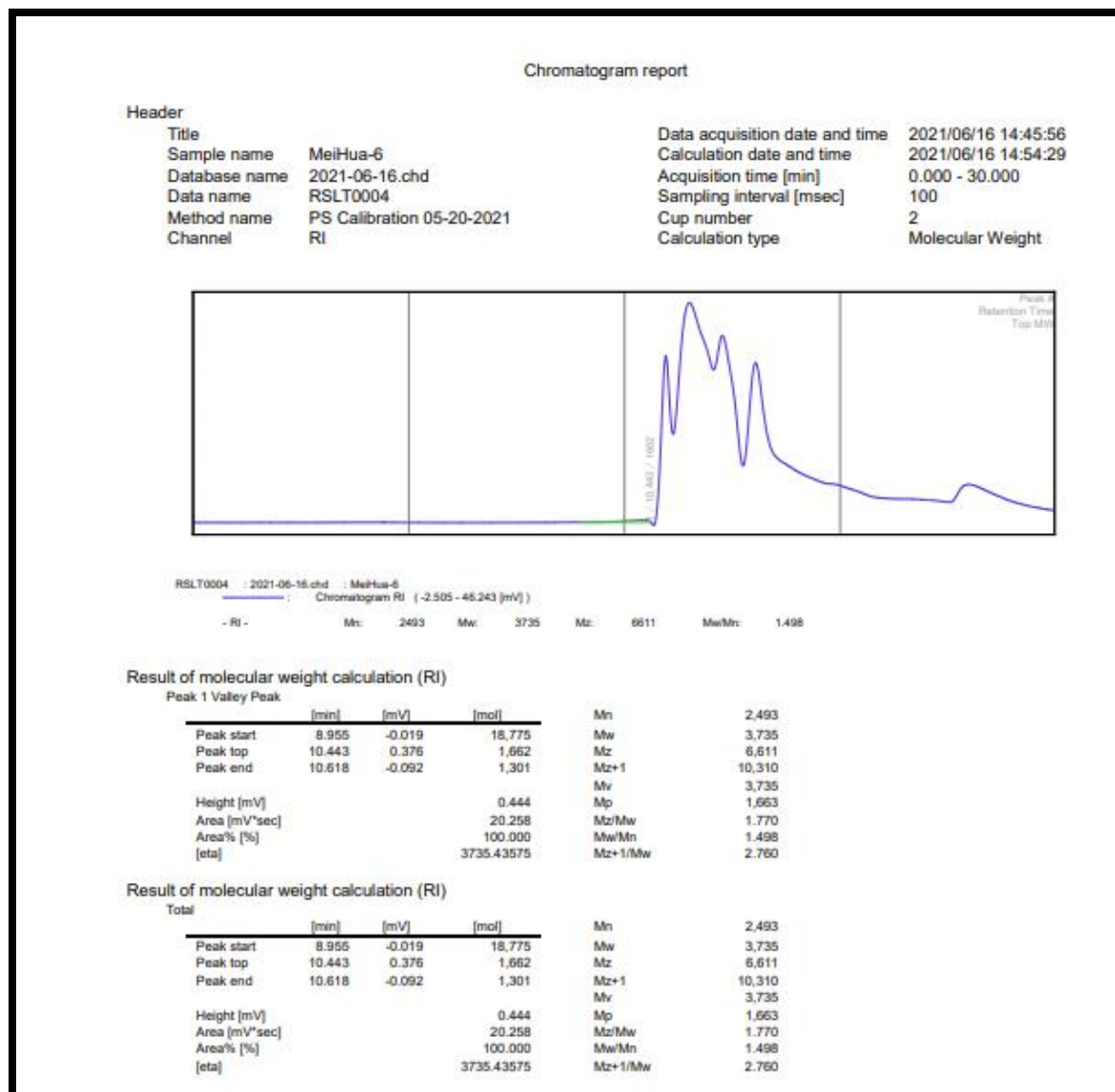
Appendix K2: Gel Permeation Chromatography (GPC) for homo-polymerization run #5 of $CF_2=FCOCF_2CF_2SO_2F$ in THF



Appendix L1: ^{19}F NMR spectrum of homo-polymerization run #6 of $\text{CF}_2=\text{FCOCF}_2\text{CF}_2\text{SO}_2\text{F}$, 400 MHz, CD_3CN



Appendix L2: Gel Permeation Chromatography (GPC) for homo-polymerization run #6 of $CF_2=FCOCF_2CF_2SO_2F$ in THF



VITA

JOSIAH MARSHALL

- Education: M.S. Chemistry, East Tennessee State University, Johnson
City, Tennessee, 2021
- B.S. ACS Chemistry-Biochemistry Concentration, East Tennessee
State University, Johnson City, Tennessee, 2016
- B.S. Criminal Justice & Criminology, East Tennessee State
University, Johnson City, Tennessee, 2016
- Sullivan County Public Schools, Kingsport, Tennessee
- Professional Experience: Lab Tech, Eastman Chemical Company; Kingsport, Tennessee,
2017-2021
- Honors and Awards: Boris Franzus Award in Organic Chemistry, East Tennessee State
University, Johnson City, Tennessee 2021
- Outstanding Graduate Student 2020-2021, East Tennessee State
University, Johnson City, Tennessee, 2021
- Margaret Sells Scholarship Endowment Award, East Tennessee
State University, Johnson City, Tennessee, 2018-2019